



저작자표시-비영리-변경금지 2.0 대한민국

이용자는 아래의 조건을 따르는 경우에 한하여 자유롭게

- 이 저작물을 복제, 배포, 전송, 전시, 공연 및 방송할 수 있습니다.

다음과 같은 조건을 따라야 합니다:



저작자표시. 귀하는 원저작자를 표시하여야 합니다.



비영리. 귀하는 이 저작물을 영리 목적으로 이용할 수 없습니다.



변경금지. 귀하는 이 저작물을 개작, 변형 또는 가공할 수 없습니다.

- 귀하는, 이 저작물의 재이용이나 배포의 경우, 이 저작물에 적용된 이용허락조건을 명확하게 나타내어야 합니다.
- 저작권자로부터 별도의 허가를 받으면 이러한 조건들은 적용되지 않습니다.

저작권법에 따른 이용자의 권리는 위의 내용에 의하여 영향을 받지 않습니다.

이것은 [이용허락규약\(Legal Code\)](#)을 이해하기 쉽게 요약한 것입니다.

[Disclaimer](#)

이 학 석 사 학 위 논 문

Precision Synthesis of Various
Low-Bandgap Donor-Acceptor
Alternating Conjugated Polymers
via Living Suzuki-Miyaura
Catalyst-Transfer Polymerization

리빙 스즈키-미야우라 촉매-이동 중합을 통한 낮
은 밴드갭을 갖는 다양한 전자 주개-받개 교대 공
중합체의 정교한 합성

2022 년 8 월

서울대학교 대학원

화학부 유기화학 전공

김 황 석

Precision Synthesis of Various Low-Bandgap Donor-Acceptor Alternating Conjugated Polymers via Living Suzuki-Miyaura Catalyst-Transfer Polymerization

지도 교수 최 태 림

이 논문을 이학석사 학위논문으로 제출함

2022 년 8 월

서울대학교 대학원

화학부 유기화학 전공

김 황 석

김황석의 이학석사 학위论문을 인준함

2022 년 8 월

위 원 장 _____ 김 경 택 (인)

부위원장 _____ 최 태 림 (인)

위 원 _____ 이 홍 근 (인)

Abstract

Precision Synthesis of Various Low-Bandgap Donor-Acceptor Alternating Conjugated Polymers via Living Suzuki-Miyaura Catalyst-Transfer Polymerization

Hwangseok Kim

Organic Chemistry in Department of Chemistry

The Graduate School

Seoul National University

Here we report that living Suzuki-Miyaura catalyst-transfer polymerization (SCTP) using RuPhos Pd G3 precatalyst is a versatile method for the precision synthesis of various donor-acceptor alternating conjugated polymers (DA ACPs). First, the living SCTP of biaryl monomers with combinations of both medium to strong A and D were optimized and DA ACPs with controlled number average molecular weight (M_n), narrow dispersity (D , 1.05–1.29) were produced in high yield (>87%). Moreover, the expansion of SCTP to an A_1 -D- A_2 -D quateraryl monomer containing diketopyrrolopyrrole (DPP; strong A) successfully obtained its controlled polymerization (M_n = 9.2–40.0 kg/mol). Additionally, the living SCTP even enabled the efficient one-pot synthesis of various diblock and triblock copolymers. Lastly, the DA ACPs showed tunable optical bandgap (E_g^{opt} , from 1.29 to 1.77 eV) and highest occupied molecular orbital (HOMO) level (from -5.57 to -4.75 eV), while their block copolymers exhibited broad absorption ranges and promising visible light-harvesting properties.

Key words : Conjugated polymer, Catalyst-transfer polymerization, Organic semiconductor, Donor-acceptor copolymer, Suzuki-Miyaura coupling

Student Number : 2020-26902

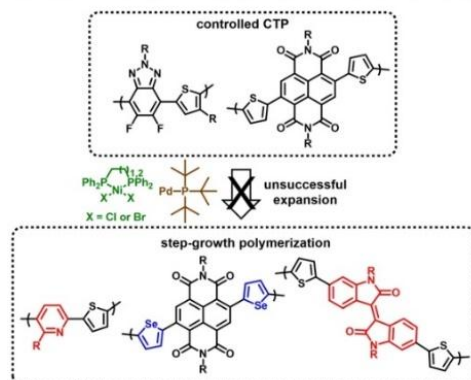
Contents

Abstract	1
Contents	3
1. Introduction	4
2. Results and Discussion	8
3. Conclusion	19
4. Experimental and Supporting Information	20
References	69
Abstract (Korean)	74

1. Introduction

Conjugated polymers (CPs) are one of the most studied organic semiconducting materials widely used in light-emitting diodes, field-effect transistors, and polymer solar cells (PSCs) owing to their flexibility, light weight, and solution processability.^{1,2} Especially, donor-acceptor alternating CPs (DA ACPs), bearing high coplanarity that leads to a low optical bandgap (E_g^{opt}), have significantly improved the device performance.³⁻⁶ Conventionally DA ACPs have been synthesized via transition-metal catalyzed Suzuki-Miyaura⁷⁻¹⁰ and Stille cross-coupling,¹¹⁻¹³ as well as direct arylation polymerization.¹⁴⁻¹⁷ However, most of these methods are step-growth polymerization, resulting in uncontrolled molecular weight, high dispersity (\mathcal{D}), low end-group fidelity, and poor batch-to-batch reproducibility. The lack of control may negatively affect the device performance.^{18,19}

(a) Previous works: controlled CTP of DA ACPs with limited scope



(b) This work

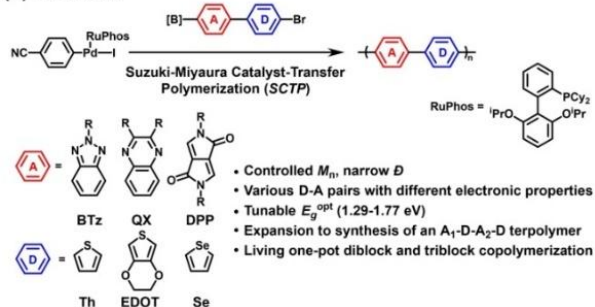


Figure 1. a) Previous works on CTP of DA ACPs showing limited scope. b) SCTP of various DA ACPs using RuPhos Pd G3 precatalyst.

On the other hand, the living chain-growth polymerization is a powerful tool for synthesizing polymers with high precision, allowing the control of both molecular weight and complex microstructures, such as block or graft copolymers. Pioneered by Yokozawa's group, catalyst-transfer polymerization (CTP), where the propagating catalysts do not dissociate from the growing polymers, has been a representative method for the chain-growth polymerization of (hetero)arene monomers.²⁰⁻²³ Thus far, CTP based on Kumada (KCTP),²⁰⁻²⁹ Suzuki-Miyaura (SCTP),³⁰⁻³⁶ and Stille cross-couplings³⁷ have been extensively investigated for the polymerization of simple (hetero)arenes (e.g., thiophene, phenylene, fluorene, and benzotriazole), as well as DD biaryl monomers (e.g., thiophene-phenylene,³⁸ bichalcogenophene,^{39,40} and cyclopentadithiophene-phenylene⁴¹). However, only a few reports with limited scope have demonstrated the controlled synthesis of DA ACPs because of challenges in efficient ring-walking between D and A. For example, well-known catalysts such as [1,3-bis(diphenylphosphino)propane]dichloronickel (Ni(dppp)Cl₂) and (tri-*tert*-butylphosphine)palladium (PdP(*t*-Bu)₃) successfully promoted the CTP of difluorobenzotriazole-thiophene and fluorene-benzothiadiazaole,^{42,43} but the same catalytic system resulted in uncontrolled or even step-growth polymerization of thiophene-pyridine monomer (**Figure 1a**).^{44,45} Besides, Kiriy *et al.* succeeded in the CTP of arylenediimide-dithiophene utilizing the same series of catalysts.⁴⁶⁻⁴⁸ Nonetheless, undesired step-growth polymerization occurred upon changing the monomer moiety from arylenediimide to isoindigo,⁴⁹ and from thiophene to selenophene,⁵⁰ thereby implying a significantly limited scope of this catalytic system (**Figure 1a**). In addition, controlled CTP of strong D-strong A to obtain a low E_g^{opt} was not achieved so far, because of the low ring-walking ability of conventional catalytic systems on DA units with vastly different electronic properties.⁵¹⁻⁵⁵ Thus, a universal methodology to synthesize various DA ACPs, including strong D-strong A, with excellent control, is still desired for the precision synthesis of organic semiconducting materials with tunable energy levels and E_g^{opt} .

Our group developed an efficient SCTP system for monomers with a wide range of electronic characters, from strong D (3,4-propylenedioxythiophene) to strong A (quinoxaline, QX).⁵⁶⁻⁵⁹ The Pd catalyst coordinated by Buchwald ligands such as RuPhos- and SPhos-Pd exhibited extraordinary catalyst-transfer ability,

achieving a universal polymerization of (hetero)arenes with very distinctive electronic properties by a novel strategy that included utilizing *N*-coordinated boronates such as 4,4,8,8-tetramethyl-1,3,6,2-dioxazaborocane (Me₄DABO) and its *N*-benzylated derivative (*N*-BnMe₄DABO). Therefore, this versatility encouraged us to expand the catalytic system to more challenging DA biaryl monomers. Herein, we report controlled SCTP to produce diverse DA ACPs with various combinations of D/A units (**Figure 1b**). First, biaryl monomers containing benzotriazole (BTz; medium A), quinoxaline (QX; strong A), thiophene (Th; medium D), and two strong D units (3,4-ethylenedioxythiophene (EDOT) and selenophene (Se)) were successfully polymerized using RuPhos Pd G3 precatalyst to produce four DA ACPs (PBTzEDOT, PQXTh, PQXEDOT, and PQXSe) with controlled number average molecular weight (M_n), narrow \mathcal{D} and high yield. Furthermore, the SCTP was applied on a quateraryl monomer with another carbonyl-containing strong A, diketopyrrolopyrrole, which conventional KCTP is not tolerant to, and obtained the controlled synthesis of an A₁-D-A₂-D terpolymer (PBTzThDPPTTh) showing narrow E_g^{opt} with near-infrared absorption. Additionally, the living nature of SCTP enabled the one-pot synthesis of D-DA (P3HT-*b*-PQXTh), A-DA (PQX-*b*-PQXSe), and novel DA-DA (PBTzEDOT-*b*-PQXTh) diblock copolymers, as well as the A-D-DA (PQX-*b*-P3HT-*b*-PQXSe) triblock copolymer by sequential addition of monomers with dramatically different electronic characters. Lastly, P3HT-*b*-PQXTh and PQX-*b*-P3HT-*b*-PQXSe displayed wide absorption ranges, as well as light-harvesting properties by fluorescence resonance energy transfer (FRET).

2. Results and Discussion

Table 1: SCTP of BTz–EDOT monomer using RuPhos Pd G3 precatalyst^[a]

P1: PBTzEDOT								
Entry	M/I	Catalyst (equiv)	Ligand (equiv)	Temp. (°C)	Time (h)	$M_{n,theo}$ ^[b]	M_n (\bar{D}) ^[c]	Yield ^[d] (%)
1	25	RuPhos Pd G3 (0.04)	RuPhos (0.24)	45	3	13.4k	11.9k (1.07)	97
2	50	RuPhos Pd G3 (0.02)	RuPhos (0.12)	45	6	26.9k	29.0k (1.26)	90
3	50	RuPhos Pd G3 (0.02)	RuPhos (0.12)	35	11	26.9k	26.5k (1.18)	92
4	15	RuPhos Pd G3 (0.067)	RuPhos (0.40)	35	5	8.1k	8.0k (1.11)	88
5	25	RuPhos Pd G3 (0.04)	RuPhos (0.24)	35	8	13.4k	14.0k (1.05)	89
6	75	RuPhos Pd G3 (0.013)	RuPhos (0.08)	35	16	40.3k	36.7k (1.21)	94

[a] Reaction conditions: **M1** (0.05 mmol, 1 equiv), RuPhos Pd G3, RuPhos, 4-iodobenzonitrile (0.95 equiv relative to the catalyst), K_3PO_4 (0.3 mmol, 6 equiv) THF/ H_2O (0.01M, v/v = 30/1). [b] Estimated by multiplying molecular weight of repeat unit by M/I. [c] Absolute molecular weight was determined by THF SEC using a MALLS detector. [d] Isolated yield.

To expand SCTP toward DA ACPs with a wide range of energy levels and E_g^{opt} , we designed various biaryl monomers, as presented in **Figure 1b**. Boron moieties were introduced on phenyl-based acceptors (BTz and QX) instead of heterocycle-based donors (Th, EDOT, and Se) to maximize the conversion by suppressing protodeboronation.⁶⁰ First, BTz–EDOT monomer (medium A–strong D) protected with *N*-BnMe₄DABO (**M1**), which was recently shown to be an optimal boronate for the SCTP of BTz,⁵⁸ was prepared. The conventional SCTP conditions using RuPhos Pd G3 with 4-iodobenzonitrile as the external initiator at a monomer to initiator ratio (M/I ratio) of 25 and 45 °C produced the desired PBTzEDOT

with M_n of 11.9 kg/mol and narrow \mathcal{D} (1.07) (Table 1, entry 1). However, \mathcal{D} broadened to 1.26 for the case of M/I = 50 (Table 1, entry 2). Notably, decreasing the temperature to 35 ° C minimized chain transfer and led to improved control (M_n = 26.5 kg/mol, \mathcal{D} = 1.18; Table 1, entry 3). At these optimal conditions, PBTzEDOT, P1, was synthesized with linear increase in molecular weight (M_n = 8.0–36.7 kg/mol) in a controlled manner (\mathcal{D} = 1.05–1.21) over a wide range of M/I ratios (15–75) (Table 1, entries 3–6; Figure 2a).

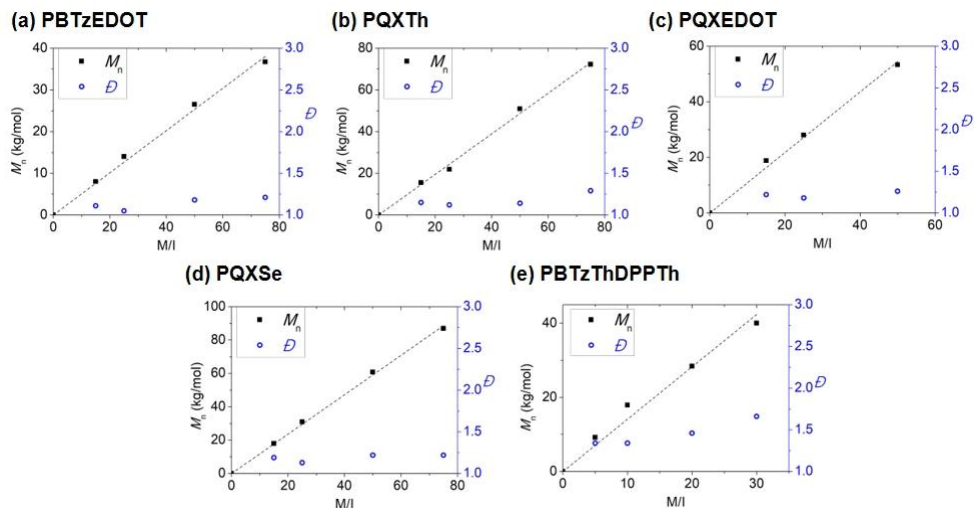


Figure 2. Plots of M_n vs. M/I ratios and their corresponding \mathcal{D} values for a) PBTzEDOT, b) PQXTh, c) PQXEDOT, d) PQXSe, and e) PBTzThDPPTTh.

Table 2: SCTP of QX–Th, QX–EDOT, and QX–Se monomers using RuPhos Pd G3 precatalyst^[a]

Entry	M/I	Monomer	Catalyst (equiv)	Ligand (equiv)	THF/H ₂ O (concn, v/v)	Time (h)	<i>M_n</i> ,theo ^[b]	<i>M_n</i> (D) ^[c]	Yield ^[d] (%)
1	25	M2	RuPhos Pd G3 (0.04)	RuPhos (0.24)	0.01M, 30/1	15	23.9k	22.5k (1.19)	87
2	50	M2	RuPhos Pd G3 (0.02)	RuPhos (0.12)	0.01M, 30/1	29	47.8k	48.2k (1.37)	82
3	50	M2	RuPhos Pd G3 (0.02)	RuPhos (0.12)	0.03M, 10/1	10	47.8k	50.9k (1.14)	93
4	15	M2	RuPhos Pd G3 (0.067)	RuPhos (0.40)	0.03M, 10/1	3	14.3k	15.5k (1.15)	88
5	25	M2	RuPhos Pd G3 (0.04)	RuPhos (0.24)	0.03M, 10/1	5	23.9k	21.9k (1.12)	90
6	75	M2	RuPhos Pd G3 (0.013)	RuPhos (0.08)	0.03M, 10/1	14	71.7k	72.2k (1.29)	92
7	15	M3	RuPhos Pd G3 (0.067)	RuPhos (0.40)	0.02M, 15/1	5	15.2k	18.8k (1.22)	87
8	25	M3	RuPhos Pd G3 (0.04)	RuPhos (0.24)	0.02M, 15/1	9	25.3k	28.0k (1.18)	94
9	50	M3	RuPhos Pd G3 (0.02)	RuPhos (0.12)	0.02M, 15/1	12	50.7k	53.3k (1.26)	92
10	50	M4	RuPhos Pd G3 (0.02)	RuPhos (0.12)	0.02M, 15/1	11	50.1k	61.0k (1.35)	90
11 ^e	50	M4	RuPhos Pd G3 (0.02)	RuPhos (0.12)	0.02M, 15/1	18	50.1k	60.8k (1.22)	93
12 ^e	15	M4	RuPhos Pd G3 (0.067)	RuPhos (0.40)	0.02M, 15/1	5	15.0k	18.0k (1.19)	90
13 ^e	25	M4	RuPhos Pd G3 (0.04)	RuPhos (0.24)	0.02M, 15/1	8	25.1k	30.9k (1.13)	92
14 ^e	75	M4	RuPhos Pd G3 (0.013)	RuPhos (0.08)	0.02M, 15/1	25	75.2k	86.9k (1.22)	95

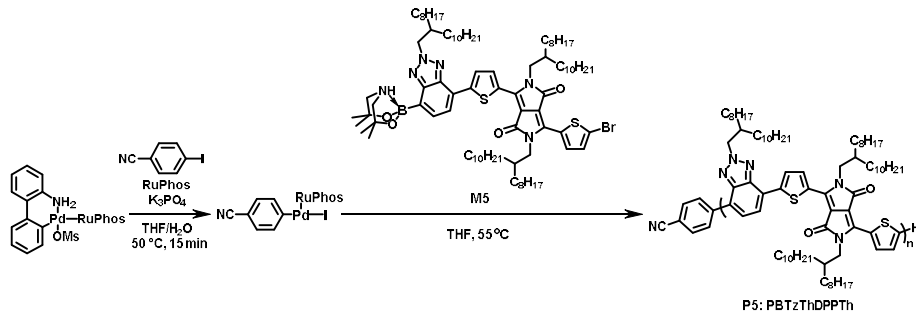
[a] Reaction conditions: monomer (0.05 mmol, 1 equiv), RuPhos Pd G3, RuPhos, 4-iodobenzonitrile (0.95 equiv relative to the catalyst), K₃PO₄ (0.3 mmol, 6 equiv). [b] Estimated by multiplying molecular weight of repeat unit by M/I. [c] Absolute molecular weight was determined by THF SEC using a MALLS detector. [d] Isolated yield. [e] conducted at 35 °C.

Encouraged by the successful SCTP of BTz-EDOT, we designed a series of monomers containing strong A (QX). First, we prepared the QX-Th monomer with $-B(OH)_2$ moiety (**M2**) to target poly(quinoxaline-*alt*-thiophene) (PQXTh), which demonstrated high performance in PSC.^{18,61,62} Although the SCTP of **M2** at 0.01 M led to M_n of 22.5 kg/mol and $\mathcal{D} = 1.19$ at M/I = 25, an attempt to increase M_n under the same condition was unsatisfactory, marking 29 h to reach full conversion at M/I = 50 and displaying broad \mathcal{D} (1.37) (**Table 2**, entries 1 and 2). Accelerating transmetalation by increasing the reaction concentration to 0.03M enhanced both the rate (10 h) and controllability ($M_n = 50.9$ kg/mol, $\mathcal{D} = 1.14$; **Table 2**, entry 3). Again, using these optimal conditions, we achieved SCTP of QX-Th with controlled M_n (15.5–72.2 kg/mol), narrow \mathcal{D} (1.12–1.29), and high yields of over 88% at M/I ratios from 15 to 75 (**Table 2**, entries 3–6; **Figure 2b**). These results show the excellent catalyst-transfer of RuPhos-Pd on DA monomers, even when a highly electron-deficient arene is involved.

Next, we moved on to the SCTP of more challenging QX-EDOT monomer (**M3**), containing stronger D of EDOT, thereby providing a considerably different electron density from the strong A unit. The same protocol using **M3** led to successful controlled synthesis ($M_n = 18.8$ –53.3 kg/mol, $\mathcal{D} = 1.18$ –1.26; **Figure 2c**) of poly(quinoxaline-*alt*-EDOT) (PQXEDOT) at M/I = 15–50 (**Table 2**, entries 7–9). Moreover, the SCTP of **M4**, containing a different strong D (selenophene), was attempted to further expand the scope, because selenophene is known to enhance the quinoidal character of CPs to absorb long-wavelength visible light and improve charge transfer ability.^{63–65} The synthesis of poly(quinoxaline-*alt*-selenophene) (PQXSe) at M/I = 50 under the same conditions led to an increase in the high molecular weight shoulder ($\mathcal{D} = 1.35$), presumably owing to undesired chain coupling (**Table 2**, entry 10). Nevertheless, lowering the temperature to 35 °C resulted in improved controllability^{57,66} ($M_n = 60.8$ kg/mol, $\mathcal{D} = 1.22$). At these conditions, the controlled SCTP of **M4** at M/I ratios = 15–75 to produce PQXSe in high yield (>90%; **Table 2**, entries 11–14) was realized ($M_n = 18.0$ –86.9 kg/mol, $\mathcal{D} = 1.13$ –1.22; **Figure 2d**). In addition, the M_n of **P1–P4** matched well with their corresponding

theoretical M_n values ($M_{n,theo}$) (Tables 1 and 2). These results highlight the excellent and universal ring-walking ability of RuPhos–Pd between arenes with vastly different electronic properties, enabling the precision synthesis of strong D–strong A copolymers.

Table 3: SCTP of BTz–Th–DPP–Th monomer using RuPhos Pd G3 precatalyst^[a]



Entry	M/I	Catalyst (equiv)	Ligand (equiv)	Time (h)	M_n (\mathcal{D}) ^[b]	Yield ^[c] (%)
1	5	RuPhos Pd G3 (0.20)	RuPhos (1.20)	12	9.2k (1.34)	90
2	10	RuPhos Pd G3 (0.10)	RuPhos (0.60)	13	17.9k (1.34)	91
3	20	RuPhos Pd G3 (0.05)	RuPhos (0.30)	13	28.4k (1.46)	97
4	30	RuPhos Pd G3 (0.033)	RuPhos (0.20)	15	40.0k (1.66)	98

[a] Reaction conditions: monomer (0.02 mmol, 1 equiv), RuPhos Pd G3, RuPhos, 4-iodobenzonitrile (0.95 equiv relative to the catalyst), K_3PO_4 (0.12 mmol, 6 equiv), THF/ H_2O (0.01M, v/v = 75/1) [b] Determined by THF SEC calibrated by PS standards. [c] Isolated yield.

Based on the successful SCTP of various DA biaryl monomers, we were inspired to expand its scope even further to a more complex quateraryl structure. Hence, we chose an A_1 –D– A_2 –D monomer containing BTz, Th, and diketopyrrolopyrrole (DPP), a strong A, as a target because such polymers were reported to have very low E_g^{opt} below 1.4 eV.^{67,68} Moreover, this investigation would demonstrate the advantage of mild conditions during SCTP as the conventional KCTP of DPP is prohibited owing to the incompatibility between the Grignard reagent and carbonyl functionality. In this context, a BTz–Th–DPP–Th monomer (**M5**) containing stable Me₄DABO on the BTz unit was prepared and polymerized at mild conditions using RuPhos

Pd G3. To our delight, this Sctp produced **P5** (PBTzThDPpTh) with a linear increase of M_n (9.2–40.0 kg/mol) at M/I = 5–30 (**Table 3**, entries 1–4; **Figure 2e**) and excellent yield (>90%). However, \mathcal{D} became broader (1.34–1.66) than in other cases, implying that ring–walking on this quateraryl backbone was indeed more challenging and chain transfer reactions inevitably occurred especially at high DP (entry 4, **Figure S1b**).⁶⁹ To the best of our knowledge, this is the first report of controlled polymerization using a monomer with more than three different arene units, demonstrating the excellent catalyst–transfer ability of RuPhos–Pd and the high functional group tolerance of Sctp.

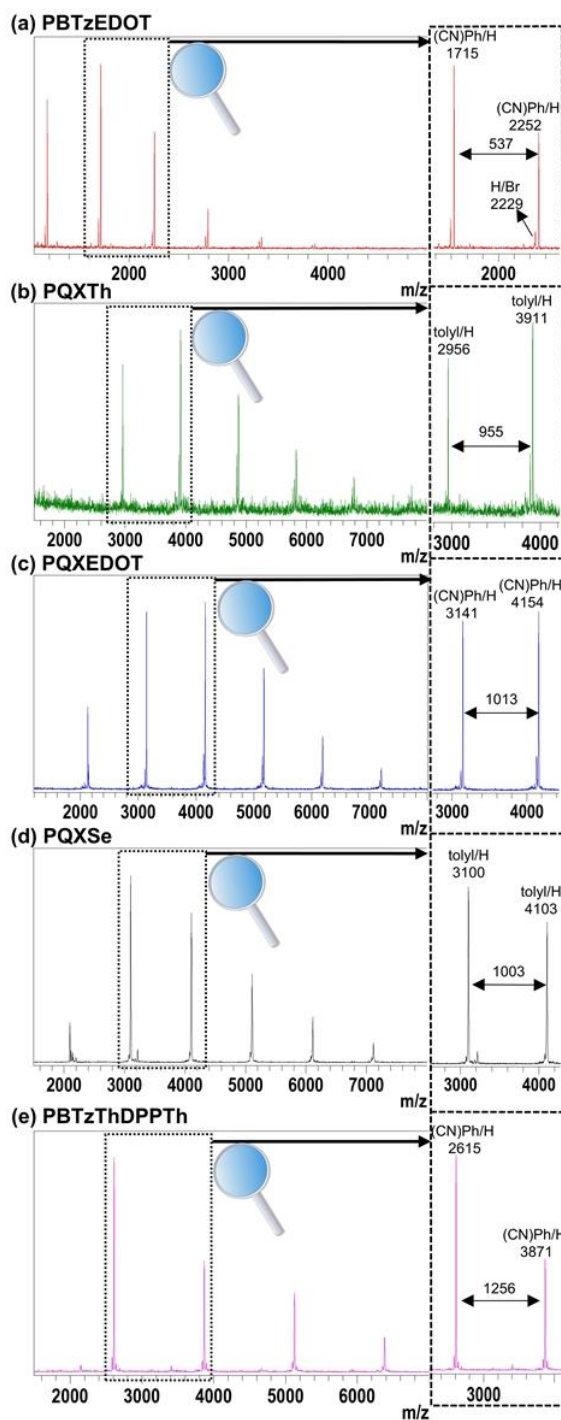


Figure 3. MALDI-TOF spectra of a) PBTzEDOT (Table 1, entry 4), b) PQXTh (Table S1, entry 1), c) PQXEDOT (Table 2, entry 7), d) PQXSe (Table S1, entry 2), and e) PBTzThDPPTTh (Table S2, entry 1).

Matrix-assisted laser desorption/ionization time-of-flight (MALDI-TOF) analysis was conducted to support the chain-growth mechanism of the Sctp.^{70,71} The MALDI-TOF spectra of PBTzEDOT (**Figure 3a**) and PQXEDOT (**Figure 3c**) revealed the high fidelity of the (CN)Ph/H end group, even though a minor peak series corresponding to H/Br appeared for PBTzEDOT. These results indicate highly efficient external initiation from RuPhos Pd G3 with 4-iodobenzonitrile followed by living chain-growth polymerization. PQXTh and PQXSe also demonstrated high end-group fidelity of tolyl/H when polymerized with 2-iodotoluene as an initiator (**Figure 3b** and **3d**, respectively; also, see the polymerization results in **Table S1**, entries 1 and 2). Unexpectedly, PBTzThDPPTH synthesized with RuPhos Pd G3 showed (CN)Ph/H and significant (CN)Ph/carbazole end groups (**Figure S1a**), even though the carbazole group was not detected by ¹H NMR spectroscopy. This observation implies that a few carbazoles released from the G3 precatalyst after initiation were capped at the end of some polymer chains, presumably via Buchwald-Hartwig coupling.^{72,73} Therefore, to prevent carbazole capping, we tested RuPhos Pd G4 catalyst at M/I = 5, which releases unreactive 9-methylcarbazole instead, and obtained **P5** with controlled molecular weight distribution by SEC analysis (M_n = 10.4 kg/mol, \mathcal{D} = 1.34; **Table S2**, entry 1) and nearly exclusive (CN)Ph/H end groups by MALDI, confirming living chain-growth polymerization was dominant at low DP (**Figure 3e**). Lastly, the degree of polymerization (DP) for each polymer was calculated from ¹H NMR spectra (PBTzEDOT = 14, PQXTh = 15, PQXEDOT = 15, PQXSe = 15; see the details in the **SI**). The obtained values matched well with their initial M/I feed ratio (15), thereby confirming the efficient external initiation and living nature of Sctp.

(P3HT₂₀-*b*-PQXTh₂₀) was successfully obtained in a controlled manner, showing a clear shift of the SEC trace to high molecular weight region ($M_n = 18.6$ kg/mol, $\mathcal{D} = 1.12$; **Figure 4a**). Similarly, after synthesizing the PQX₂₀ acceptor ($M_n = 16.5$ kg/mol, $\mathcal{D} = 1.10$) first block, 20 equiv. of QX-Se monomer (**M4**) was added to provide PQX₂₀-*b*-PQXSe₂₀ (A-DA) with a narrow \mathcal{D} ($M_n = 35.1$ kg/mol, $\mathcal{D} = 1.18$; **Figure 4b**). Moreover, to push the system to more challenging BCP, we synthesized PBTzEDOT₂₀-*b*-PQXTh₂₀ ($M_n = 27.0$ kg/mol, $\mathcal{D} = 1.21$; **Figure 4c**) by achieving chain elongation even from PBTzEDOT₂₀, a DA block macroinitiator ($M_n = 10.1$ kg/mol, $\mathcal{D} = 1.16$). This is the first example of controlled synthesis of a fully conjugated DA-DA polymer via CTP. Lastly, we even pushed our limit to the unprecedented one-pot synthesis of A-B-C type triblock copolymer (TCP) via series of chain elongation with CTP.⁷⁴⁻⁷⁷ By preparing acceptor PQX₁₅ ($M_n = 11.6$ kg/mol, $\mathcal{D} = 1.12$) as the first block, the sequential addition of the donor **M6** followed by the DA type **M4** (15 equiv. each) produced the PQX₁₅-*b*-P3HT₁₅-*b*-PQXSe₁₅ TCP ($M_n = 32.7$ kg/mol, $\mathcal{D} = 1.19$) as confirmed by clear shift of SEC traces (**Figure 4d**). This successful synthesis highlights the capacity of RuPhos-Pd-promoted SCTP in achieving a highly efficient catalyst transfer among the A, D, and DA units with significantly distinct electronic characters. Additionally, ¹H NMR analysis of the resulting BCPs and TCP (see the **SI**) revealed that the DP of each block was consistent with the initial feed ratio of each monomer (P3HT = 23 and PQXTh = 19 for P3HT₂₀-*b*-PQXTh₂₀, PQX = 18 and PQXSe = 21 for PQX₂₀-*b*-PQXSe₂₀, PBTzEDOT = 19 and PQXTh = 19 for PBTzEDOT₂₀-*b*-PQXTh₂₀, PQX = 14 P3HT = 17 and PQXSe = 16 for PQX₁₅-*b*-P3HT₁₅-*b*-PQXSe₁₅) to support the living character of SCTP on several DA monomers.

Table 4: Optical and electrochemical properties of DA ACPs prepared by SCTP

Entry	Polymer	λ_{max} in film (nm)	λ_{onset} in film (nm)	$E_g^{\text{opt, [a]}}$ (eV)	$E_{\text{HOMO}}^{\text{[b]}}$ (eV)	$E_{\text{LUMO}}^{\text{[c]}}$ (eV)
1	PBTzEDOT	573	701	1.77	-4.75	-2.98
2	PQXTh	631	712	1.73	-5.57	-3.84
3	PQXEDOT	639	713	1.73	-5.11	-3.38
4	PQXSe	681	759	1.64	-5.45	-3.81
5	PBTzThDPPTTh	766, 845	960	1.29	-5.21	-3.92

[a] $E_g^{\text{opt}} = 1240/\lambda_{\text{onset}}$. [b] Measured by cyclic voltammetry. [c] Estimated by $E_{\text{LUMO}} = E_{\text{HOMO}}$

+ E_g^{opt} .

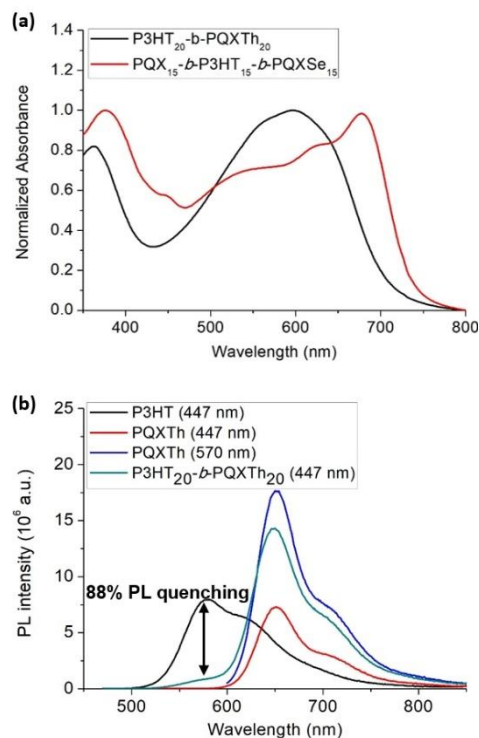


Figure 5. a) UV-vis absorption spectra of P3HT-*b*-PQXTh (black) and PQX-*b*-P3HT-*b*-PQXSe (red) in thin films. b) Emission spectra of P3HT (0.003 g/mL) and PQXTh (0.017 g/mL) at 447 nm excitation (black and red, respectively), P3HT-*b*-PQXTh (0.020 g/mL) at 570 nm (blue) and 447 nm excitation (green) in CHCl₃.

Notably, the broad scope of SCTP allowed for fine-tuning of the optical and electrochemical properties of the polymers. First, E_g^{opt} values (calculated from λ_{onset} of UV-vis-NIR absorption spectra in thin film states; see **Figure S2**) between 1.64 and 1.77 eV were obtained from the biaryl DA ACPs (**P1-P4**) depending on their electronic character (**Table 4**, entries 1-4). Remarkably, E_g^{opt} of **P5**, containing the DPP unit, significantly decreased to 1.29 eV to exhibit near-infrared absorption (**Table 4**, entry 5). Overall, all these polymers exhibited significantly narrower E_g^{opt} values compared to the DA ACPs previously synthesized by other CTP systems,^{42,43,46,47} highlighting the versatility of the current SCTP system and demonstrating its potential to produce applicable CPs that are widely used in current polymer electronics. Additionally, the highest occupied molecular orbital (HOMO) level measured by cyclic voltammetry (See **Figure S5** for the cyclic voltammograms) was raised by a strong D or reduced by a strong A, leading to a broad

range of values from -5.57 to -4.75 eV (**Table 4**). In addition, the absorption spectrum of P3HT-*b*-PQXTh includes a full width at half maximum of 220 nm (460–680 nm; **Figure 5a**) and showed promising aspects for intramolecular FRET owing to the significant overlap between the PQXTh absorption and the P3HT emission (**Figure S2** and **S3**). Excitation of P3HT-*b*-PQXTh at 447 nm (λ_{max} of P3HT) led to 88% intramolecular fluorescence quenching and amplified emission of the PQXTh block, which corresponds to 88% FRET efficiency, suggesting its potential utility in PSC (**Figure 5b**).⁸⁰ Lastly, PQX-*b*-P3HT-*b*-PQXSe TCP showed vastly broad UV/Vis spectra with half-maximum absorption from 350 to 717 nm, absorbing all visible light (**Figure 5a**). This absorption property originates from the complementary contribution of all three blocks, suggesting PQX-*b*-P3HT-*b*-PQXSe TCP as a potential material for high-performance light-harvesting applications.

3. Conclusion

In summary, we report the versatile SCTP using RuPhos Pd G3 to achieve the precision synthesis of DA ACPs. First, various DA ACPs (PBTzEDOT, PQXTh, PQXEDOT, and PQXSe) were synthesized in controlled M_n , narrow \mathcal{D} , and high yields (>87%) from DA biaryl monomers with medium to strong D and A. Notably, the precision synthesis of an A_1-D-A_2-D terpolymer (PBTzThDPPTTh) containing carbonyl groups, which are intolerant of the Grignard nucleophiles used in conventional KCTP, further highlighted the excellent ring-walking ability of RuPhos-Pd and high functional group tolerance of SCTP. Also, MALDI-TOF and ^1H NMR analyses supported the living chain-growth mechanism. The controlled polymerization of DA ACPs with a wide range of electronic properties granted the modulation of E_g^{opt} (from 1.29 to 1.77 eV) and HOMO level (from -5.57 to -4.75 eV). Finally, the living SCTP method led to the synthesis of various di(tri)block copolymers with wide absorption ranges and complex microstructures, such as D-DA (P3HT-*b*-PQXTh), A-DA (PQX-*b*-PQXSe), DA-DA (PBTzEDOT-*b*-PQXTh), and A-D-DA (PQX-*b*-P3HT-*b*-PQXSe). The considerably expanded scope of the controlled synthesis of DA ACPs in this study can significantly contribute to the production of novel organic electronic materials. Furthermore, we are developing a more atom-economical methodology to produce structurally complex but widely used conjugated polymers.

4. Experimental and Supporting Information

Materials

Unless otherwise noted, all reagents were purchased from commercial sources and used without further purification. Tetrahydrofuran (THF) was distilled over sodium and benzophenone, and degassed by argon bubbling for 20 minutes before using on polymerization. For size exclusion chromatography (SEC) analysis, HPLC grade THF (stabilized by BHT) was purchased from Fisher Chemical™. (7-bromo-2-(2-octyldodecyl)-2H-benzo[d][1,2,3]triazol-4-yl)boronic acid (1), (8-bromo-2,3-bis(3-((2-octyldodecyl)oxy)phenyl)quinoxalin-5-yl)boronic acid (M7), 1,1'-(benzylazanediyl)bis(2-methylpropan-2-ol) (7), 1,1'-azanediylbis(2-methylpropan-2-ol) (20), 2-(2,3-dihydrothieno[3,4-b][1,4]dioxin-5-yl)-4,4,5,5-tetramethyl-1,3,2-dioxaborolane (3), trimethyl(selenophen-2-yl)stannane (14), and 2,5-bis(2-octyldodecyl)-3,6-bis(5-(trimethylstannyl)thiophen-2-yl)-2,5-dihydropyrrolo [3,4-c]pyrrole-1,4-dione (17) were prepared by the previously reported synthetic methods.

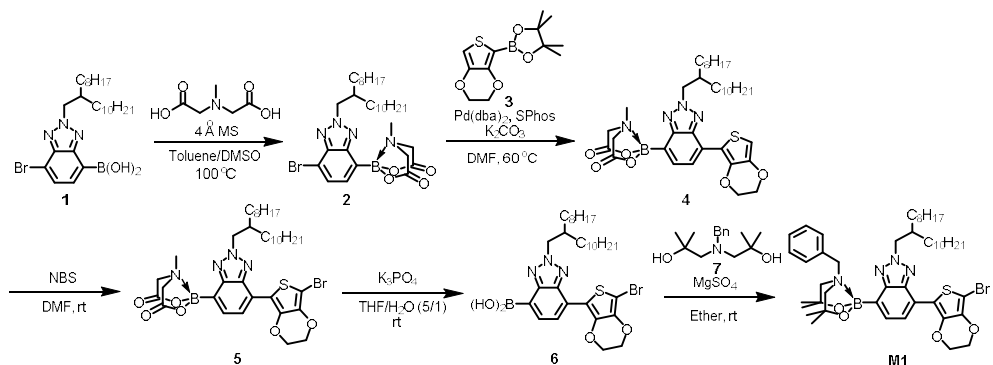
General analytical information

¹H NMR and ¹³C NMR spectra were recorded by Varian/Oxford As-500 (500 MHz for ¹H; scan number 64 and relaxation delay time 5 sec for polymers, and 125 MHz for ¹³C). Size exclusion chromatography (SEC) analysis was carried out using Shodex GPC LF-804 column eluted with THF (HPLC grade, Fisher) in Waters system (1515 pump and 2707 autosampler) and a Wyatt Optilab TrEX refractive index detector. The flow rate was 1.0 mL/min and temperature of the column was maintained at 35 ° C. For injection into the SEC, samples were diluted in 0.001–0.002 wt% by THF and filtered through a 0.20 μm PTFE filter. For the MALLS-VIS-RI analysis, Wyatt triple detector equipped with 785 nm interference filters and Dawn 8+/Viscostar II/Optilab T-rEX were used. MALDI-TOF spectra of polymers were obtained by Bruker Daltonics autoflex II TOF/TOF using pyrene (for PBTzEDOT, PQXEDOT, and PBTzThDPPTTh), TPBD (for PQXTh), and terthiophene (for PQXSe) as matrices. High-resolution mass spectroscopy (HRMS) analyses were performed by ultra-high resolution ESI Q-TOF mass spectrometer (Bruker, Germany) in Organic Chemistry Research Center, Sogang University. UV-vis absorption spectra were obtained by Jasco Inc. UV-vis Spectrometer V-650. Cyclic voltammetry (CV) measurements were carried out by CHI 601C Electrochemical Analyzer (CH Instruments, Inc.). Cyclic voltammograms were recorded by

using polymer films deposited on working electrode of Pt rod, counter electrode of Pt coil, and reference electrode of Ag/Ag⁺ (10 mM AgNO₃ in 0.1 M acetonitrile solution of n-Bu₄NPF₆). For calibration, the redox potential of F_c/F_c⁺ was measured under the same conditions.

Preparation and characterization of monomers

(a) Preparation and Characterization of M1



Compound 2: To a round-bottom flask equipped with a magnetic stir bar, compound **1** (1.05 g, 2.0 mmol) and *N*-methyliminodiacetic acid (327 mg, 2.2 mmol) were added. The reagents were dissolved in toluene (8 mL) and DMSO (1.6 mL). After stirring at 100 °C for 7 h, the crude mixture was diluted with diethyl ether, washed with water three times, dried over anhydrous MgSO₄, and concentrated under reduced pressure. The product was purified by flash column chromatography on silica gel (EA:Hexane = 2:1) to afford (MIDA)B-BTz-Br (compound **2**) as white solid (1.08 g, 1.74 mmol, 87 %). ¹H NMR (500 MHz, CDCl₃) δ (ppm) = 7.63 (d, *J* = 7.3 Hz, 1H), 7.59 (d, *J* = 7.3 Hz, 1H), 4.62 (d, *J* = 7.0 Hz, 2H), 4.20 (d, *J* = 16.2 Hz, 2H), 4.11 (d, *J* = 16.2 Hz, 2H), 2.61 (s, 3H), 2.23 (m, 1H), 1.35–1.15 (m, 32H), 0.86 (td, *J* = 7.0, 3.7 Hz, 6H). ¹³C NMR (125 MHz, CDCl₃) δ (ppm) = 167.36, 146.42, 143.37, 132.83, 129.19, 112.58, 63.07, 60.70, 47.00, 39.06, 31.89, 31.84, 31.28, 30.30, 29.82, 29.62, 29.59, 29.50, 29.45, 29.31, 29.24, 26.13, 22.67, 22.64, 14.12, 14.10. HRMS (ESI): *m/z* for C₃₁H₅₀BBrNaN₄O₄ [M+Na]⁺, calcd: 655.3006, found: 655.3006.

Compound 4: To a round-bottom flask equipped with a magnetic stir bar, compound **2** (934 mg, 1.5 mmol), compound **3** (483 mg, 1.8 mmol), bis(dibenzylideneacetone)palladium(0) (43.5 mg, 0.075 mmol), SPhos (49.3 mg, 0.12 mmol), and potassium carbonate (622 mg, 4.5 mmol) were added. The flask was evacuated and backfilled with argon three times. The reagents

were dissolved in DMF (7.5 mL). After stirring at 60 ° C for 10 h, the crude mixture was diluted with diethyl ether, washed with water three times, dried over anhydrous MgSO₄, and concentrated under reduced pressure. The product was purified by flash column chromatography on silica gel (EA:Hexane = 2:1) to afford (MIDA)B–BTzEDOT (compound **4**) as pale yellow solid (861 mg, 1.24 mmol, 83 %). ¹H NMR (500 MHz, CDCl₃) δ (ppm) = 8.09 (d, *J* = 7.3 Hz, 1H), 7.77 (d, *J* = 7.3 Hz, 1H), 6.50 (s, 1H), 4.63 (d, *J* = 6.5 Hz, 2H), 4.37 (m, 2H), 4.27 (m, 2H), 4.22 (d, *J* = 16.2 Hz, 2H), 4.11 (d, *J* = 16.2 Hz, 2H), 2.59 (s, 3H), 2.20 (m, 1H), 1.38–1.15 (m, 32H), 0.86 (td, *J* = 7.0, 3.7 Hz, 6H). ¹³C NMR (125 MHz, CDCl₃) δ (ppm) = 167.80, 146.63, 141.70, 140.87, 139.98, 132.48, 124.92, 122.91, 113.61, 101.44, 74.98, 64.94, 64.39, 63.02, 59.91, 46.91, 39.05, 31.88, 31.86, 31.48, 29.87, 29.80, 29.62, 29.61, 29.58, 29.52, 29.31, 29.27, 26.31, 24.83, 22.65, 22.63, 14.09. HRMS (ESI): *m/z* for C₃₇H₅₅BNaN₄O₆S [M+Na]⁺, calcd: 717.3833, found: 717.3834.

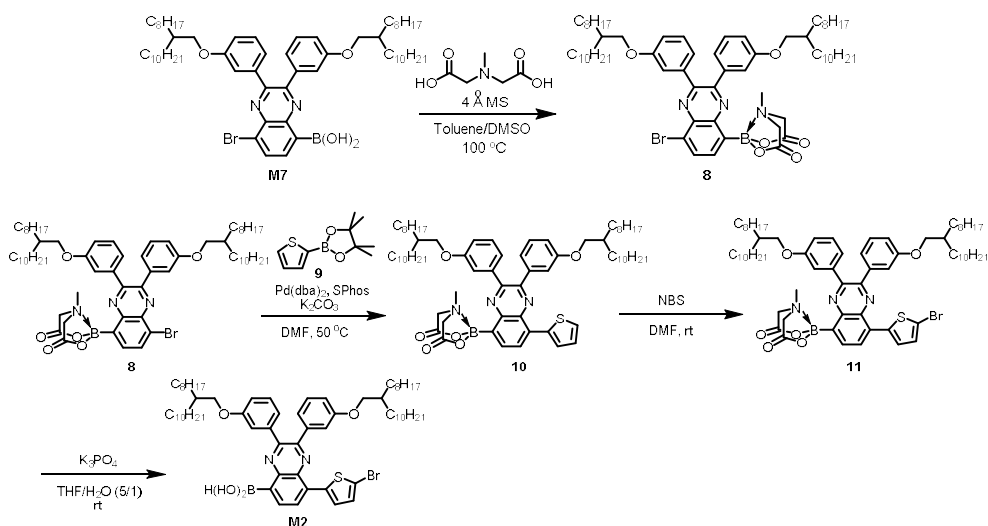
Compound 5: To a round-bottom flask equipped with a magnetic stir bar, compound **4** (861 mg, 1.24 mmol) was added and the flask was evacuated and backfilled with argon three times. The compound was dissolved in DMF (3 mL). Then, *N*-Bromosuccinimide (234 mg, 1.30 mmol) in DMF (2 mL) was added. After stirring at rt for 2 h, the crude mixture was diluted with diethyl ether, washed with water three times, dried over anhydrous MgSO₄, and concentrated under reduced pressure to afford (MIDA)B–BTzEDOT–Br (compound **5**) as pale yellow solid (936 mg, 1.21 mmol, 98 %). ¹H NMR (500 MHz, CDCl₃) δ (ppm) = 8.06 (d, *J* = 7.3 Hz, 1H), 7.77 (d, *J* = 7.3 Hz, 1H), 4.64 (d, *J* = 6.4 Hz, 2H), 4.38 (dd, *J* = 12.8, 5.0 Hz, 4H), 4.21 (d, *J* = 16.2 Hz, 2H), 4.07 (d, *J* = 16.2 Hz, 2H), 2.61 (s, 3H), 2.19 (m, 1H), 1.38–1.17 (m, 32H), 0.86 (td, *J* = 7.0, 3.6 Hz, 6H). ¹³C NMR (125 MHz, CDCl₃) δ (ppm) = 167.54, 146.51, 140.61, 139.93, 139.29, 132.54, 124.17, 122.87, 114.04, 90.28, 64.88, 64.84, 63.04, 59.86, 46.90, 39.12, 31.90, 31.87, 31.51, 29.92, 29.81, 29.65, 29.62, 29.57, 29.33, 29.30, 26.33, 22.67, 22.65, 14.11. HRMS (ESI): *m/z* for C₃₇H₅₄BBrNaN₄O₆S [M+Na]⁺, calcd: 795.2938, found: 795.2939.

Compound 6: To a round-bottom flask equipped with a magnetic stir bar, compound **5** (936 mg, 1.21 mmol) was added. The compound was dissolved in THF (6 mL). Then, potassium phosphate tribasic (3.93 g, 18.2 mmol) in water (1.2 mL) was added. After stirring at rt for 15 h, the crude mixture was diluted with diethyl ether, washed with saturated NH₄Cl(aq) two times, dried over anhydrous MgSO₄, and concentrated under reduced pressure. The product was purified by trituration in EA to afford (HO)₂B–BTzEDOT–Br (compound **6**) as yellow solid (580 mg, 0.93 mmol, 77 %). ¹H NMR (500 MHz, CDCl₃) δ (ppm) = 8.13 (d, *J* = 7.3 Hz, 1H), 7.92 (d, *J* = 7.3 Hz, 1H),

5.91 (broad, 2H), 4.69 (d, $J = 6.6$ Hz, 2H), 4.42 (dd, $J = 5.7, 2.0$ Hz, 2H), 4.38 (dd, $J = 5.6, 1.9$ Hz, 2H), 2.26 (m, 1H), 1.46–1.18 (m, 32H), 0.87 (td, $J = 7.0, 3.6$ Hz, 6H). ^{13}C NMR (125 MHz, CDCl_3) δ (ppm) = 148.21, 140.06, 139.96, 139.67, 134.52, 125.62, 122.82, 114.08, 90.96, 64.91, 64.81, 59.88, 39.13, 31.91, 31.88, 31.41, 29.88, 29.64, 29.63, 29.62, 29.56, 29.34, 29.30, 26.25, 22.68, 22.66, 14.13. HRMS (ESI): m/z for $\text{C}_{32}\text{H}_{49}\text{BBrNaN}_3\text{O}_4\text{S}$ $[\text{M}+\text{Na}]^+$, calcd: 684.2618, found: 684.2620.

M1: To a round-bottom flask equipped with a magnetic stir bar, compound **6** (63 mg, 0.10 mmol) and MgSO_4 (500 mg) were added. Then, compound **7** (25.4 mg, 0.10 mmol) in diethyl ether (1.0 mL) was added. After stirring at rt for 15 h, the crude mixture was filtrated, washed with diethyl ether, and concentrated under reduced pressure. **M1** was obtained as yellow solid (86 mg, 0.098 mmol, 98 %) and used without further purification. ^1H NMR (500 MHz, CDCl_3) δ (ppm) = 8.06 (d, $J = 7.3$ Hz, 1H), 7.92 (d, $J = 7.3$ Hz, 1H), 7.41 – 7.37 (m, 3H), 7.26 (m, 2H), 4.68 (d, $J = 6.4$ Hz, 2H), 4.39 (dd, $J = 11.5, 5.2$ Hz, 4H), 4.21 (s, 2H), 3.54 (d, $J = 12.2$ Hz, 2H), 3.02 (d, $J = 12.2$ Hz, 2H), 2.26 (m, 1H), 1.62 (s, 6H), 1.56 (s, 6H), 1.39 – 1.11 (m, 32H), 0.92 – 0.85 (td, $J = 7.0, 3.6$ Hz, 6H). ^{13}C NMR (125 MHz, CDCl_3) δ (ppm) = 148.36, 141.20, 139.82, 138.23, 133.34, 133.24, 131.15, 129.03, 128.89, 123.17, 121.63, 115.33, 88.75, 75.39, 67.88, 64.94, 64.79, 62.90, 59.79, 39.22, 31.92, 31.87, 31.71, 31.57, 29.97, 29.86, 29.63, 29.58, 29.35, 29.28, 26.60, 22.70, 22.67, 14.14. HRMS (ESI): m/z for $\text{C}_{47}\text{H}_{70}\text{BBrNaN}_4\text{O}_4\text{S}$ $[\text{M}+\text{Na}]^+$, calcd: 899.4292, found: 899.4293.

(b) Preparation and Characterization of M2



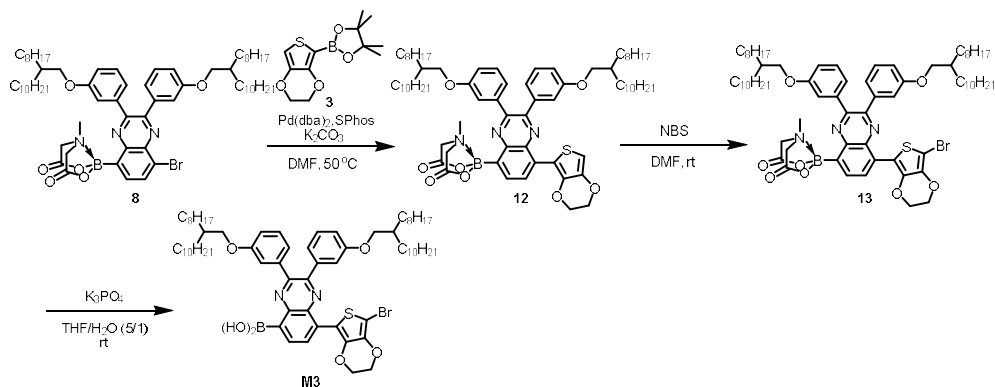
Compound 8: To a round-bottom flask equipped with a magnetic stir bar, **M7** (1.49 g, 1.5 mmol) and *N*-methyliminodiacetic acid (269 mg, 1.8 mmol) were added. The reagents were dissolved in toluene (6 mL) and DMSO (1.2 mL). After stirring at 100 ° C for 7 h, the crude mixture was diluted with diethyl ether, washed with water three times, dried over anhydrous MgSO₄, and concentrated under reduced pressure. The product was purified by flash column chromatography on silica gel (EA:Hexane = 1:1) to afford (MIDA)B-QX-Br (compound **8**) as white solid (1.52 g, 1.37 mmol, 91 %). ¹H NMR (500 MHz, CDCl₃) δ (ppm) = 8.14 (m, 2H), 7.34–7.30 (m, 1H), 7.25–7.21 (m, 2H), 7.11 (d, *J* = 6.6 Hz, 2H), 6.97–6.88 (m, 3H), 4.82–4.21 (broad, 2H), 3.96 (d, *J* = 15.0 Hz, 2H), 3.70 (d, *J* = 4.2 Hz, 2H), 3.62 (d, *J* = 4.2 Hz, 2H), 2.70 (s, 3H), 1.71 (m, 2H), 1.40–1.18 (m, 64H), 0.90 (t, *J* = 6.7 Hz, 12H). ¹³C NMR (125 MHz, CDCl₃) δ (ppm) = 167.69, 159.46, 159.19, 153.27, 153.15, 143.91, 139.48, 139.06, 138.90, 137.14, 133.43, 129.82, 129.26, 126.73, 122.34, 121.58, 117.03, 116.59, 115.63, 114.48, 71.17, 70.96, 64.50, 47.53, 37.81, 31.95, 31.28, 31.26, 30.11, 30.09, 29.77, 29.75, 29.71, 29.67, 29.40, 26.81, 22.71, 14.14. HRMS (ESI): *m/z* for C₆₅H₉₉BBBrNaN₃O₆ [M+Na]⁺, calcd: 1130.6708, found: 1130.6714.

Compound 10: To a round-bottom flask equipped with a magnetic stir bar, compound **8** (1.52 g, 1.37 mmol), compound **9** (379 mg, 1.78 mmol), bis(dibenzylideneacetone)palladium(0) (39.1 mg, 0.068 mmol), SPhos (41.8 mg, 0.102 mmol), and potassium carbonate (567 mg, 4.1 mmol) were added. The flask was evacuated and backfilled with argon three times. The reagents were dissolved in DMF (5.5 mL). After stirring at 50 ° C for 12 h, the crude mixture was diluted with diethyl ether, washed with water three times, dried over anhydrous MgSO₄, and concentrated under reduced pressure. The product was purified by flash column chromatography on silica gel (EA:Hexane = 1:1) to afford (MIDA)B-QXTh (compound **10**) as yellow solid (1.33 g, 1.20 mmol, 87 %). ¹H NMR (500 MHz, CDCl₃) δ (ppm) = 8.32 (d, *J* = 7.5 Hz, 1H), 8.19 (d, *J* = 7.5 Hz, 1H), 7.93 (d, *J* = 3.6 Hz, 1H), 7.54 (d, *J* = 5.1 Hz, 1H), 7.35–7.30 (m, 1H), 7.27–7.19 (m, 4H), 7.13 (d, *J* = 7.5 Hz, 1H), 6.98–6.89 (m, 3H), 4.30 (broad, 2H), 3.94 (d, *J* = 15.6 Hz, 2H), 3.74 (d, *J* = 5.6 Hz, 2H), 3.68 (d, *J* = 5.6 Hz, 2H), 2.73 (s, 3H), 1.73 (m, 2H), 1.44–1.26 (m, 64H), 0.90 (t, *J* = 6.4 Hz, 12H). ¹³C NMR (125 MHz, CDCl₃) δ (ppm) = 167.79, 159.50, 159.19, 152.23, 151.68, 143.49, 140.01, 139.36, 138.45, 137.43, 137.02, 134.54, 129.75, 129.23, 129.07, 127.10, 127.03, 126.66, 122.60, 121.64, 116.80, 116.68, 115.56, 114.53, 71.22, 71.02, 64.53, 47.48, 37.86, 31.94, 31.34, 31.28, 30.11, 29.75, 29.70, 29.66, 29.40, 26.81, 22.70, 14.13. HRMS (ESI): *m/z* for C₆₉H₁₀₂BNaNa₃O₆S [M+Na]⁺, calcd: 1134.7480, found: 1134.7482.

Compound 11: To a round-bottom flask equipped with a magnetic stir bar, compound **10** (1.33 g, 1.20 mmol) was added and the flask was evacuated and backfilled with argon three times. The compound was dissolved in DMF (3 mL). Then, *N*-Bromosuccinimide (225 mg, 1.26 mmol) in DMF (2 mL) was added. After stirring at rt for 12 h, the crude mixture was diluted with diethyl ether, washed with water three times, dried over anhydrous MgSO₄, and concentrated under reduced pressure to afford (MIDA)B-QXTh-Br (compound **5**) as pale yellow solid (1.36 g, 1.14 mmol, 95 %). ¹H NMR (500 MHz, CDCl₃) δ (ppm) = 8.08 (d, *J* = 8.1 Hz, 1H), 7.98 (m, 2H), 7.52 (d, *J* = 7.6 Hz, 1H), 7.42–7.35 (m, 2H), 7.28–7.24 (m, 3H), 7.00–6.93 (m, 3H), 3.95 (d, *J* = 16.4 Hz, 2H), 3.85 (d, *J* = 16.3 Hz, 2H), 3.72 (d, *J* = 5.7 Hz, 2H), 3.59 (d, *J* = 5.8 Hz, 2H), 2.75 (s, 3H), 1.79–1.66 (m, 2H), 1.43–1.24 (m, 64H), 0.92–0.87 (m, 12H). ¹³C NMR (125 MHz, CDCl₃) δ (ppm) = 166.52, 159.35, 158.91, 153.21, 152.67, 143.32, 139.38, 139.27, 138.69, 133.53, 133.07, 129.58, 129.30, 128.88, 127.59, 122.97, 122.56, 122.43, 116.74, 116.49, 115.98, 115.78, 71.07, 61.44, 47.26, 37.83, 37.70, 31.95, 31.31, 31.23, 30.10, 29.75, 29.70, 29.66, 29.40, 26.84, 26.76, 22.71, 14.14. HRMS (ESI): *m/z* for C₆₉H₁₀₁BBBrNaN₃O₆S [M+Na]⁺, calcd: 1212.6585, found: 1212.6588.

M2: To a round-bottom flask equipped with a magnetic stir bar, compound **11** (1.36 g, 1.14 mmol) was added. The compound was dissolved in THF (5.5 mL). Then, potassium phosphate tribasic (3.63 g, 17.1 mmol) in water (1.1 mL) was added. After stirring at rt for 20 h, the crude mixture was diluted with diethyl ether, washed with saturated NH₄Cl(aq) two times, dried over anhydrous MgSO₄, and concentrated under reduced pressure. The product was purified by flash column chromatography on silica gel (EA:Hexane = 1:6) to afford **M2** as pale yellow solid (864 mg, 0.80 mmol, 70 %). ¹H NMR (500 MHz, CDCl₃) δ (ppm) = 8.38 (d, *J* = 7.4 Hz, 1H), 8.16 (d, *J* = 7.4 Hz, 1H), 7.85 (broad s, 2H), 7.62 (d, *J* = 3.6 Hz, 1H), 7.40 (s, 1H), 7.29 (t, *J* = 7.9 Hz, 1H), 7.24–6.94 (m, 7H), 3.83 (d, *J* = 5.2 Hz, 2H), 3.71 (d, *J* = 5.2 Hz, 2H), 1.75 (m, 2H), 1.47–1.21 (m, 64H), 0.86 (m, 12H). ¹³C NMR (125 MHz, CDCl₃) δ (ppm) = 159.47, 159.41, 152.03, 151.77, 144.65, 139.38, 139.17, 138.90, 138.21, 136.60, 134.47, 129.62, 129.10, 129.00, 126.39, 125.65, 122.77, 121.76, 118.18, 117.03, 116.57, 115.31, 115.10, 71.08, 71.00, 37.98, 37.79, 31.93, 31.37, 31.26, 30.11, 30.08, 29.74, 29.69, 29.66, 29.38, 26.93, 26.81, 22.70, 14.13. HRMS (ESI): *m/z* for C₆₄H₉₇BBBrN₂O₄S [M+H]⁺, calcd: 1079.6445, found: 1079.6457.

(c) Preparation and Characterization of M3



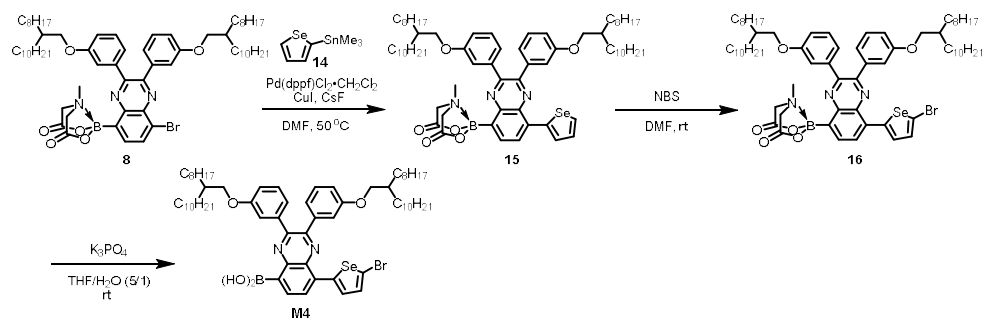
Compound 12: To a round-bottom flask equipped with a magnetic stir bar, compound **8** (1.11 g, 1.0 mmol), compound **3** (403 mg, 1.5 mmol), bis(dibenzylideneacetone)palladium(0) (29 mg, 0.05 mmol), SPhos (32.9 mg, 0.08 mmol), and potassium carbonate (415 mg, 3.0 mmol) were added. The flask was evacuated and backfilled with argon three times. The reagents were dissolved in DMF (5 mL). After stirring at 50 °C for 10 h, the crude mixture was diluted with diethyl ether, washed with water three times, dried over anhydrous MgSO₄, and concentrated under reduced pressure. The product was purified by flash column chromatography on silica gel (EA:Hexane = 1:1) to afford (MIDA)B-QXEDOT (compound **12**) as orange solid (784 mg, 0.67 mmol, 67 %). ¹H NMR (500 MHz, CDCl₃) δ (ppm) = 8.63 (d, *J* = 7.7 Hz, 1H), 8.31 (d, *J* = 7.7 Hz, 1H), 7.34–7.29 (m, 2H), 7.22 (d, *J* = 5.1 Hz, 2H), 7.13 (d, *J* = 7.5 Hz, 1H), 6.96 – 6.88 (m, 3H), 6.58 (s, 1H), 4.48–4.31 (m, 4H), 3.93 (d, *J* = 15.2 Hz, 2H), 3.74 (d, *J* = 5.6 Hz, 2H), 3.67 (d, *J* = 5.6 Hz, 2H), 2.71 (s, 3H), 1.78–1.68 (m, 2H), 1.43 – 1.18 (m, 64H), 0.90 (t, *J* = 6.5 Hz, 12H). ¹³C NMR (125 MHz, CDCl₃) δ (ppm) = 167.87, 159.46, 159.16, 151.89, 151.00, 143.25, 141.48, 140.87, 140.08, 139.26, 137.47, 137.21, 133.04, 129.72, 129.01, 128.85, 127.93, 122.71, 121.67, 116.73, 116.57, 115.69, 114.54, 112.78, 103.79, 71.18, 70.99, 65.05, 64.33, 47.45, 37.86, 37.83, 31.95, 31.33, 31.27, 30.12, 29.77, 29.72, 29.67, 29.41, 26.82, 22.71, 14.14. HRMS (ESI): *m/z* for C₇₁H₁₀₄BNa₃O₈S [M+Na]⁺, calcd: 1192.7535, found: 1192.7536.

Compound 13: To a round-bottom flask equipped with a magnetic stir bar, compound **12** (784 mg, 0.67 mmol) was added and the flask was evacuated and backfilled with argon three times. The compound was dissolved in DMF (1.5 mL). Then, *N*-Bromosuccinimide (126 mg, 0.70 mmol) in DMF (1.5 mL) was added. After stirring at rt for 1 h, the crude mixture was diluted with diethyl ether, washed with water three times, dried over anhydrous MgSO₄, and concentrated under reduced pressure to afford (MIDA)B–

QXEDOT-Br (compound **13**) as orange solid (811 mg, 0.65 mmol, 97 %). ^1H NMR (500 MHz, CDCl_3) δ (ppm) = 8.66 (d, J = 7.7 Hz, 1H), 8.30 (d, J = 7.7 Hz, 1H), 7.40 (s, 1H), 7.31 (t, J = 6.3 Hz, 1H), 7.20 (t, J = 7.9 Hz, 1H), 7.08 (dd, J = 16.1, 7.4 Hz, 2H), 6.95 (m, 3H), 4.45 (dd, J = 21.8, 3.9 Hz, 4H), 3.91 (d, J = 15.5 Hz, 2H), 3.79 (d, J = 5.4 Hz, 2H), 3.75 (d, J = 5.4 Hz, 2H), 2.71 (s, 3H), 1.74 (m, 2H), 1.46–1.24 (m, 64H), 0.89 (t, J = 5.8 Hz, 12H). ^{13}C NMR (125 MHz, CDCl_3) δ (ppm) = 167.71, 159.40, 152.18, 151.06, 143.18, 140.31, 139.91, 139.59, 138.89, 137.25, 137.00, 132.43, 129.66, 128.93, 127.45, 122.81, 121.66, 116.87, 116.75, 115.26, 114.47, 112.97, 93.33, 71.17, 70.92, 64.97, 64.71, 47.41, 38.01, 37.80, 31.92, 31.35, 31.25, 30.09, 29.74, 29.70, 29.68, 29.65, 29.39, 26.93, 26.78, 22.68, 14.11. HRMS (ESI): m/z for $\text{C}_{71}\text{H}_{103}\text{BBBrNaN}_3\text{O}_8\text{S}$ $[\text{M}+\text{Na}]^+$, calcd: 1270.6640, found: 1270.6639.

M3: To a round-bottom flask equipped with a magnetic stir bar, compound **13** (811 mg, 0.65 mmol) was added. The compound was dissolved in THF (3.5 mL). Then, potassium phosphate tribasic (2.08 g, 9.8 mmol) in water (0.7 mL) was added. After stirring at rt for 20 h, the crude mixture was diluted with diethyl ether, washed with saturated NH_4Cl (aq) two times, dried over anhydrous MgSO_4 , and concentrated under reduced pressure. The product was purified by flash column chromatography on silica gel (EA:Hexane = 1:6) to afford **M3** as orange solid (558 mg, 0.49 mmol, 75 %). ^1H NMR (500 MHz, CDCl_3) δ (ppm) = 8.70 (d, J = 7.3 Hz, 1H), 8.37 (d, J = 7.6 Hz, 1H), 7.43 (broad s, 2H), 7.28 (t, J = 7.9 Hz, 2H), 7.19 (t, J = 7.9 Hz, 1H), 7.12 (d, J = 6.9 Hz, 1H), 7.05 (m, 2H), 6.95 (d, J = 7.1 Hz, 2H), 4.42 (dd, J = 22.0, 3.9 Hz, 4H), 3.84 (d, J = 5.4 Hz, 2H), 3.69 (d, J = 5.4 Hz, 2H), 1.74 (m, 2H), 1.48–1.22 (m, 64H), 0.87 (t, J = 5.8 Hz, 12H). ^{13}C NMR (125 MHz, CDCl_3) δ (ppm) = 159.51, 159.42, 151.32, 151.22, 144.41, 140.76, 139.60, 139.51, 138.87, 138.49, 136.76, 133.40, 130.90, 129.60, 128.93, 127.31, 122.90, 121.82, 116.95, 116.51, 115.42, 115.17, 112.98, 100.24, 94.15, 68.53, 64.98, 64.67, 51.22, 38.04, 37.82, 31.94, 31.41, 31.29, 30.12, 30.09, 29.75, 29.72, 29.69, 29.65, 29.39, 26.97, 26.82, 22.71, 14.13. HRMS (ESI): m/z for $\text{C}_{66}\text{H}_{98}\text{BBBrNaN}_2\text{O}_6\text{S}$ $[\text{M}+\text{Na}]^+$, calcd: 1159.6320, found: 1159.6322.

(d) Preparation and Characterization of M4



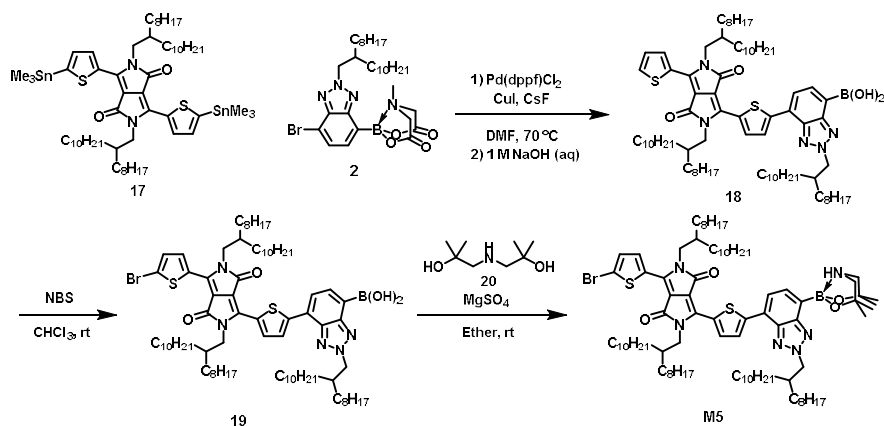
Compound 15: To a round-bottom flask equipped with a magnetic stir bar, compound **8** (890 mg, 0.80 mmol), compound **14** (282 mg, 0.96 mmol), [1,1-bis(diphenylphosphino)ferrocene]dichloropalladium(II) dichloromethane adduct (39.1 mg, 0.04 mmol), copper(I) iodide (15.2 mg, 0.08 mmol) and cesium fluoride (243 mg, 1.6 mmol) were added. The flask was evacuated and backfilled with argon three times. The reagents were dissolved in DMF (4 mL). After stirring at 50 °C for 5 h, the crude mixture was diluted with diethyl ether, washed with water three times, dried over anhydrous MgSO₄, and concentrated under reduced pressure. The product was purified by flash column chromatography on silica gel (EA:Hexane = 1:1) to afford (MIDA)B-QXSe (compound **15**) as yellow solid (733 mg, 0.63 mmol, 79 %). ¹H NMR (500 MHz, CDCl₃) δ (ppm) = 8.28 (d, J = 7.6 Hz, 1H), 8.26 (d, J = 7.6 Hz, 1H), 8.23 (d, J = 5.7 Hz, 1H), 8.09 (d, J = 3.9 Hz, 1H), 7.45 (dd, J = 5.6, 4.1 Hz, 1H), 7.30 (t, J = 7.9 Hz, 1H), 7.25–7.17 (m, 3H), 7.12 (d, J = 7.6 Hz, 1H), 6.95–6.87 (m, 3H), 4.19 (br s, 2H), 3.94 (d, J = 15.6 Hz, 2H), 3.71–3.63 (m, 4H), 2.69 (s, 3H), 1.71 (m, 2H), 1.41–1.24 (m, 64H), 0.88 (t, J = 6.6 Hz, 12H). ¹³C NMR (125 MHz, CDCl₃) δ (ppm) = 167.86, 159.36, 159.14, 152.47, 151.80, 143.63, 141.37, 139.78, 139.16, 136.97, 136.73, 136.57, 135.84, 129.72, 129.02, 128.86, 127.76, 125.16, 122.78, 121.63, 116.79, 116.58, 115.80, 114.63, 71.16, 71.04, 64.46, 47.48, 37.84, 37.80, 31.92, 31.32, 31.26, 30.08, 29.74, 29.73, 29.68, 29.67, 29.64, 29.38, 29.37, 26.80, 26.78, 22.68, 14.10. HRMS (ESI): m/z for C₆₉H₁₀₂BNa₃O₆Se [M+Na]⁺, calcd: 1182.6925, found: 1182.6937.

Compound 16: To a round-bottom flask equipped with a magnetic stir bar, compound **15** (733 mg, 0.63 mmol) was added and the flask was evacuated and backfilled with argon three times. The compound was dissolved in DMF (2 mL). Then, *N*-Bromosuccinimide (119 mg, 0.66 mmol) in DMF (1.5 mL) was added. After stirring at rt for 4 h, the crude mixture was diluted with diethyl ether, washed with water three times, dried over anhydrous MgSO₄, and concentrated under reduced pressure to afford (MIDA)B-QXSe-Br

(compound **16**) as pale yellow solid (743 mg, 0.60 mmol, 95 %). ^1H NMR (500 MHz, CDCl_3) δ (ppm) = 8.33 (d, J = 7.6 Hz, 1H), 8.25 (d, J = 7.7 Hz, 1H), 7.83 (d, J = 4.4 Hz, 1H), 7.40 (d, J = 4.4 Hz, 1H), 7.31 (t, J = 7.9 Hz, 1H), 7.27–7.21 (m, 2H), 7.10 (d, J = 7.6 Hz, 2H), 6.98–6.88 (m, 3H), 4.45 (broad, 2H), 3.94 (d, J = 15.7 Hz, 2H), 3.75 (d, J = 5.2 Hz, 2H), 3.71 (d, J = 5.2 Hz, 2H), 2.73 (s, 3H), 1.81–1.67 (m, 2H), 1.42–1.24 (m, 64H), 0.90 (t, J = 6.3 Hz, 12H). ^{13}C NMR (125 MHz, CDCl_3) δ (ppm) = 167.70, 159.42, 159.35, 153.00, 152.06, 143.67, 142.30, 139.57, 138.81, 137.07, 136.22, 135.22, 132.03, 129.74, 129.17, 126.66, 123.96, 123.75, 122.79, 121.70, 116.91, 115.56, 114.58, 71.18, 64.49, 47.48, 37.95, 37.81, 31.95, 31.34, 31.27, 30.11, 29.76, 29.71, 29.67, 29.41, 26.87, 26.81, 22.71, 14.14. HRMS (ESI): m/z for $\text{C}_{69}\text{H}_{101}\text{BBBrNaN}_3\text{O}_6\text{Se}$ $[\text{M}+\text{Na}]^+$, calcd: 1260.6030, found: 1260.6032.

M4: To a round-bottom flask equipped with a magnetic stir bar, compound **16** (743 mg, 0.60 mmol) was added. The compound was dissolved in THF (3 mL). Then, potassium phosphate tribasic (1.91 g, 9.0 mmol) in water (0.6 mL) was added. After stirring at rt for 18 h, the crude mixture was diluted with diethyl ether, washed with saturated $\text{NH}_4\text{Cl}(\text{aq})$ two times, dried over anhydrous MgSO_4 , and concentrated under reduced pressure. The product was purified by flash column chromatography on silica gel (EA:Hexane = 1:6) to afford **M4** as yellow solid (518 mg, 0.46 mmol, 76 %). ^1H NMR (500 MHz, CDCl_3) δ (ppm) = 8.39 (d, J = 7.0 Hz, 1H), 8.23 (d, J = 7.0 Hz, 1H), 8.05 (broad s, 2H), 7.79 (d, J = 5.7 Hz, 1H), 7.47 (d, J = 5.7 Hz, 1H), 7.31–6.90 (m, 8H), 3.80 (d, J = 5.3 Hz, 2H), 3.69 (d, J = 5.3 Hz, 2H), 1.75 (m, 2H), 1.51–1.19 (m, 64H), 0.87 (m, 12H). ^{13}C NMR (125 MHz, CDCl_3) δ (ppm) = 159.38, 159.36, 152.17, 152.06, 144.86, 142.13, 139.11, 138.68, 138.26, 135.93, 132.01, 129.61, 129.14, 127.09, 124.41, 123.91, 122.82, 121.81, 116.93, 116.68, 115.63, 115.14, 71.17, 71.09, 37.93, 37.80, 31.93, 31.35, 31.27, 30.11, 30.09, 29.75, 29.69, 29.65, 29.40, 29.39, 26.87, 26.82, 22.70, 14.13. HRMS (ESI): m/z for $\text{C}_{64}\text{H}_{96}\text{BBBrNaN}_2\text{O}_4\text{Se}$ $[\text{M}+\text{Na}]^+$, calcd: 1149.5709, found: 1149.5711.

(e) Preparation and Characterization of M5



Compound 18

1) To a round-bottom flask equipped with a magnetic stir bar, compound **17** (356 mg, 0.30 mmol), compound **2** (199 mg, 0.27 mmol), [1,1-bis(diphenylphosphino)ferrocene]dichloropalladium(II) dichloromethane adduct (12.1 mg, 0.014 mmol), copper(I) iodide (5.0 mg, 0.027 mmol) and cesium fluoride (82 mg, 0.54 mmol) were added. The flask was evacuated and backfilled with argon three times. The reagents were dissolved in DMF (3 mL). After stirring at 70 °C for 6 h, the crude mixture was diluted with diethyl ether, washed with water three times, dried over anhydrous MgSO₄, and concentrated under reduced pressure.

2) The mixture from 1) was used without purification to be dissolved in diethyl ether (3 mL), added 1 M NaOH (1 mL), and stirred at rt for 2 h. The crude mixture was diluted with diethyl ether, washed with water, dried over anhydrous MgSO₄, and concentrated under vacuum. Purification via flash column chromatography on silica gel (EA:Hexane = 1:6) was conducted to afford a purple solid (137 mg, max 0.105 mmol, 39 %) including compound **18** as a major component. However, because of some inseparable impurity, the mixture obtained after column chromatography was used for the next step without further purification.

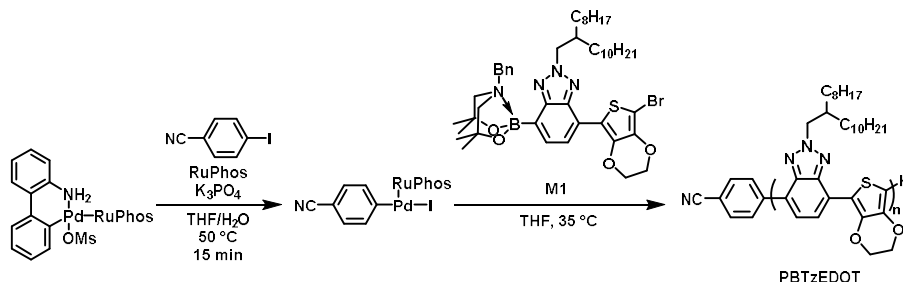
Compound 19: To a round-bottom flask equipped with a magnetic stir bar, mixture of **18** (137 mg, max 0.105 mmol) was added and the flask was evacuated and backfilled with argon three times. The compound was dissolved in CHCl₃ (1 mL). Then, *N*-Bromosuccinimide (22.7 mg, 0.126 mmol) in CHCl₃ (1 mL) was added slowly at 0 °C. After stirring at 0 °C for 6 h, the crude mixture was diluted with diethyl ether, washed with water, dried over anhydrous MgSO₄, and concentrated under reduced pressure.

The product was purified by flash column chromatography on silica gel (EA:Hexane = 1:6) to afford compound **19** as purple solid (108 mg, 0.078 mmol, 75 %). ^1H NMR (500 MHz, CDCl_3) δ (ppm) = 9.06 (d, J = 4.1 Hz, 1H), 8.65 (d, J = 4.1 Hz, 1H), 8.29 (d, J = 4.2 Hz, 1H), 7.96 (d, J = 7.1 Hz, 1H), 7.78 (d, J = 7.1 Hz, 1H), 7.22 (d, J = 4.1 Hz, 1H), 6.04 (s, 2H), 4.71 (d, J = 6.6 Hz, 2H), 4.11 (d, J = 7.6 Hz, 2H), 3.96 (d, J = 7.6 Hz, 2H), 2.31 (m, 1H), 2.02 (m, 1H), 1.91 (m, 1H), 1.41–1.16 (m, 96H), 0.90–0.81 (m, 18H). ^{13}C NMR (126 MHz, CDCl_3) δ (ppm) = 161.72, 161.44, 148.69, 145.09, 140.57, 140.48, 139.05, 138.82, 136.94, 135.12, 134.27, 131.40, 131.34, 130.11, 128.98, 126.22, 122.99, 118.63, 108.44, 60.44, 46.46, 39.18, 37.92, 37.81, 31.92, 31.89, 31.45, 31.24, 30.11, 30.01, 29.84, 29.65, 29.63, 29.58, 29.52, 29.37, 29.34, 29.31, 29.28, 26.28, 26.23, 22.68, 22.66, 14.11. HRMS (ESI): m/z for $\text{C}_{80}\text{H}_{131}\text{BBBrNaN}_5\text{O}_4\text{S}_2$ $[\text{M}+\text{Na}]^+$, calcd: 1402.8817, found: 1402.8821.

M5: To a round-bottom flask equipped with a magnetic stir bar, compound **19** (108 mg, 0.078 mmol) and MgSO_4 (300 mg) were added. Then, compound **20** (18.8 mg, 0.117 mmol) in diethyl ether (1.5 mL) was added. After stirring at rt for 15 h, the crude mixture was filtrated, washed with diethyl ether, and concentrated under reduced pressure. The product was purified by flash column chromatography on silica gel (EA:Hexane = 1:1.5) to afford **M5** as blue solid (103 mg, 0.068 mmol, 87 %). ^1H NMR (500 MHz, CDCl_3) δ (ppm) = 9.12 (d, J = 4.1 Hz, 1H), 8.59 (d, J = 3.8 Hz, 1H), 8.17 (d, J = 4.1 Hz, 1H), 7.71 (s, 2H), 7.21 (d, J = 3.9 Hz, 1H), 6.89 (broad s, 1H), 4.65 (d, J = 6.5 Hz, 2H), 4.10 (d, J = 7.6 Hz, 2H), 3.96 (d, J = 7.5 Hz, 2H), 3.43 (dd, J = 11.6, 3.9 Hz, 2H), 2.98 (dd, J = 11.6, 3.9 Hz, 2H), 2.24 (m, 1H), 2.04 (m, 1H), 1.90 (m, 1H), 1.41–1.13 (m, 108H), 0.89–0.80 (m, 18H). ^{13}C NMR (126 MHz, CDCl_3) δ (ppm) = 161.91, 161.35, 147.41, 147.32, 141.49, 140.79, 137.82, 137.61, 134.58, 131.53, 131.29, 130.48, 128.35, 127.38, 124.45, 121.11, 117.97, 108.63, 107.65, 76.32, 65.86, 62.17, 59.99, 46.32, 39.33, 37.94, 37.80, 31.92, 31.89, 31.88, 31.50, 31.22, 30.10, 30.01, 29.94, 29.74, 29.67, 29.63, 29.55, 29.36, 29.35, 29.31, 26.48, 26.26, 22.69, 22.66, 14.12. HRMS (ESI): m/z for $\text{C}_{88}\text{H}_{146}\text{BBBrNaN}_6\text{O}_4\text{S}_2$ $[\text{M}+\text{Na}]^+$, calcd: 1528.0021, found: 1528.0025.

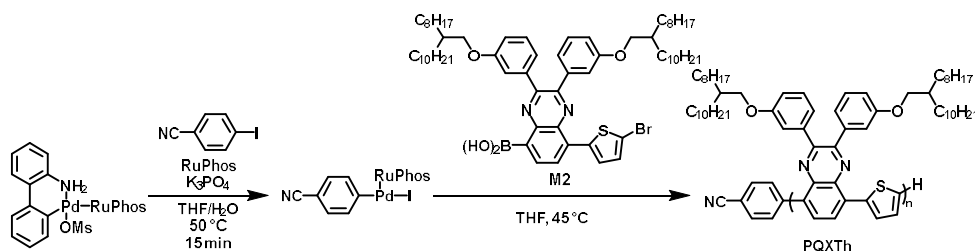
Experimental procedures for polymerization

(a) Synthesis of PBTzEDOT using M1 as a monomer



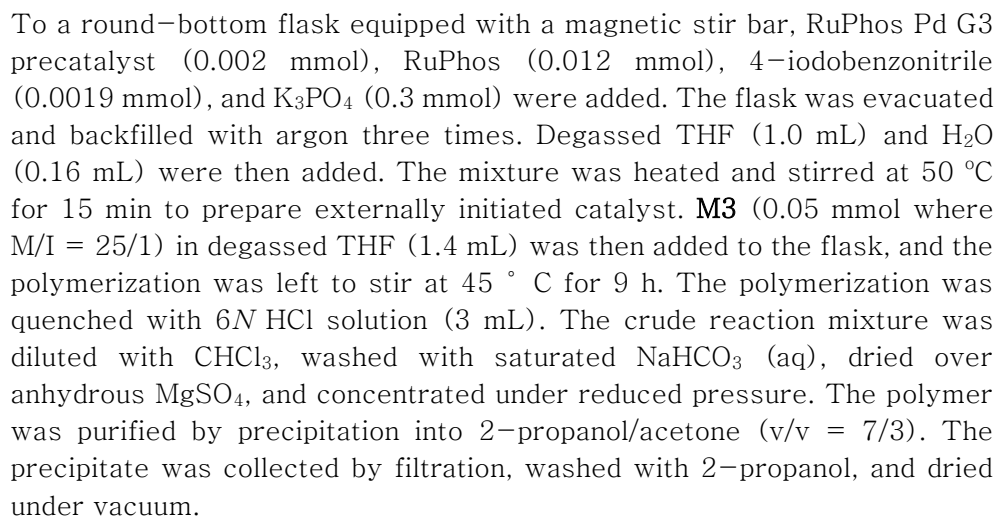
To a round-bottom flask equipped with a magnetic stir bar, RuPhos Pd G3 precatalyst (0.002 mmol), RuPhos (0.012 mmol), 4-iodobenzonitrile (0.0019 mmol), and K_3PO_4 (0.3 mmol) were added. The flask was evacuated and backfilled with argon three times. Degassed THF (2 mL) and H_2O (0.16 mL) were then added. The mixture was heated and stirred at 50 °C for 15 min to prepare externally initiated catalyst. **M1** (0.05 mmol where M/I = 25/1) in degassed THF (2.8 mL) was then added to the flask, and the polymerization was left to stir at 35 °C for 8 h. The polymerization was quenched with 6N HCl solution (3 mL). The crude reaction mixture was diluted with $CHCl_3$, washed with saturated $NaHCO_3$ (aq), dried over anhydrous $MgSO_4$, and concentrated under reduced pressure. The polymer was purified by precipitation into 2-propanol. The precipitate was collected by filtration, washed with 2-propanol, and dried under vacuum.

(b) Synthesis of PQXTh using M2 as a monomer

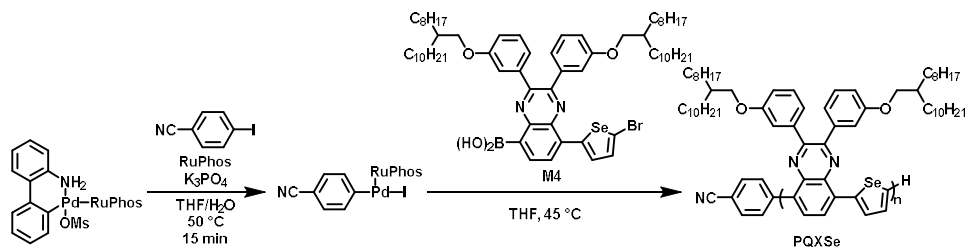


To a round-bottom flask equipped with a magnetic stir bar, RuPhos Pd G3 precatalyst (0.002 mmol), RuPhos (0.012 mmol), 4-iodobenzonitrile (0.0019 mmol), and K_3PO_4 (0.3 mmol) were added. The flask was evacuated and backfilled with argon three times. Degassed THF (0.8 mL) and H_2O (0.16 mL) were then added. The mixture was heated and stirred at 50 °C for 15 min to prepare externally initiated catalyst. **M2** (0.05 mmol where

(c) Synthesis of PQXEDOT using M3 as a monomer

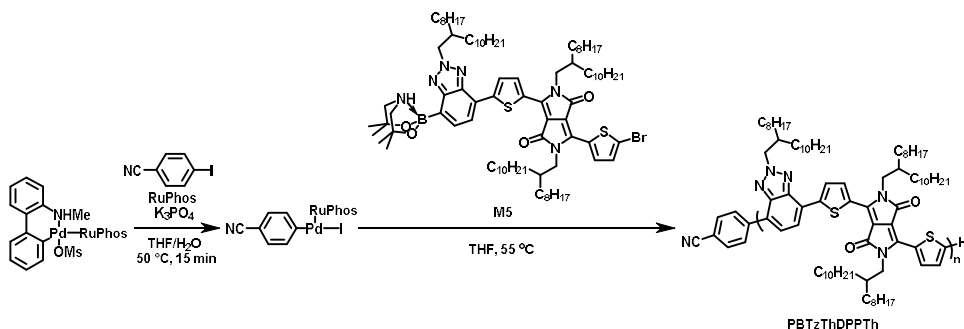


(d) Synthesis of PQXSe using M4 as a monomer



To a round-bottom flask equipped with a magnetic stir bar, RuPhos Pd G3 precatalyst (0.002 mmol), RuPhos (0.012 mmol), 4-iodobenzonitrile (0.0019 mmol), and K_3PO_4 (0.3 mmol) were added. The flask was evacuated and backfilled with argon three times. Degassed THF (1.0 mL) and H_2O (0.16 mL) were then added. The mixture was heated and stirred at 50 °C for 15 min to prepare externally initiated catalyst. **M4** (0.05 mmol where M/I = 25/1) in degassed THF (1.4 mL) was then added to the flask, and the polymerization was left to stir at 35 °C for 8 h. The polymerization was quenched with 6N HCl solution (3 mL). The crude reaction mixture was diluted with $CHCl_3$, washed with saturated $NaHCO_3$ (aq), dried over anhydrous $MgSO_4$, and concentrated under reduced pressure. The polymer was purified by precipitation into 2-propanol/acetone (v/v = 7/3). The precipitate was collected by filtration, washed with 2-propanol, and dried under vacuum.

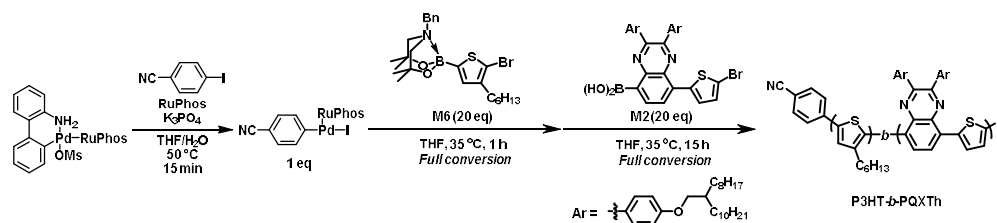
(e) Synthesis of PBTzThDPPTTh using M5 as a monomer



To a round-bottom flask equipped with a magnetic stir bar, RuPhos Pd G3 precatalyst (0.002 mmol), RuPhos (0.012 mmol), 4-iodobenzonitrile (0.0019 mmol), and K_3PO_4 (0.12 mmol) were added. The flask was evacuated and backfilled with argon three times. Degassed THF (1.0 mL) and H_2O (0.027 mL) were then added. The mixture was heated and stirred at 50 °C for 15 min to prepare externally initiated catalyst. **M5** (0.02 mmol

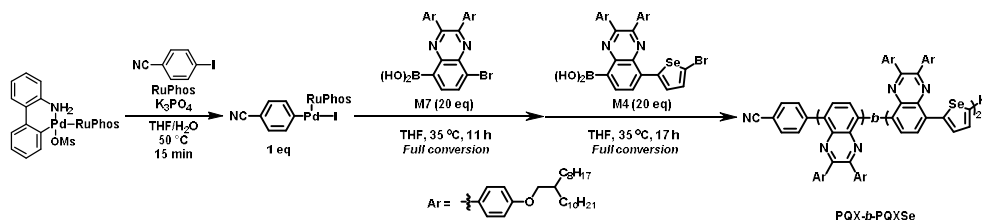
where M/I = 10/1) in degassed THF (1.0 mL) was then added to the flask, and the polymerization was left to stir at 55 ° C for 13 h. The polymerization was quenched with 6*N*HCl solution (1 mL). The crude reaction mixture was diluted with CHCl₃, washed with saturated NaHCO₃ (aq), dried over anhydrous MgSO₄, and concentrated under reduced pressure. The polymer was purified by precipitation into 2-propanol/acetone (v/v = 1/1). The precipitate was collected by filtration, washed with 2-propanol, and dried under vacuum.

(f) Synthesis of P3HT₂₀-*b*-PQXTh₂₀ by the sequential addition



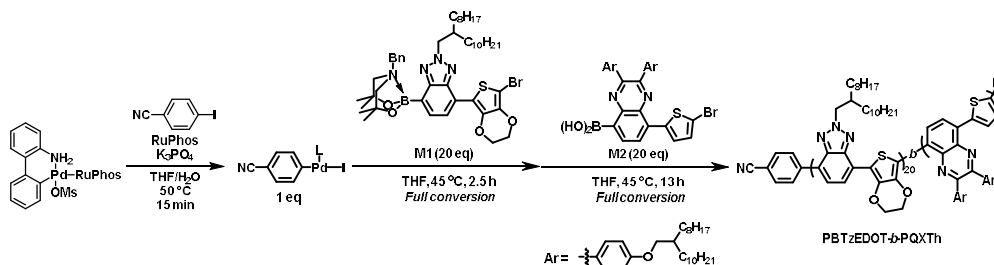
To a round-bottom flask equipped with a magnetic stir bar, RuPhos Pd G3 precatalyst (0.002 mmol), RuPhos (0.012 mmol), 4-iodobenzonitrile (0.0019 mmol), and K₃PO₄ (0.24 mmol) were added. The flask was evacuated and backfilled with argon three times. Degassed THF (1.5 mL) and H₂O (0.13 mL) were then added. The mixture was heated and stirred at 50 °C for 15 min to prepare externally initiated catalyst. **M6** (0.04 mmol) in degassed THF (2.4 mL) was then added to the flask, and the polymerization was left to stir at 35 ° C for 1 h. Subsequently, **M2** (0.04 mmol) in degassed THF (0.8 mL) was added to the flask, and the polymerization was left to stir at 35 ° C for 15 h. The polymerization was quenched with 6*N*HCl solution (3 mL). The crude reaction mixture was diluted with CHCl₃, washed with saturated NaHCO₃ (aq), dried over anhydrous MgSO₄, and concentrated under reduced pressure. The polymer was purified by precipitation into 2-propanol/acetone (v/v = 7/3). The precipitate was collected by filtration, washed with 2-propanol, and dried under vacuum.

(g) Synthesis of $\text{PQX}_{20}\text{-}b\text{-PQXSe}_{20}$ by the sequential addition



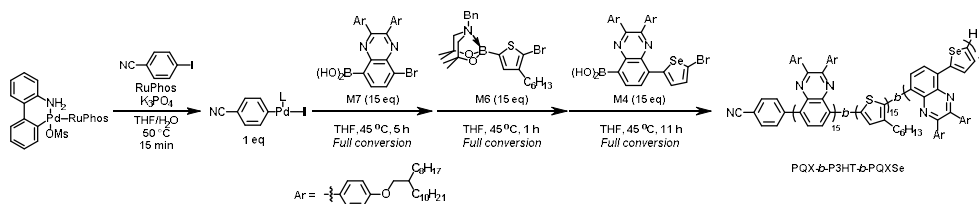
To a round-bottom flask equipped with a magnetic stir bar, RuPhos Pd G3 precatalyst (0.002 mmol), RuPhos (0.012 mmol), 4-iodobenzonitrile (0.0019 mmol), and K_3PO_4 (0.24 mmol) were added. The flask was evacuated and backfilled with argon three times. Degassed THF (1.0 mL) and H_2O (0.13 mL) were then added. The mixture was heated and stirred at 50 °C for 15 min to prepare externally initiated catalyst. **M7** (0.04 mmol) in degassed THF (1.0 mL) was then added to the flask, and the polymerization was left to stir at 35 °C for 11 h. Subsequently, **M4** (0.04 mmol) in degassed THF (0.8 mL) was added to the flask, and the polymerization was left to stir at 35 °C for 17 h. The polymerization was quenched with 6*N* HCl solution (3 mL). The crude reaction mixture was diluted with CHCl_3 , washed with saturated NaHCO_3 (aq), dried over anhydrous MgSO_4 , and concentrated under reduced pressure. The polymer was purified by precipitation into 2-propanol/acetone (v/v = 7/3). The precipitate was collected by filtration, washed with 2-propanol, and dried under vacuum.

(h) Synthesis of PBTzEDOT₂₀-*b*-PQXTh₂₀ by the sequential addition



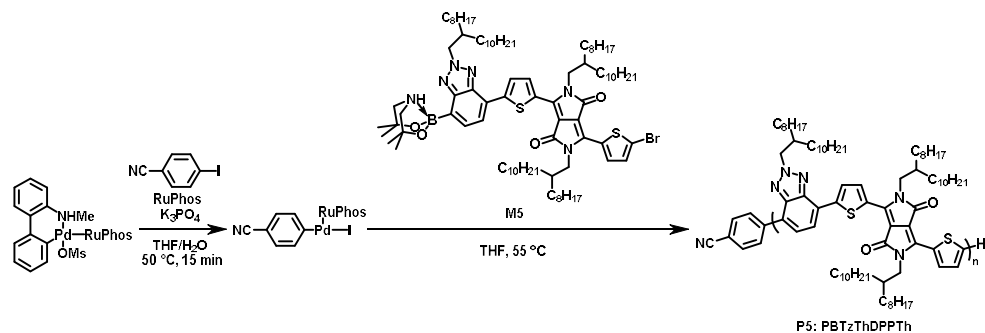
To a round-bottom flask equipped with a magnetic stir bar, RuPhos Pd G3 precatalyst (0.002 mmol), RuPhos (0.012 mmol), 4-iodobenzonitrile (0.0019 mmol), and K₃PO₄ (0.24 mmol) were added. The flask was evacuated and backfilled with argon three times. Degassed THF (1.5 mL) and H₂O (0.13 mL) were then added. The mixture was heated and stirred at 50 °C for 15 min to prepare externally initiated catalyst. **M1** (0.04 mmol) in degassed THF (2.4 mL) was then added to the flask, and the polymerization was left to stir at 45 °C for 2.5 h. Subsequently, **M2** (0.04 mmol) in degassed THF (0.8 mL) was added to the flask, and the polymerization was left to stir at 45 °C for 13 h. The polymerization was quenched with 6*N* HCl solution (3 mL). The crude reaction mixture was diluted with CHCl₃, washed with saturated NaHCO₃ (aq), dried over anhydrous MgSO₄, and concentrated under reduced pressure. The polymer was purified by precipitation into 2-propanol/acetone (v/v = 1/1). The precipitate was collected by filtration, washed with 2-propanol, and dried under vacuum.

(i) Synthesis of $\text{PQX}_{15}\text{-}b\text{-P3HT}_{15}\text{-}b\text{-PQXSe}_{15}$ by the sequential addition.



To a round-bottom flask equipped with a magnetic stir bar, RuPhos Pd G3 precatalyst (0.002 mmol), RuPhos (0.012 mmol), 4-iodobenzonitrile (0.0019 mmol), and K₃PO₄ (0.24 mmol) were added. The flask was evacuated and backfilled with argon three times. Degassed THF (1.0 mL) and H₂O (0.13 mL) were then added. The mixture was heated and stirred at 50 °C for 15 min to prepare externally initiated catalyst. **M7** (0.04 mmol) in degassed THF (0.9 mL) was then added to the flask, and the polymerization

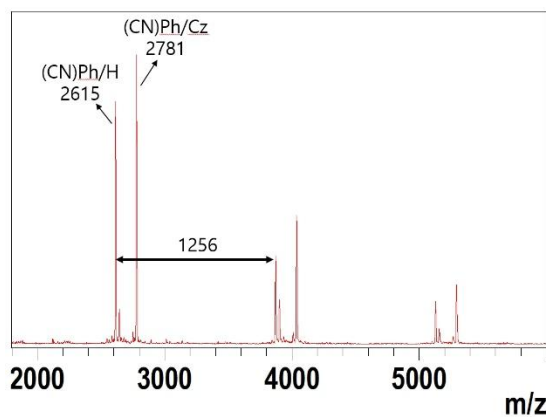
Table S2: SCTP of BTz–Th–DPP–Th Monomer Using RuPhos Pd G4 Precatalyst^[a]



Entry	M/I	Catalyst (equiv)	Ligand (equiv)	Time (h)	M_n (\mathcal{D}) ^[b]	Yield ^[c] (%)
1	5	RuPhos Pd G4 (0.20)	RuPhos (1.20)	13	10.4k (1.34)	86

[a] Reaction conditions: monomer (0.02 mmol, 1 equiv), RuPhos Pd G4, RuPhos, 4-iodobenzonitrile (0.95 equiv relative to the catalyst), K_3PO_4 (0.12 mmol, 6 equiv), THF/ H_2O (0.01M, v/v = 75/1). [b] Determined by THF GPC calibrated by PS standards. [c] Isolated yield.

(a) Table 3, entry 1



(b) Table 3, entry 4 ($M/I = 30$)

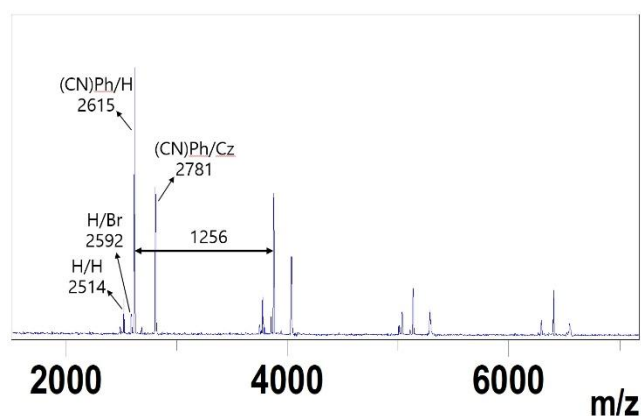
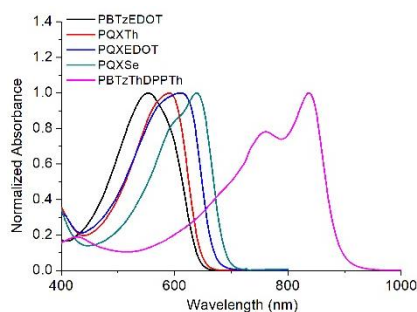


Figure S1: MALDI-TOF spectra of (a) PBTzThDPPTTh with undesired carbazole (Cz) capping, (b) PBTzThDPPTTh with minor peaks of H/H and H/Br end groups, indicating some competing chain transfer arose at $M/I = 30$.

UV-Vis-NIR absorption and emission spectra of polymers

(a) CHCl_3 solution



(b) Thin film

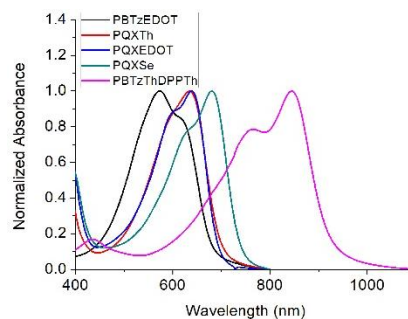


Figure S2: Absorption spectra of PBTzEDOT, PQXTh, PQXEDOT, PQXSe, and PBTzThDPPTTh in (a) CHCl_3 solution (0.02 g/mL), (b) thin film.

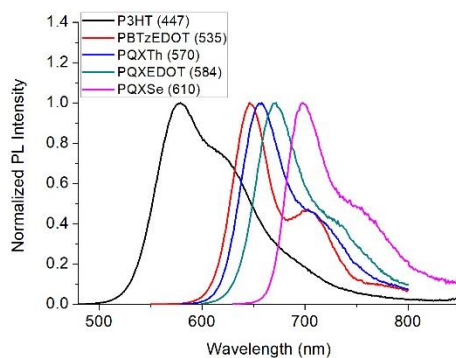
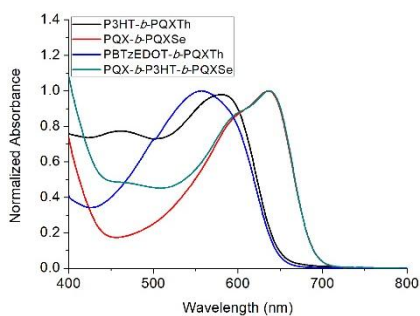


Figure S3: Emission spectra of P3HT at 447 nm excitation, PBTzEDOT at 535 nm excitation, PQXTh at 570 nm excitation, PQXEDOT at 584 nm excitation, and PQXSe at 610 nm excitation in CHCl_3 solution (0.02 g/mL). PBTzThDPPTh showed very weak PL signal.

(a) CHCl_3 solution



(b) Thin film

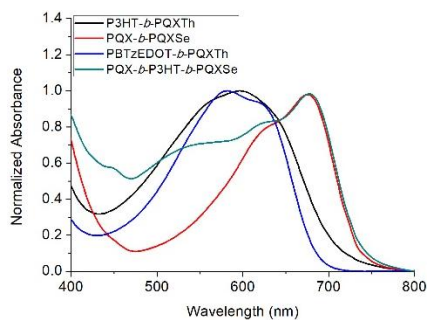
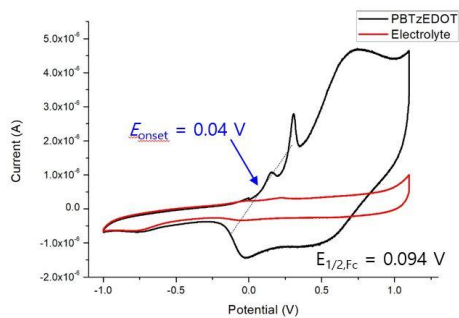


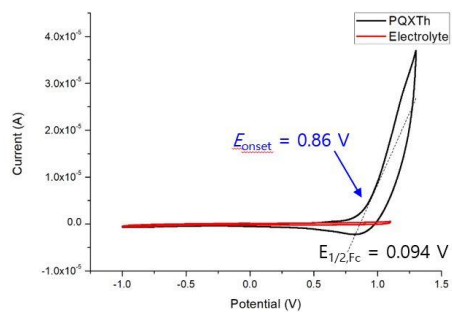
Figure S4: Absorption spectra of P3HT-*b*-PQXTh, PQX-*b*-PQXSe, PBTzEDOT-*b*-PQXTh, and PQX-*b*-P3HT-*b*-PQXSe in (a) CHCl_3 solution (0.02 g/mL) and (b) thin film.

Cyclic voltammograms of polymers

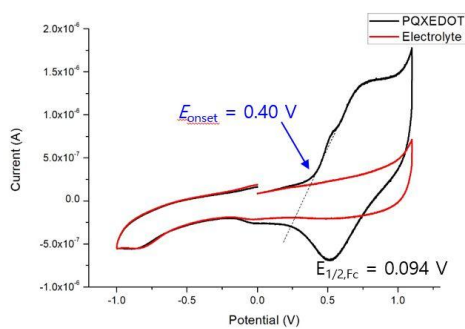
(a) PBTzEDOT



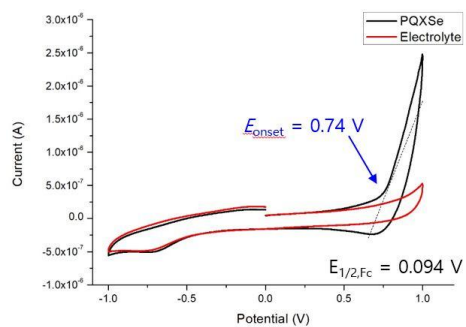
(b) PQXTh



(c) PQXEDOT



(d) PQXSe



(e) PBTzThDPPTTh

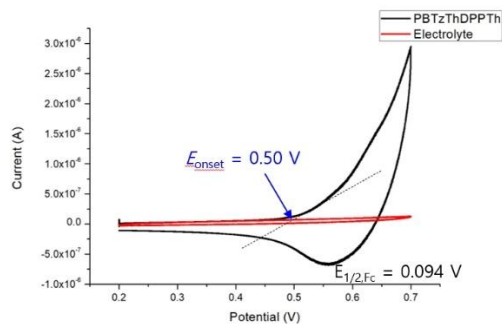
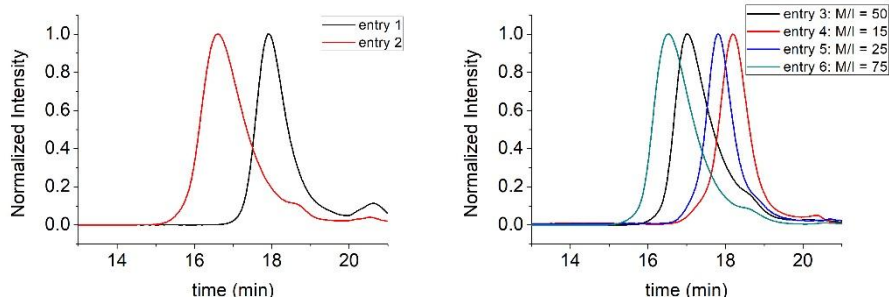


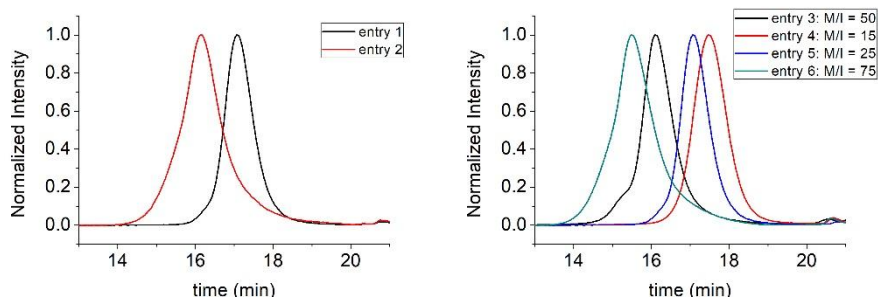
Figure S5: Cyclic voltammograms of (a) PBTzEDOT, (b) PQXTh, (c) PQXEDOT, (d) PQXSe, (e) PBTzThDPPTTh in thin films.

THF SEC traces of polymers

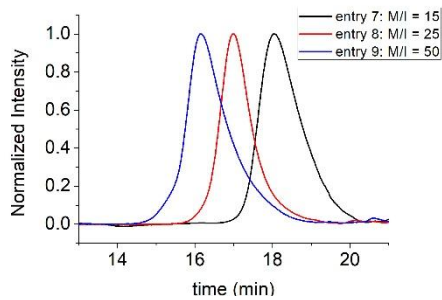
(a) Table 1: PBTzEDOT



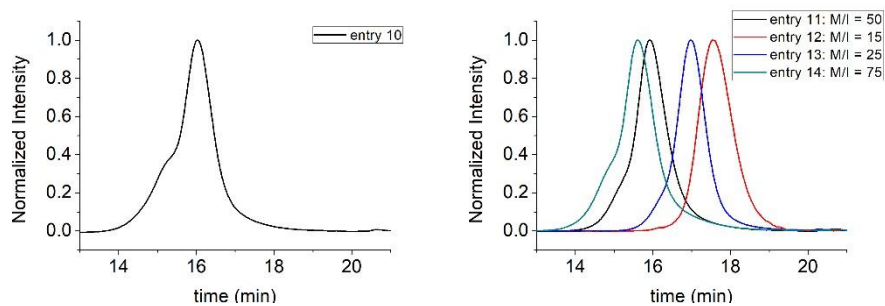
(b) Table 2, entries 1–6: PQXTh



(c) Table 2, entries 7–9: PQXEDOT



(d) Table 2, entries 10–14: PQXSe



(e) Table 3, entries 1–4: PBTzThDPPTTh

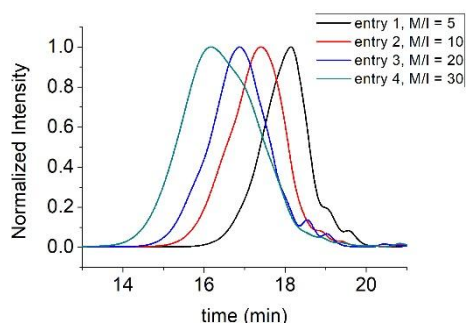
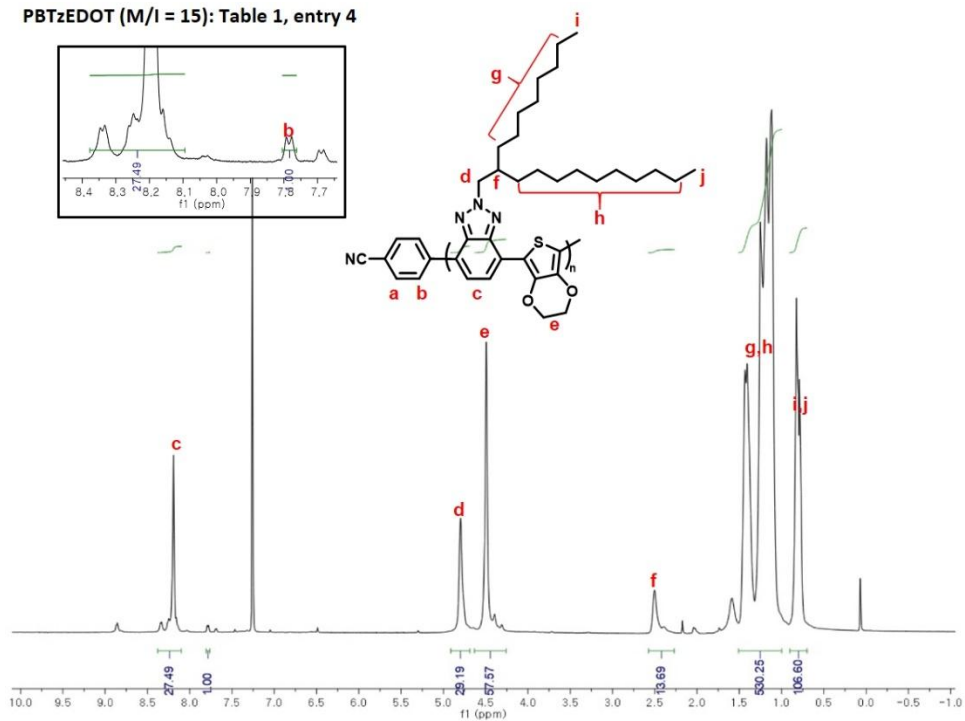


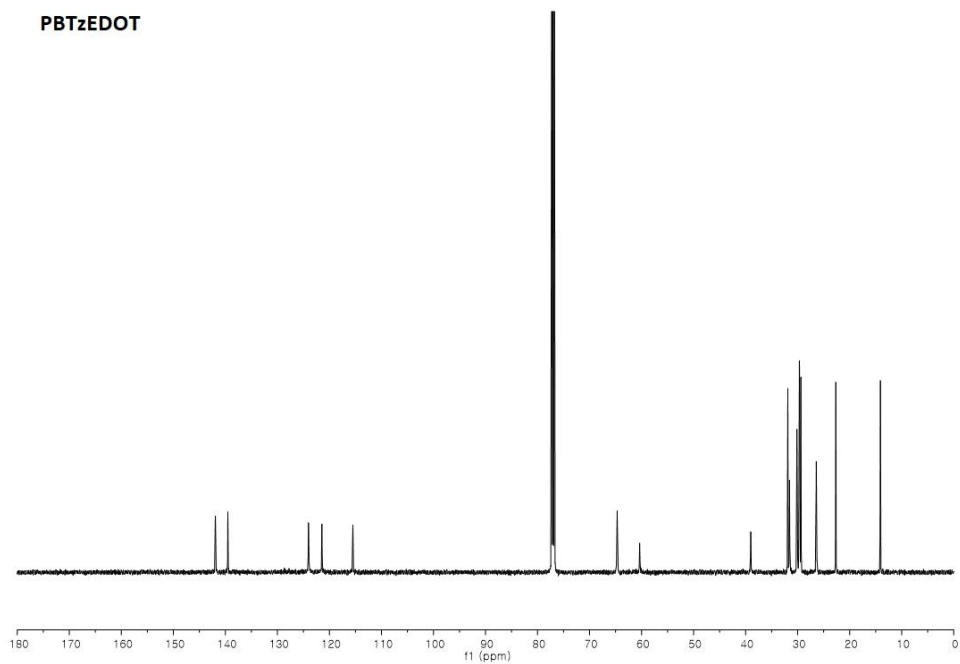
Figure S6: THF SEC traces of (a) PBTzEDOT in Table 1 (entries 1–6), (b) PQXTh in Table 2 (entries 1–6), (c) PQXEDOT in Table 2 (entries 7–9), (d) PQXSe in Table 2 (entries 10–14), and (e) PBTzThDPPTTh in Table 3 (entries 1–4).

^1H and ^{13}C NMR spectra of polymers

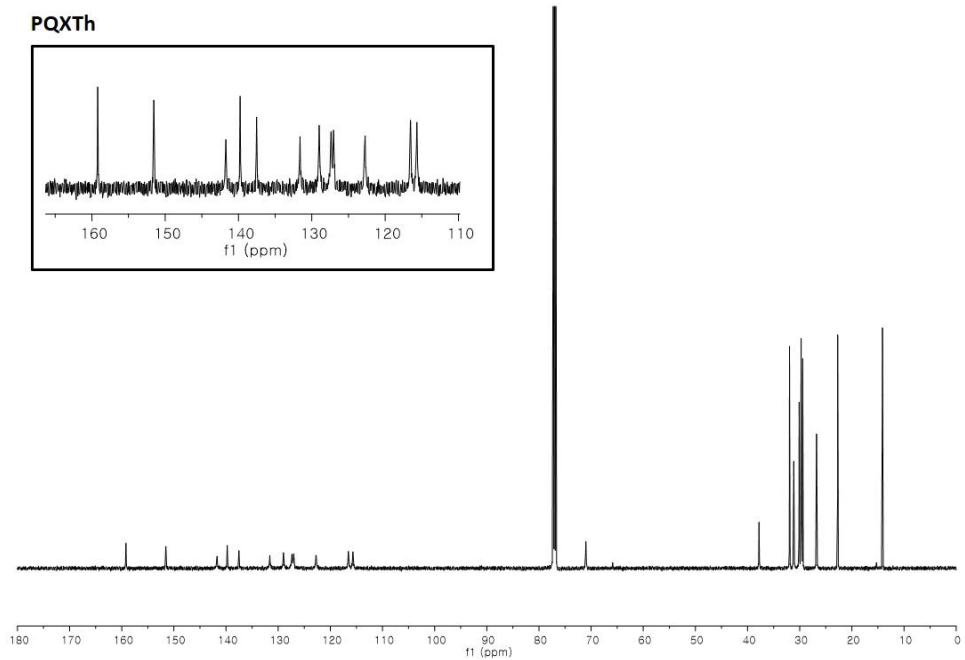
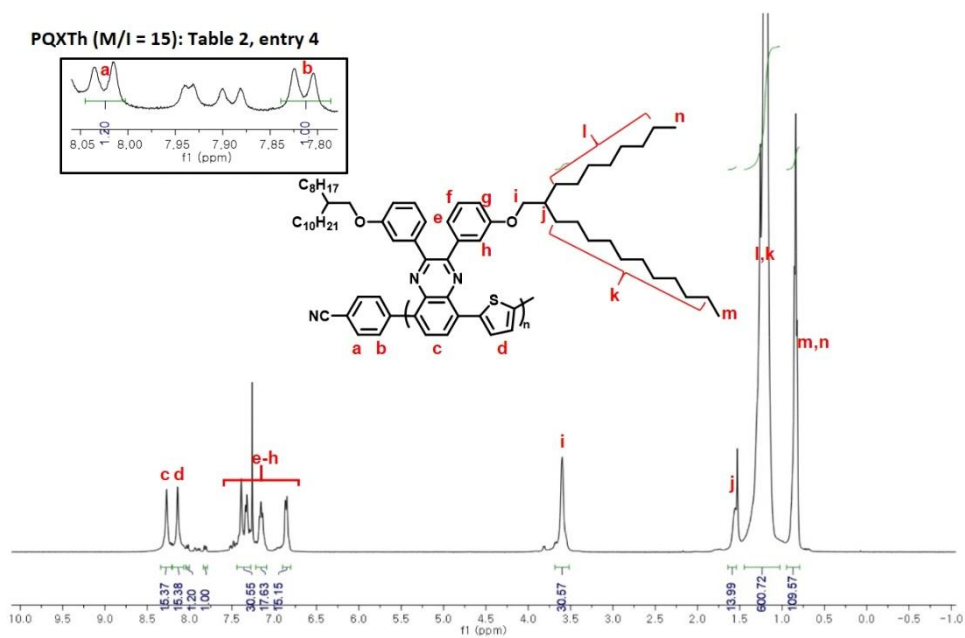
PBTzEDOT (M/I = 15): Table 1, entry 4



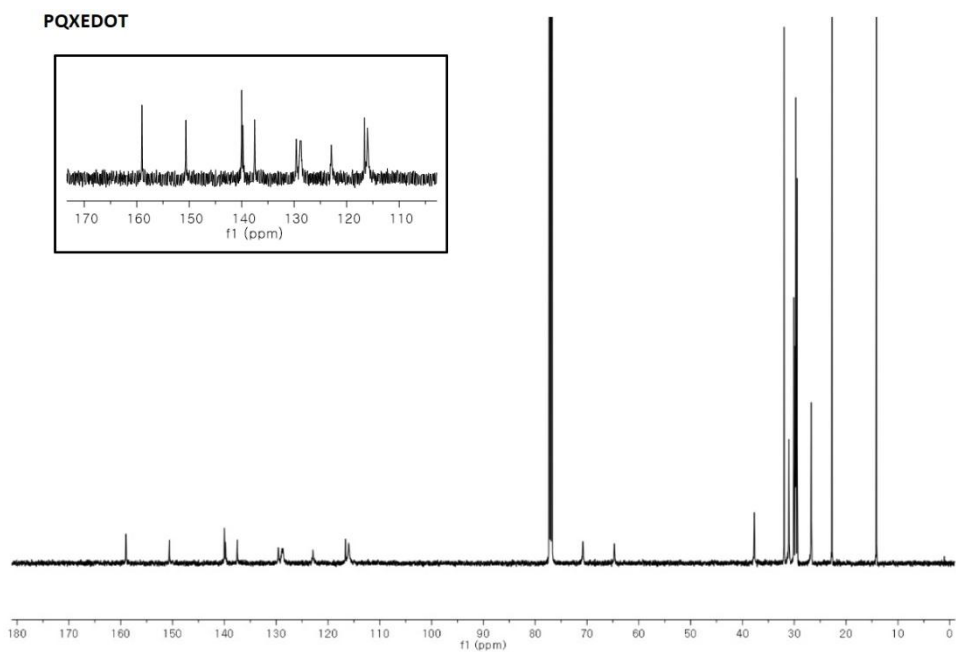
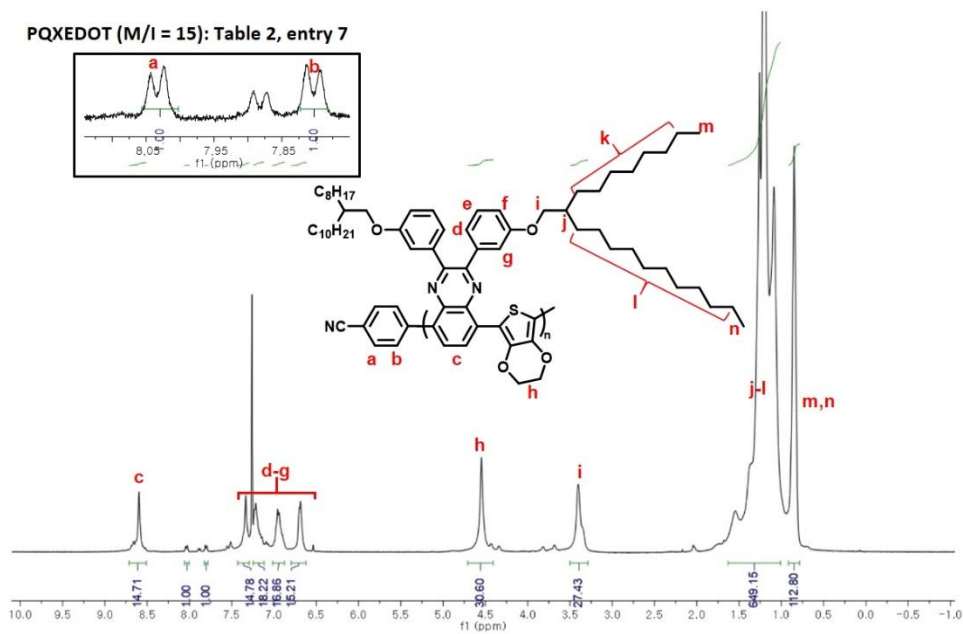
PBTzEDOT



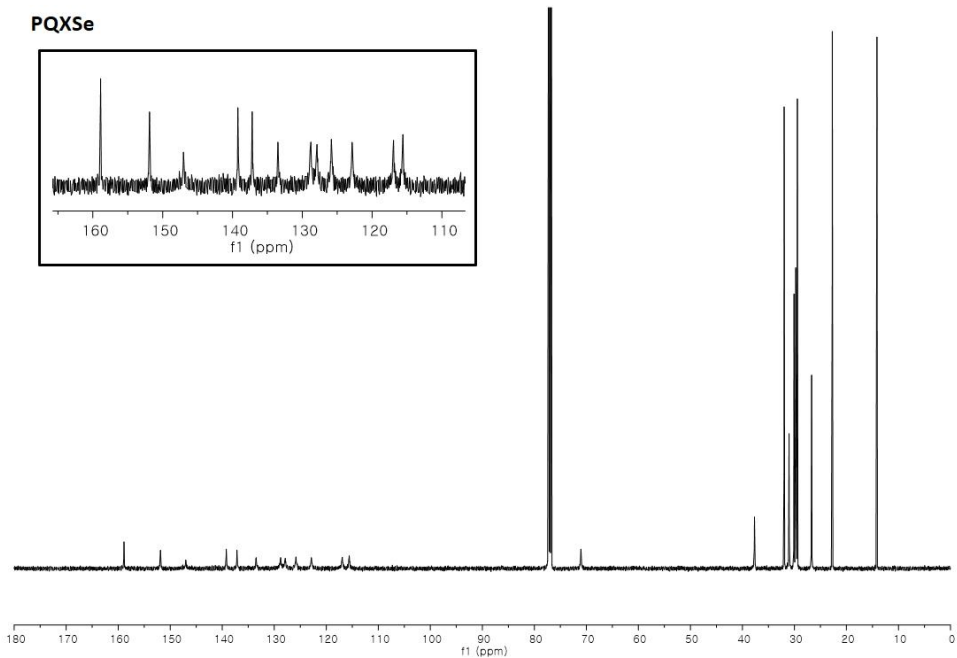
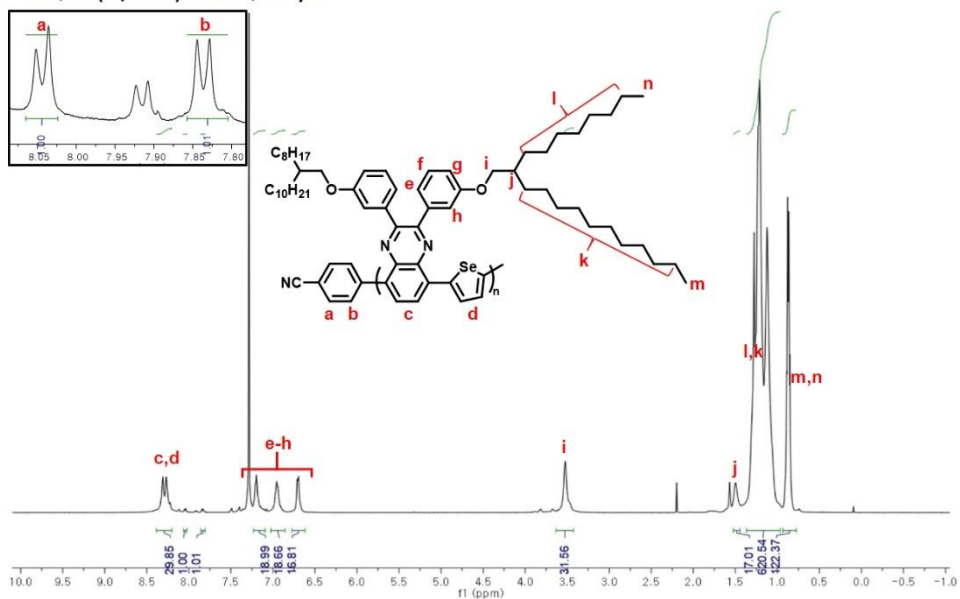
PQXTh (M/I = 15): Table 2, entry 4



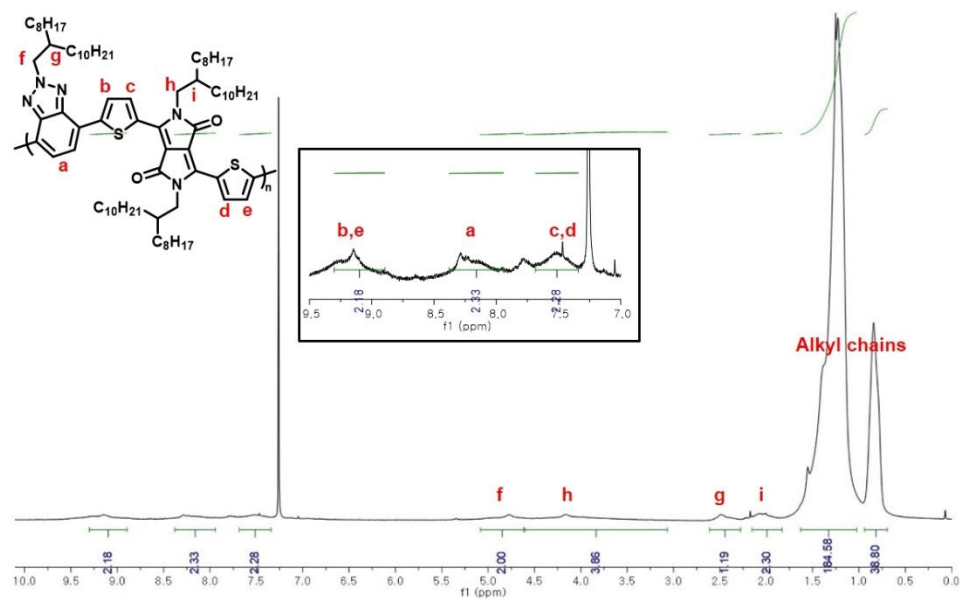
PQXEDOT (M/I = 15): Table 2, entry 7



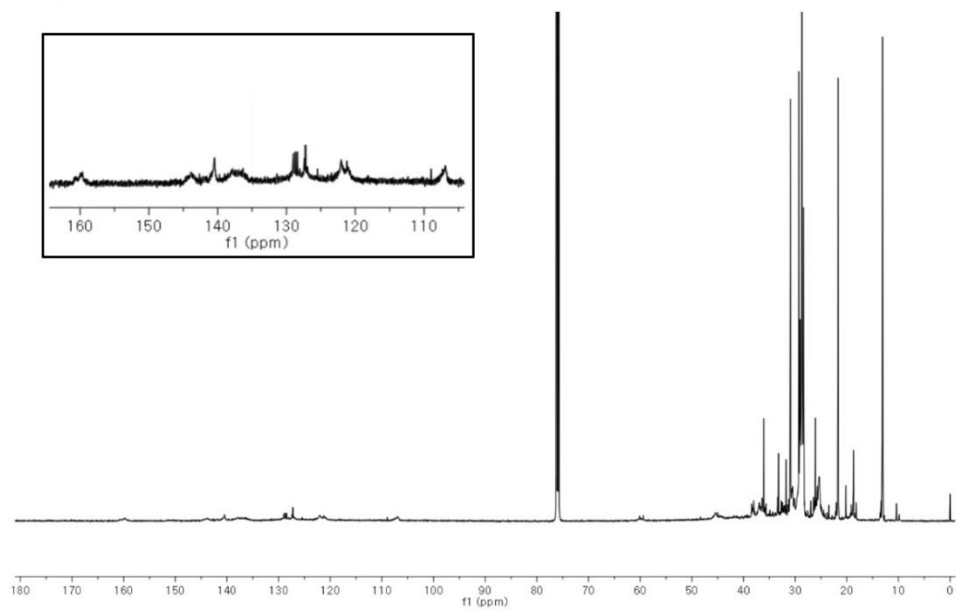
PQXSe (M/I = 15): Table 2, entry 12



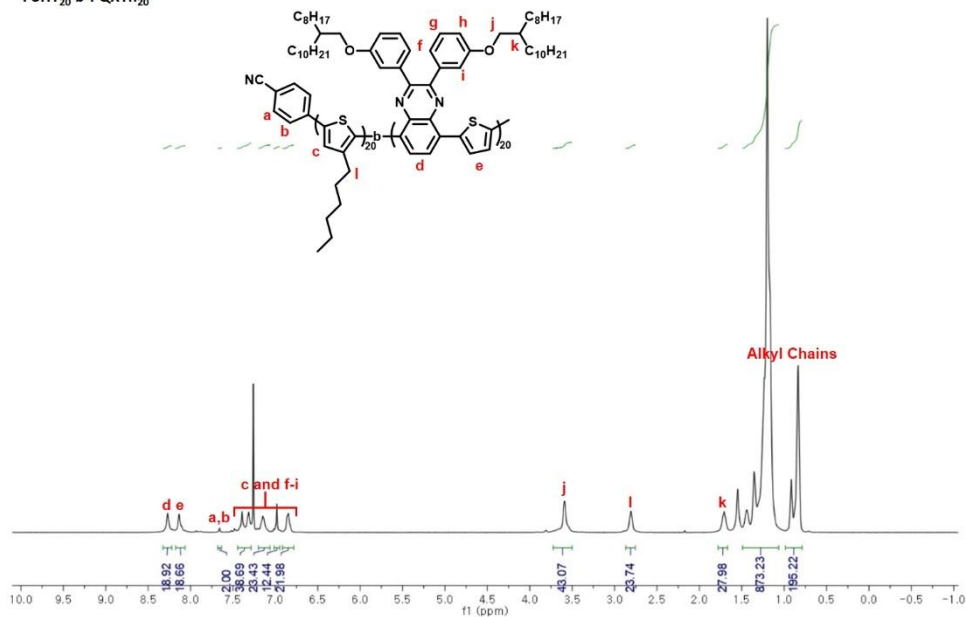
PBTzThDPPTTh (M/I = 10): Table 3, entry 2



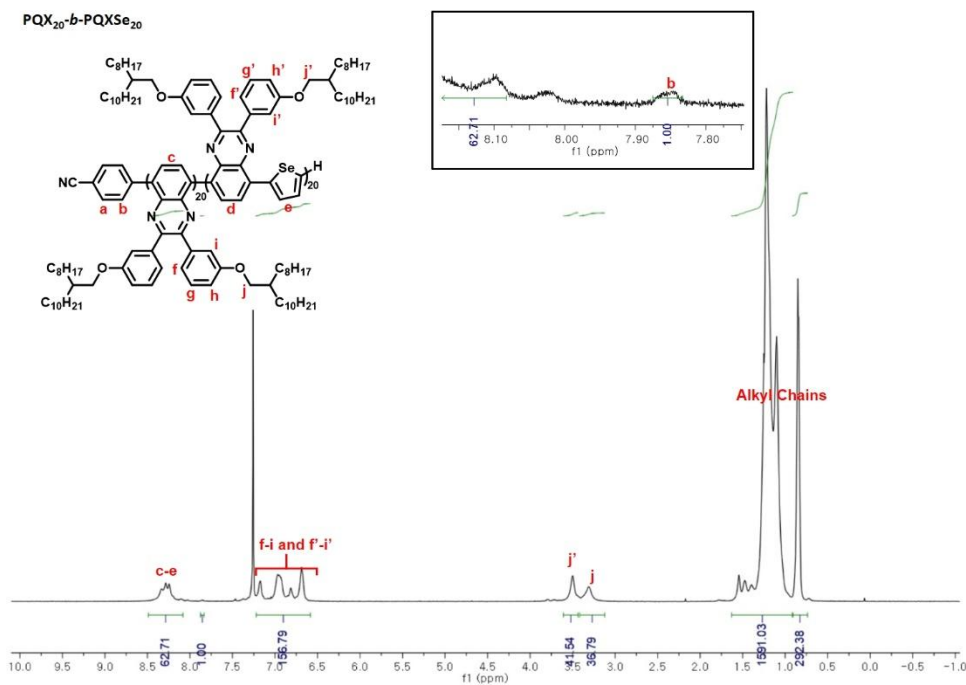
PBTzThDPPTTh



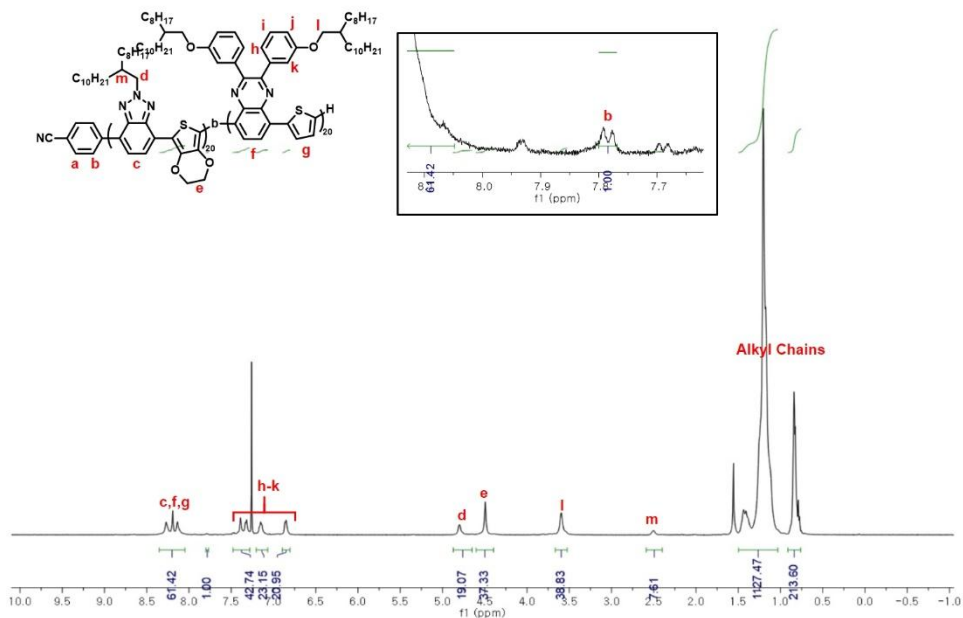
P3HT₂₀-*b*-PQXTh₂₀



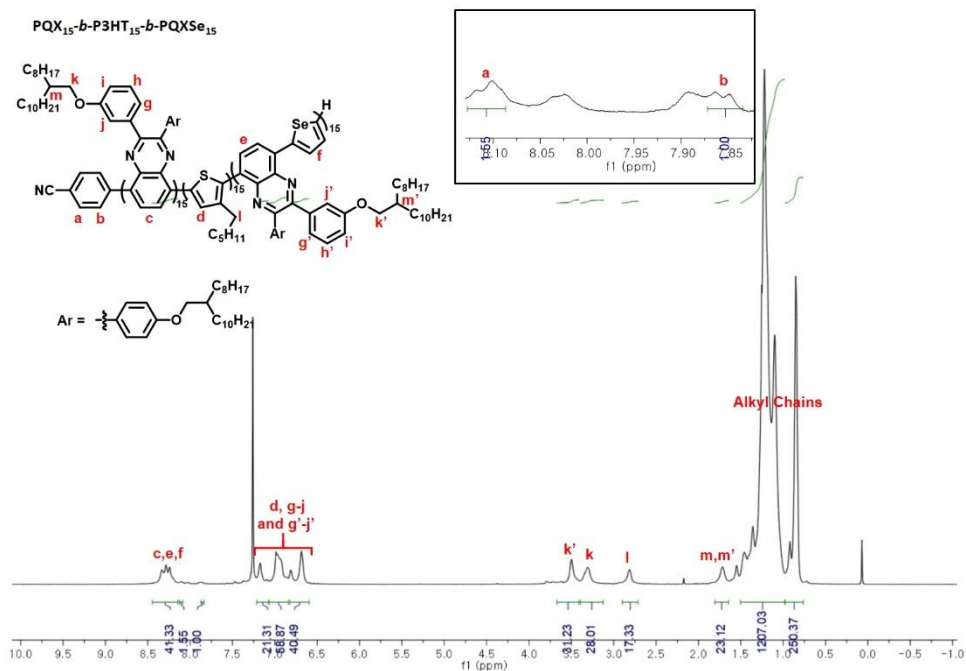
PQX₂₀-*b*-PQXSe₂₀



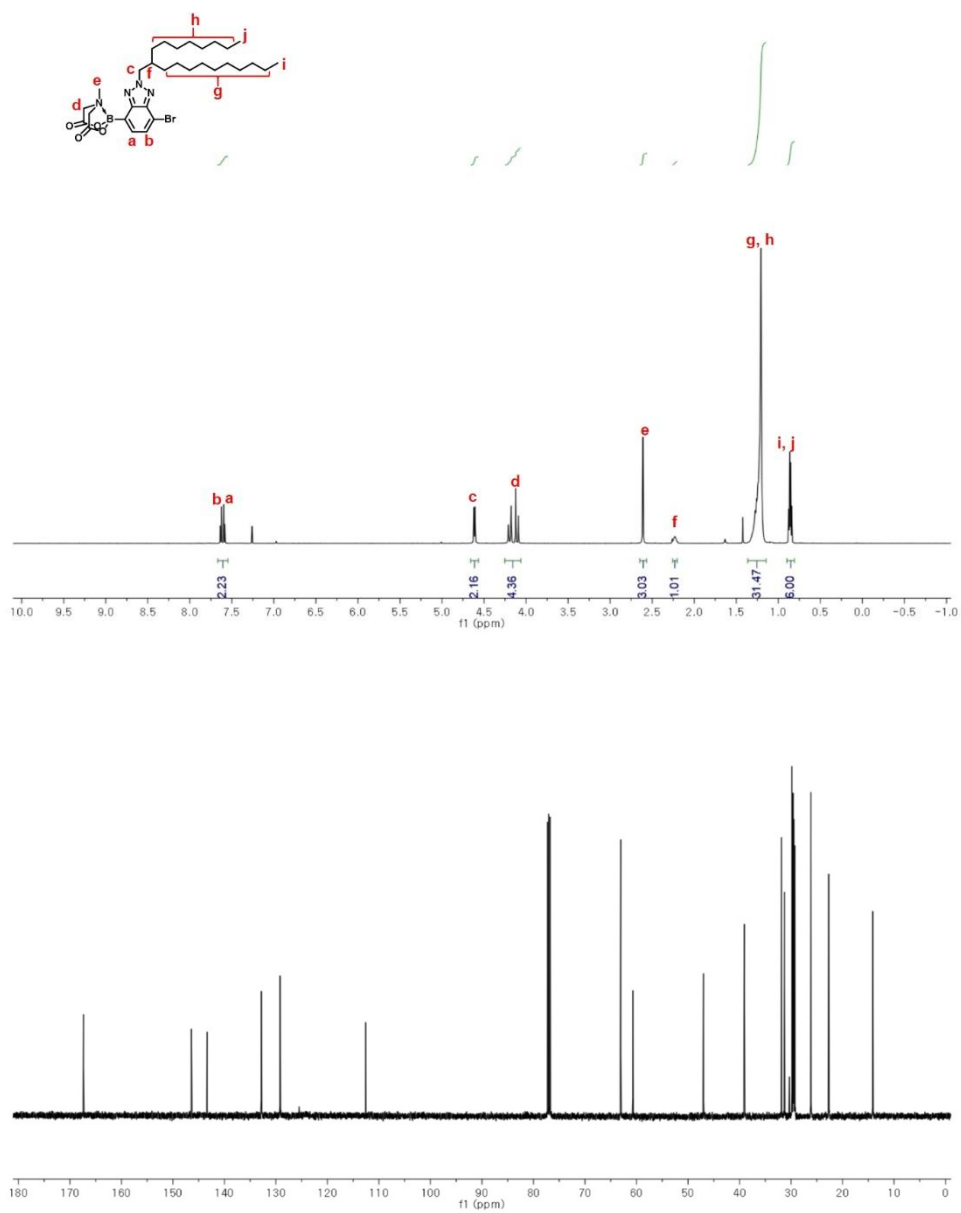
PBTzEDOT₂₀-*b*-PQXTh₂₀

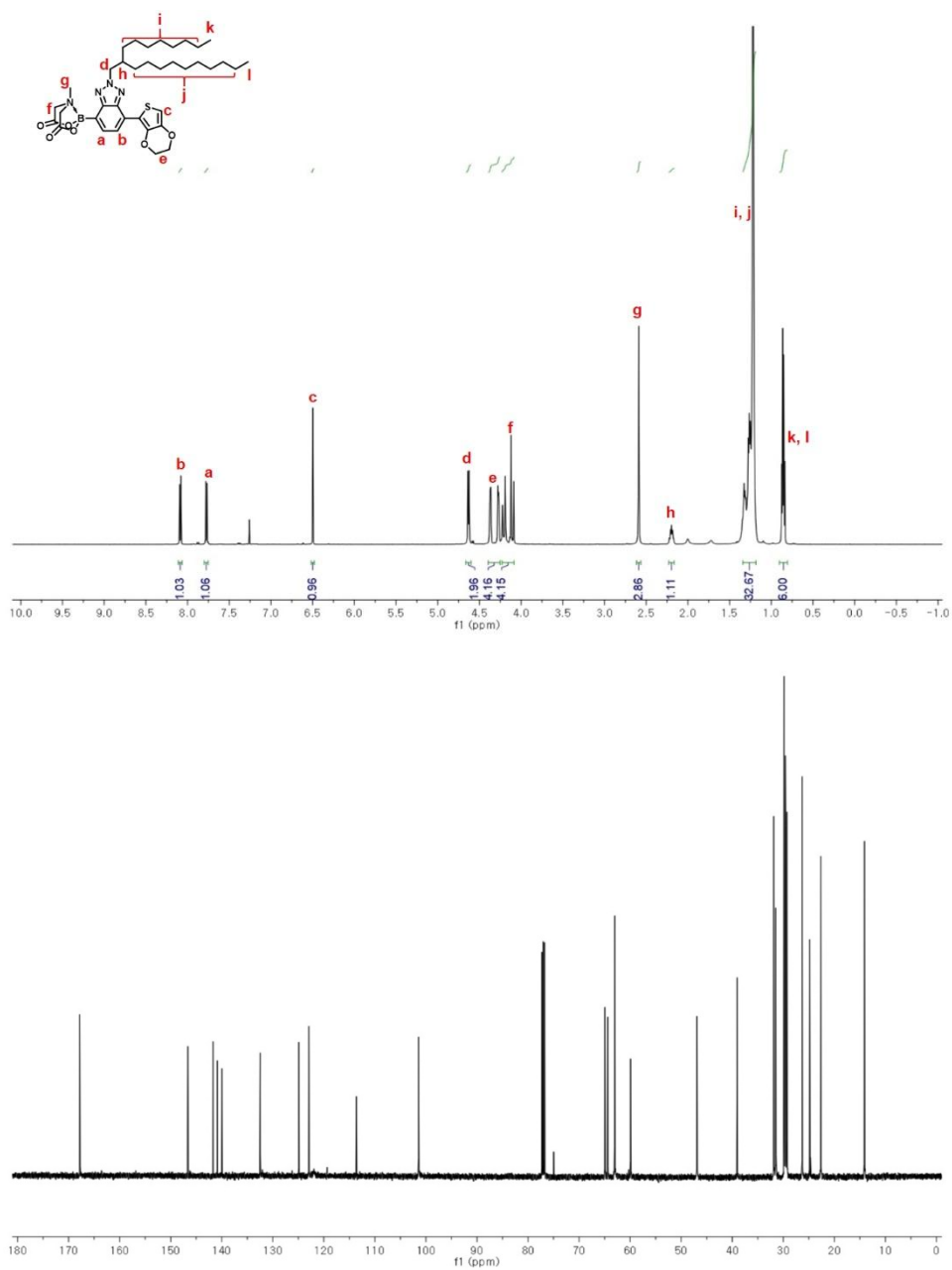


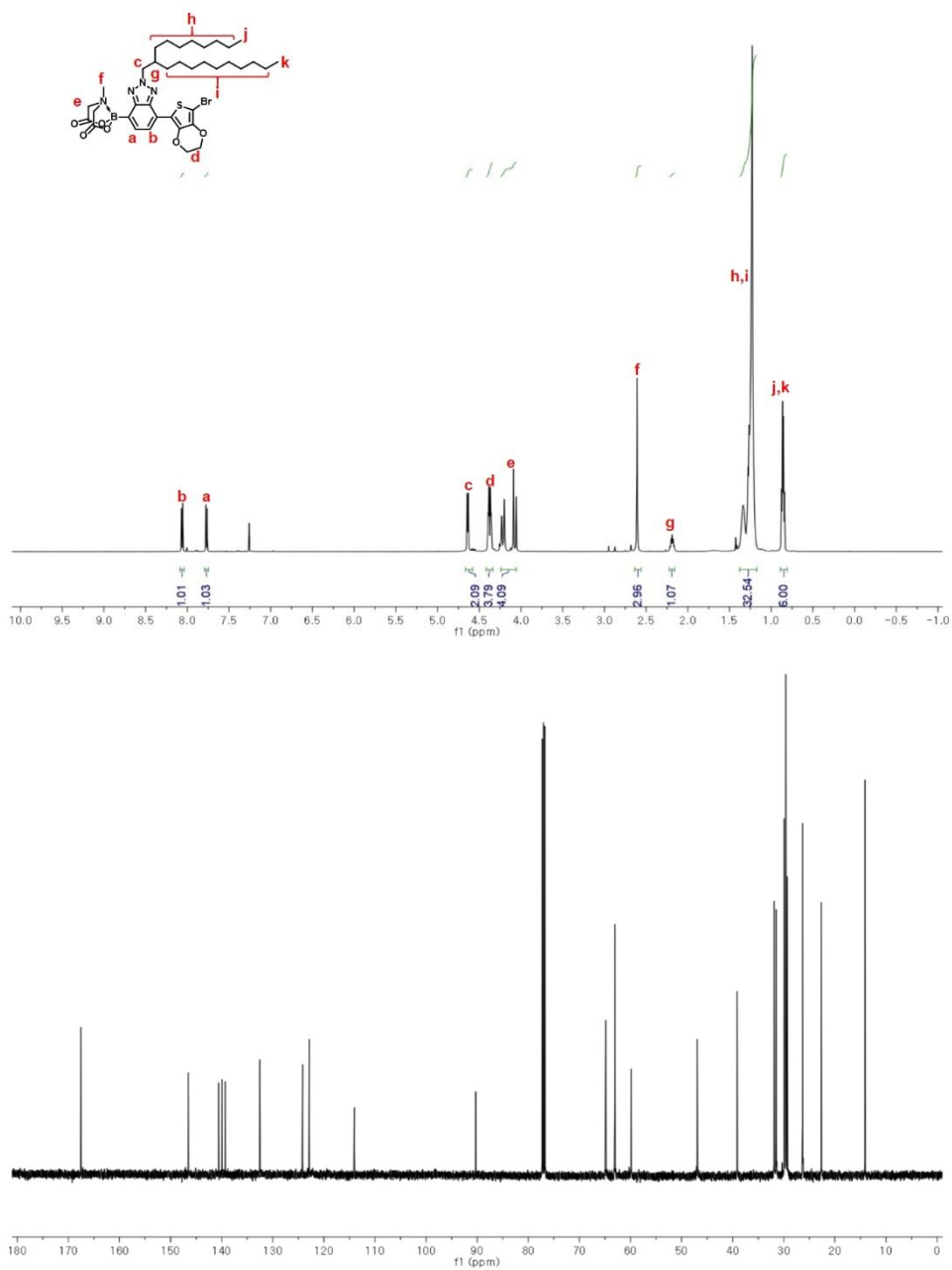
PQX₁₅-*b*-P3HT₁₅-*b*-PQXSe₁₅

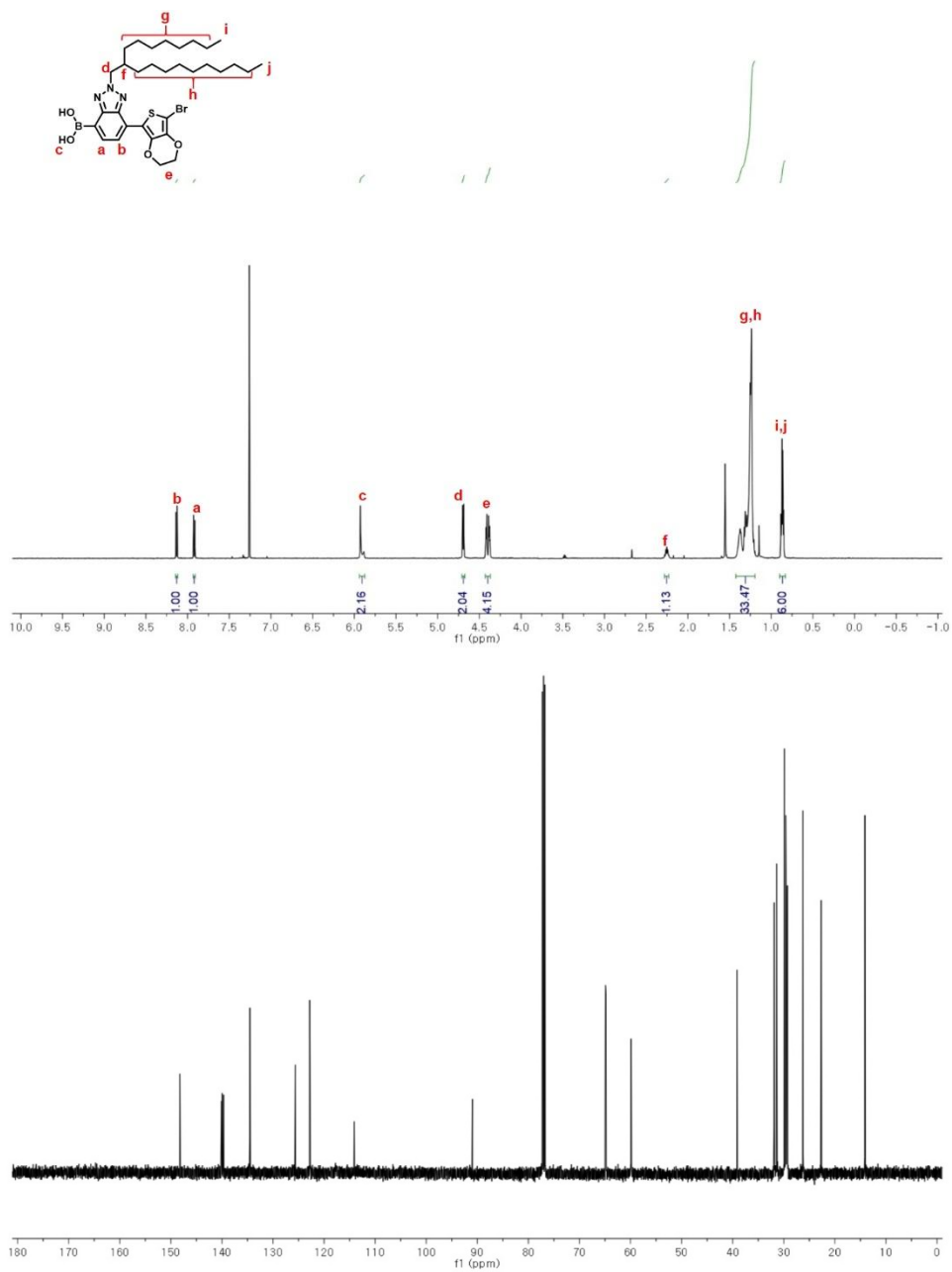


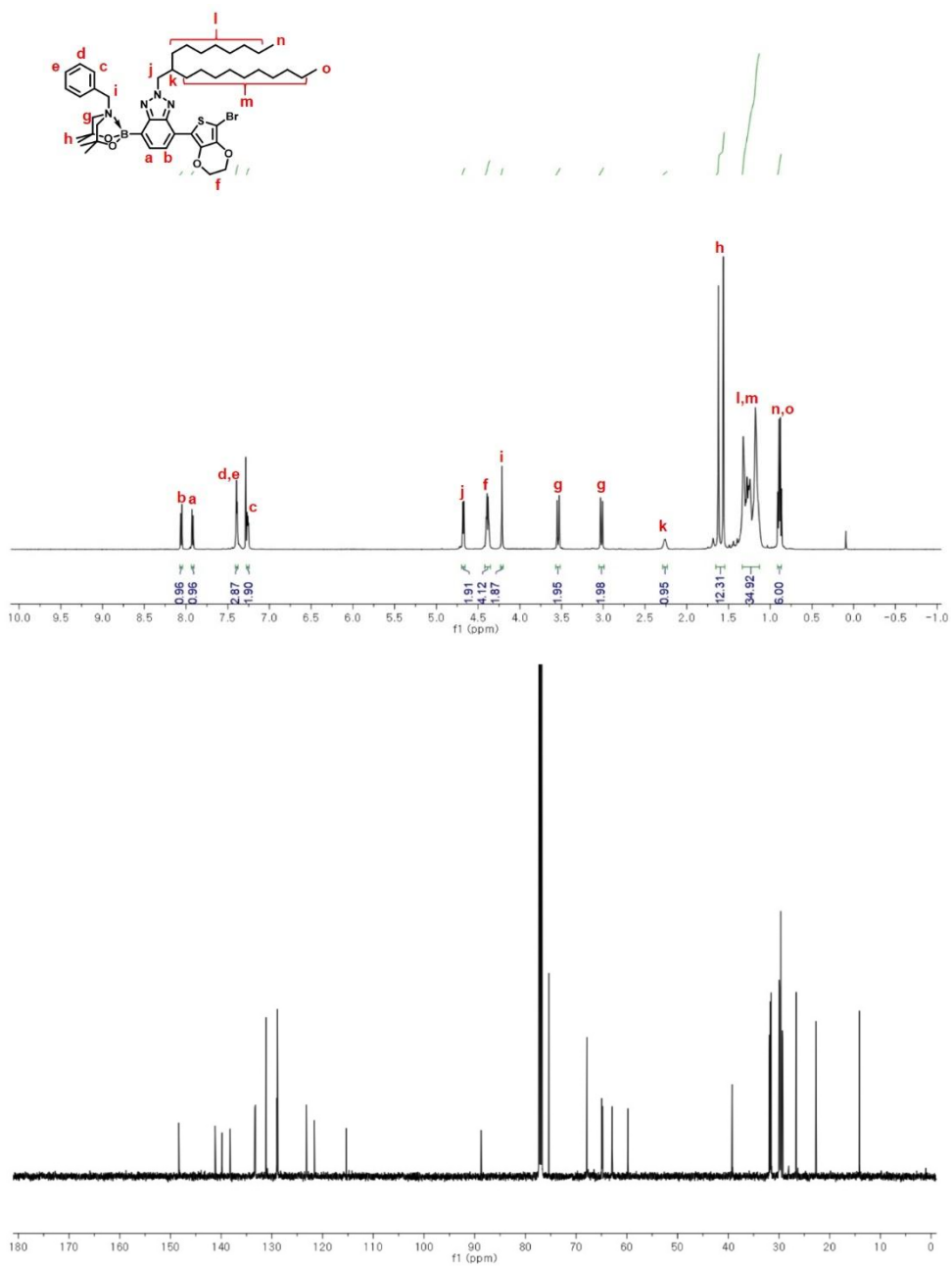
^1H , ^{13}C and ^{11}B NMR spectra of new compounds (in CDCl_3)

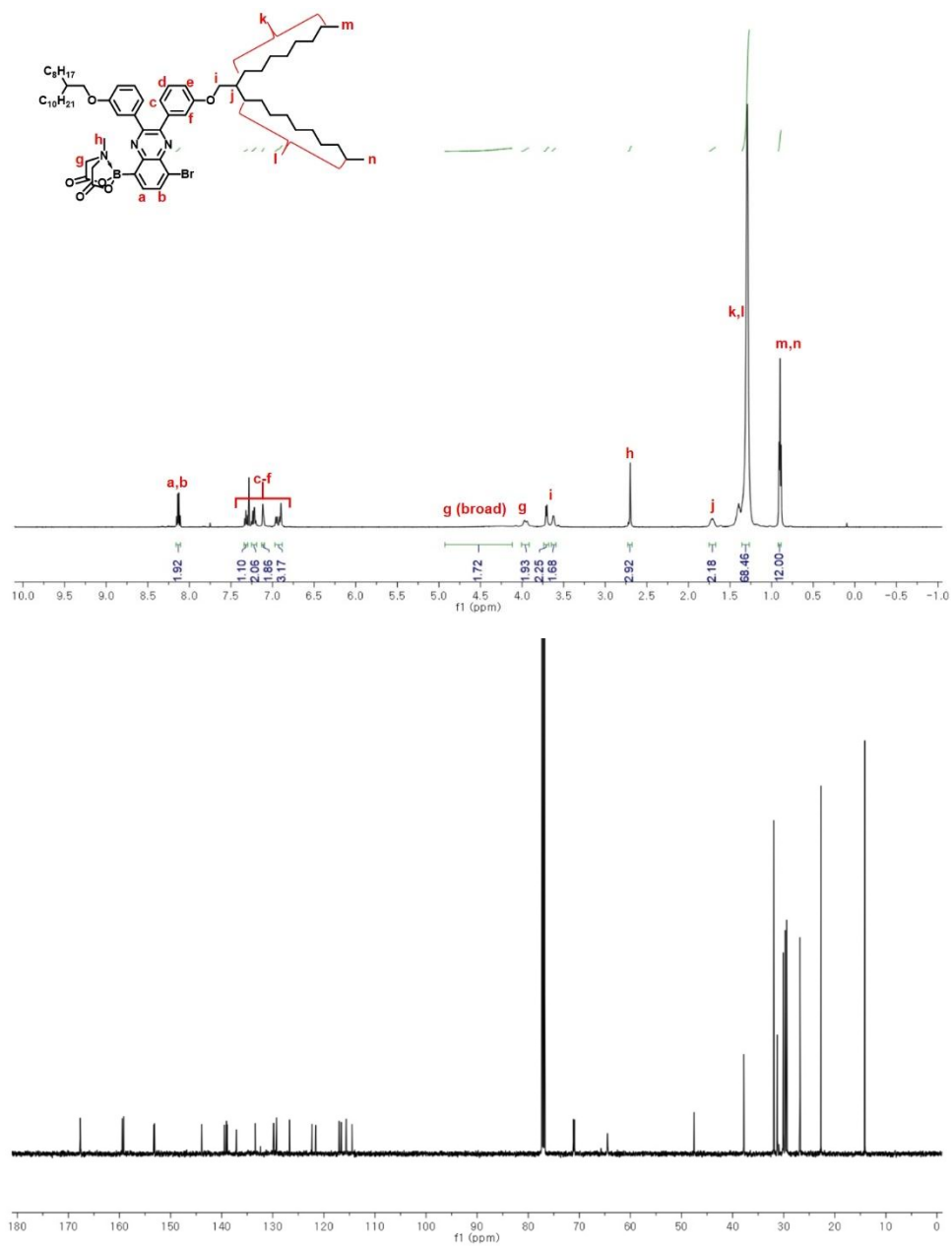


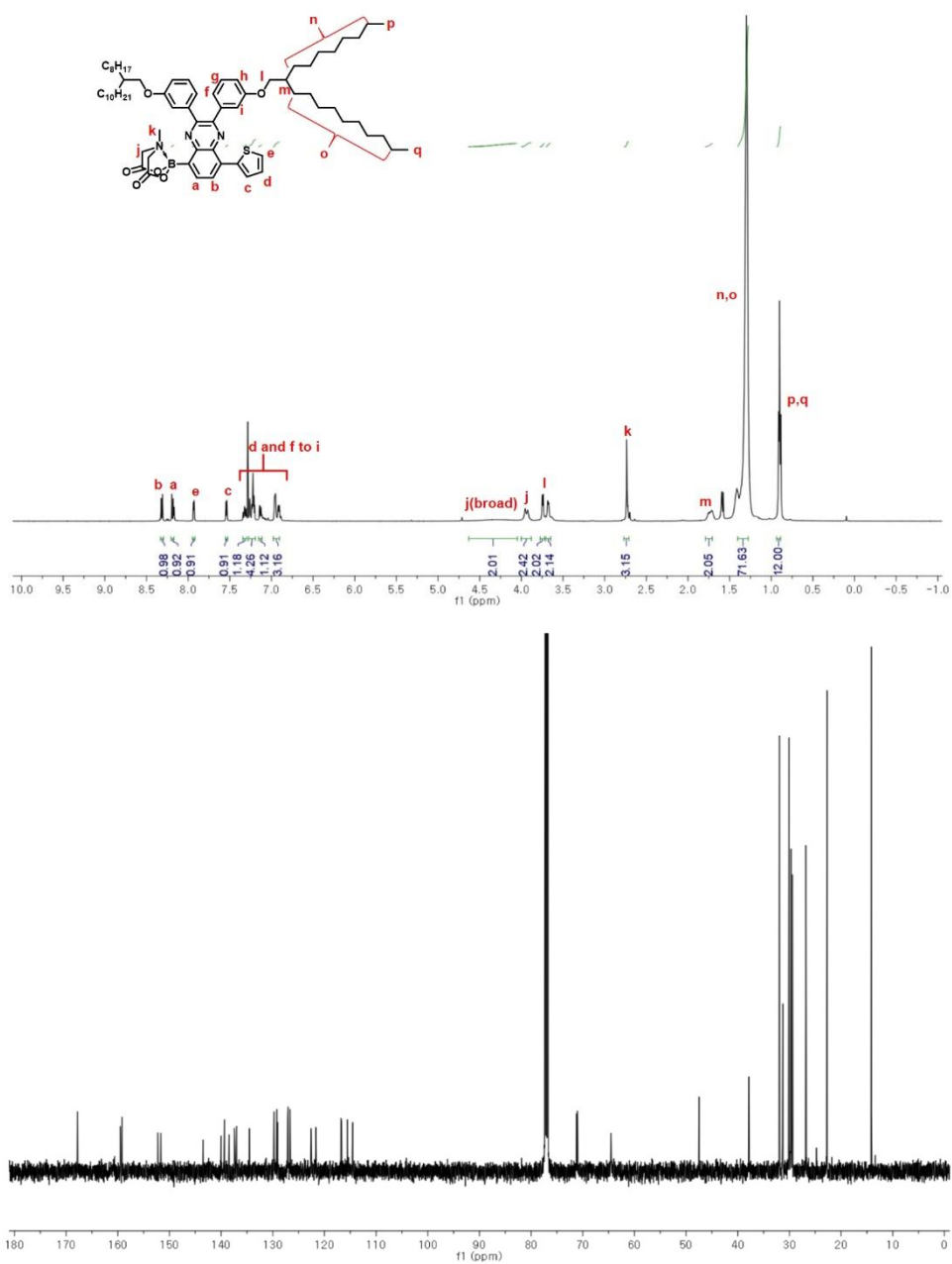


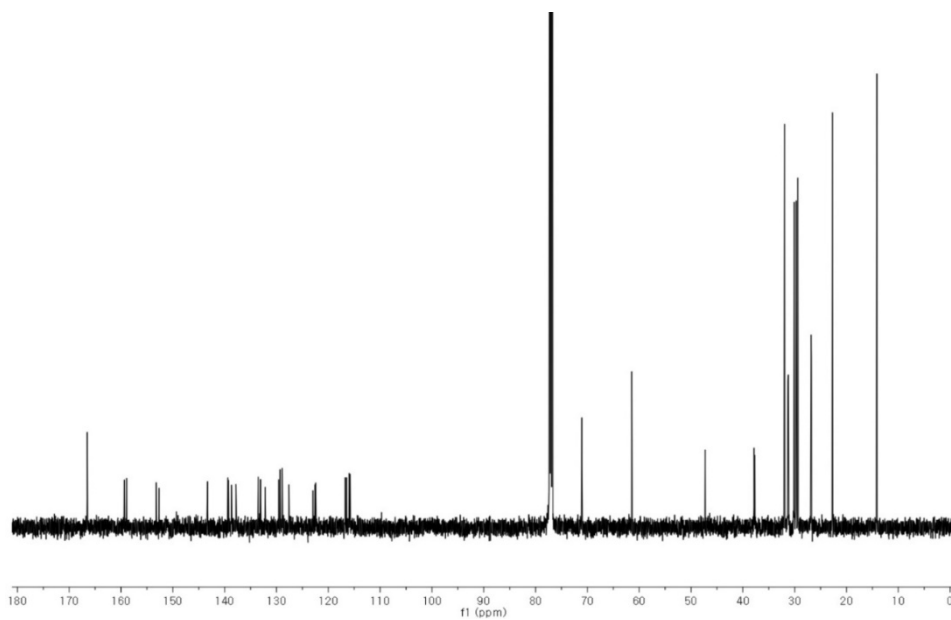
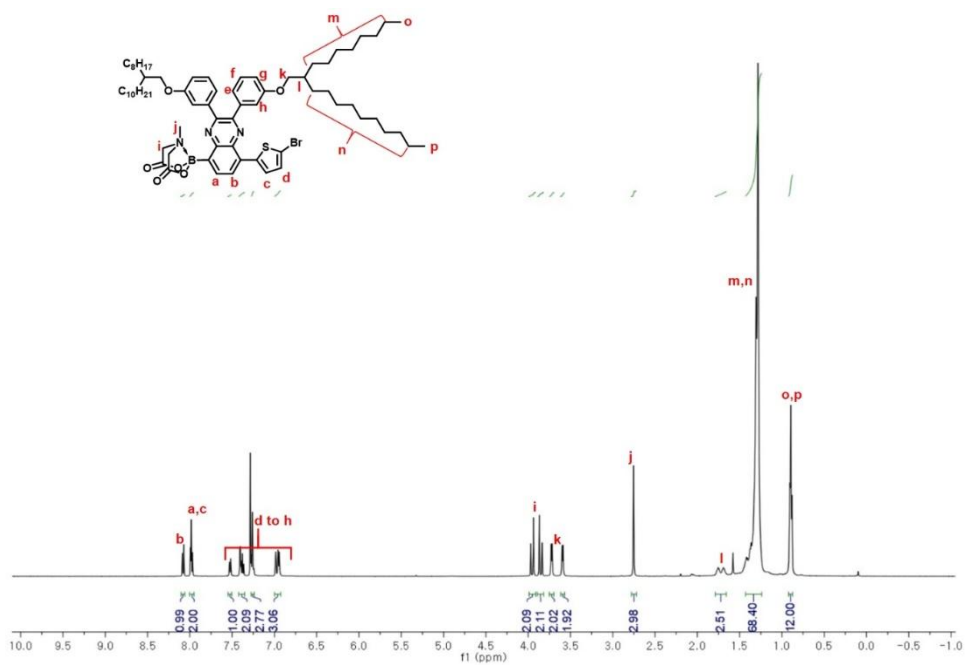


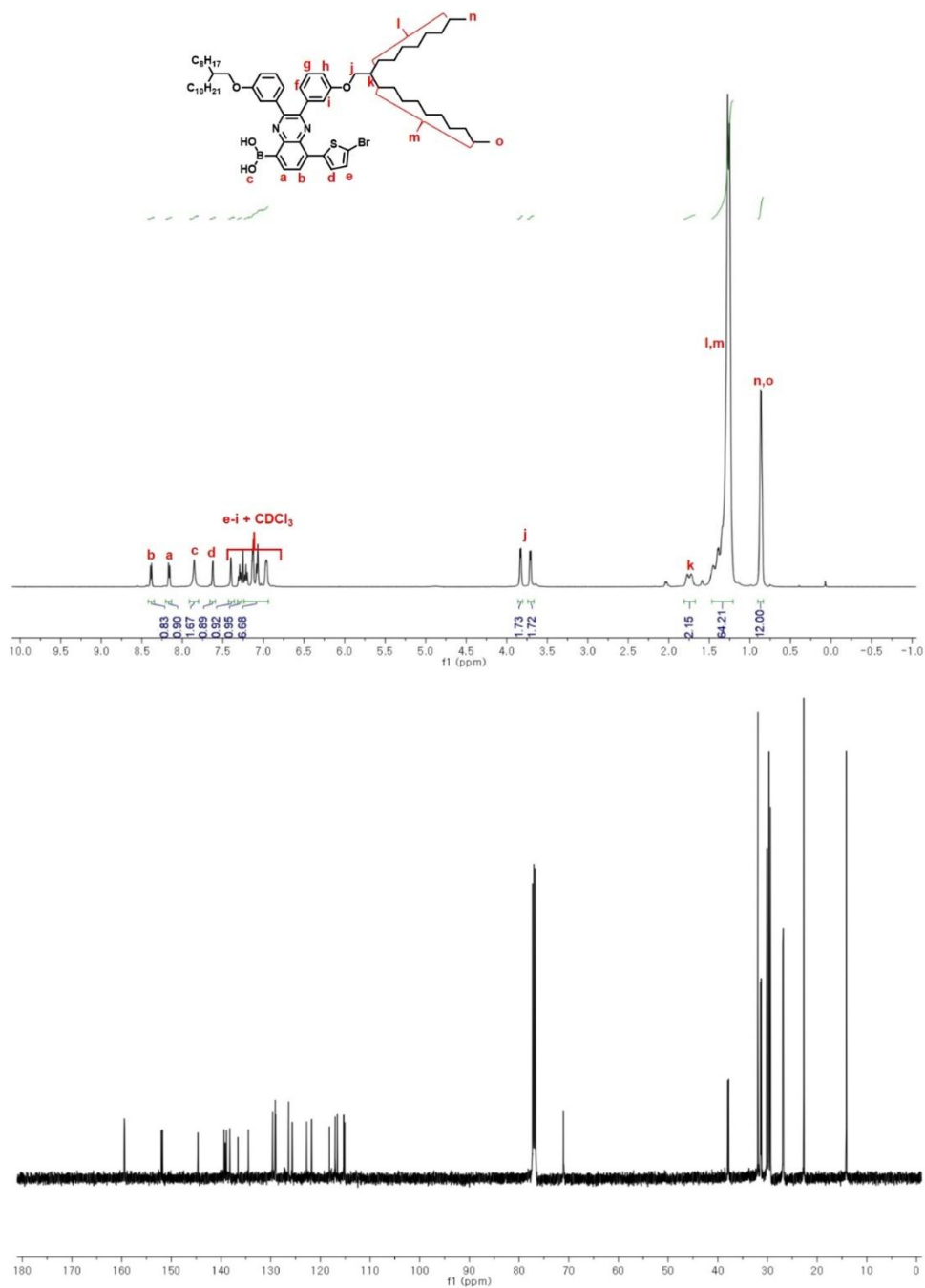


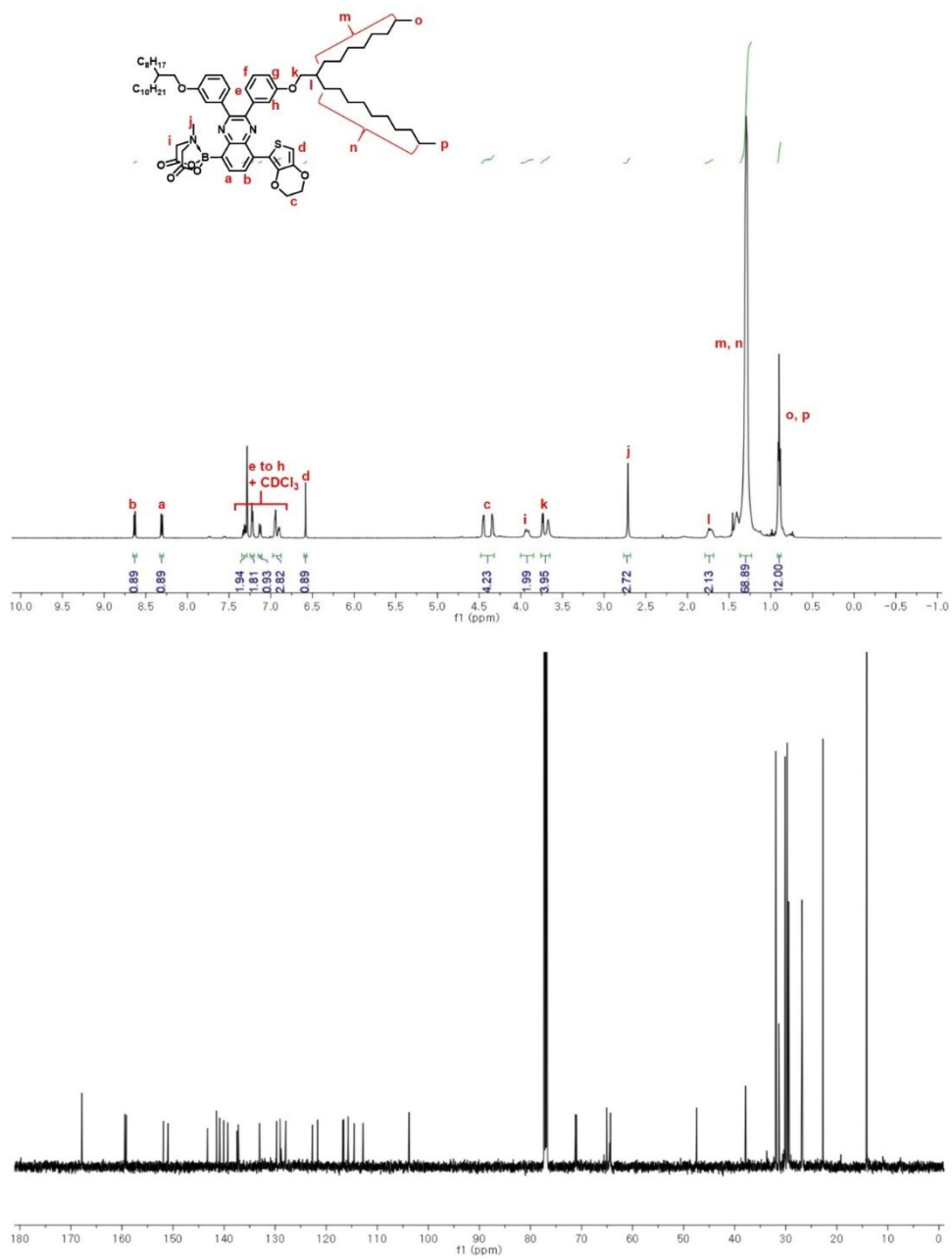


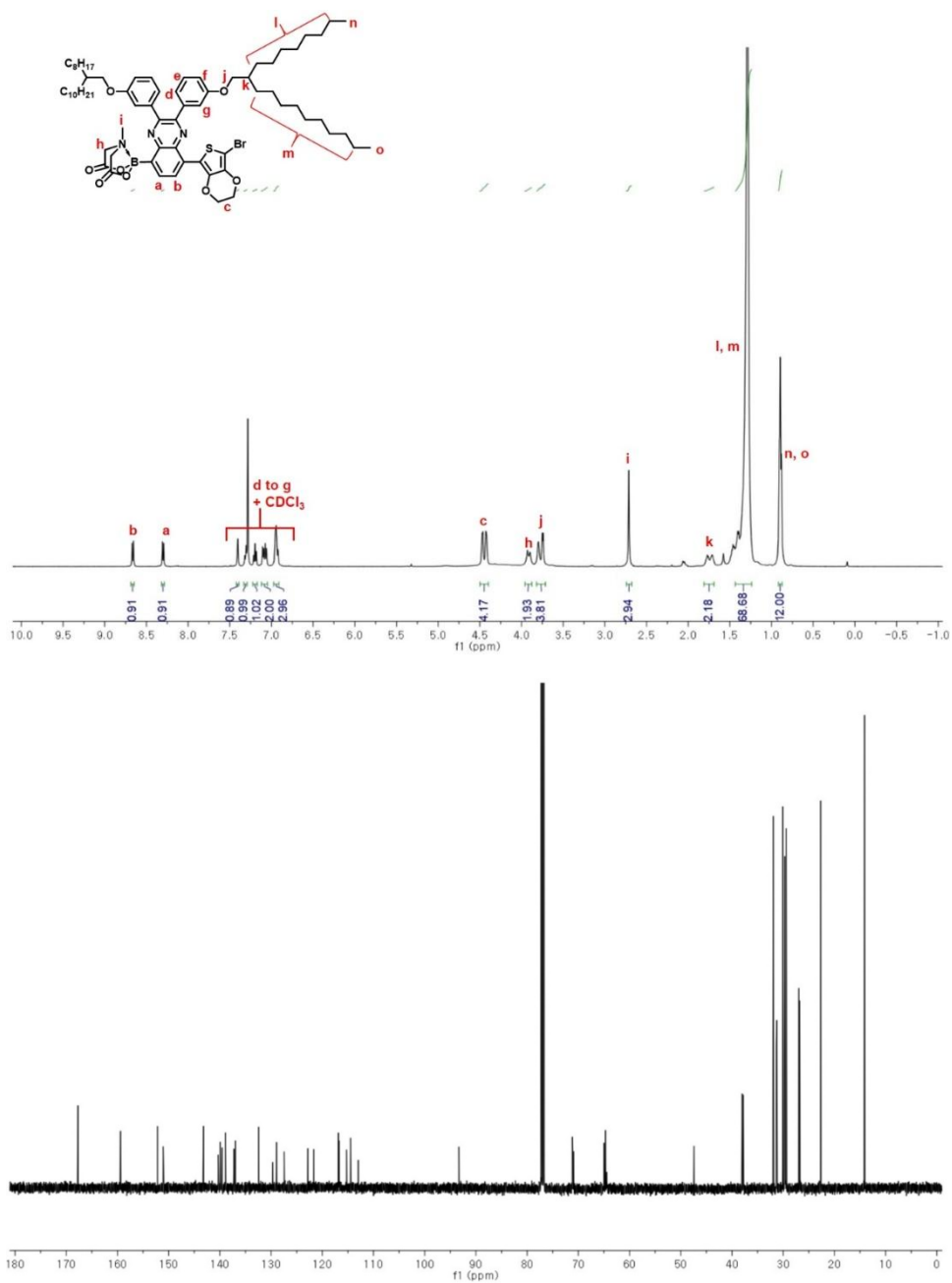


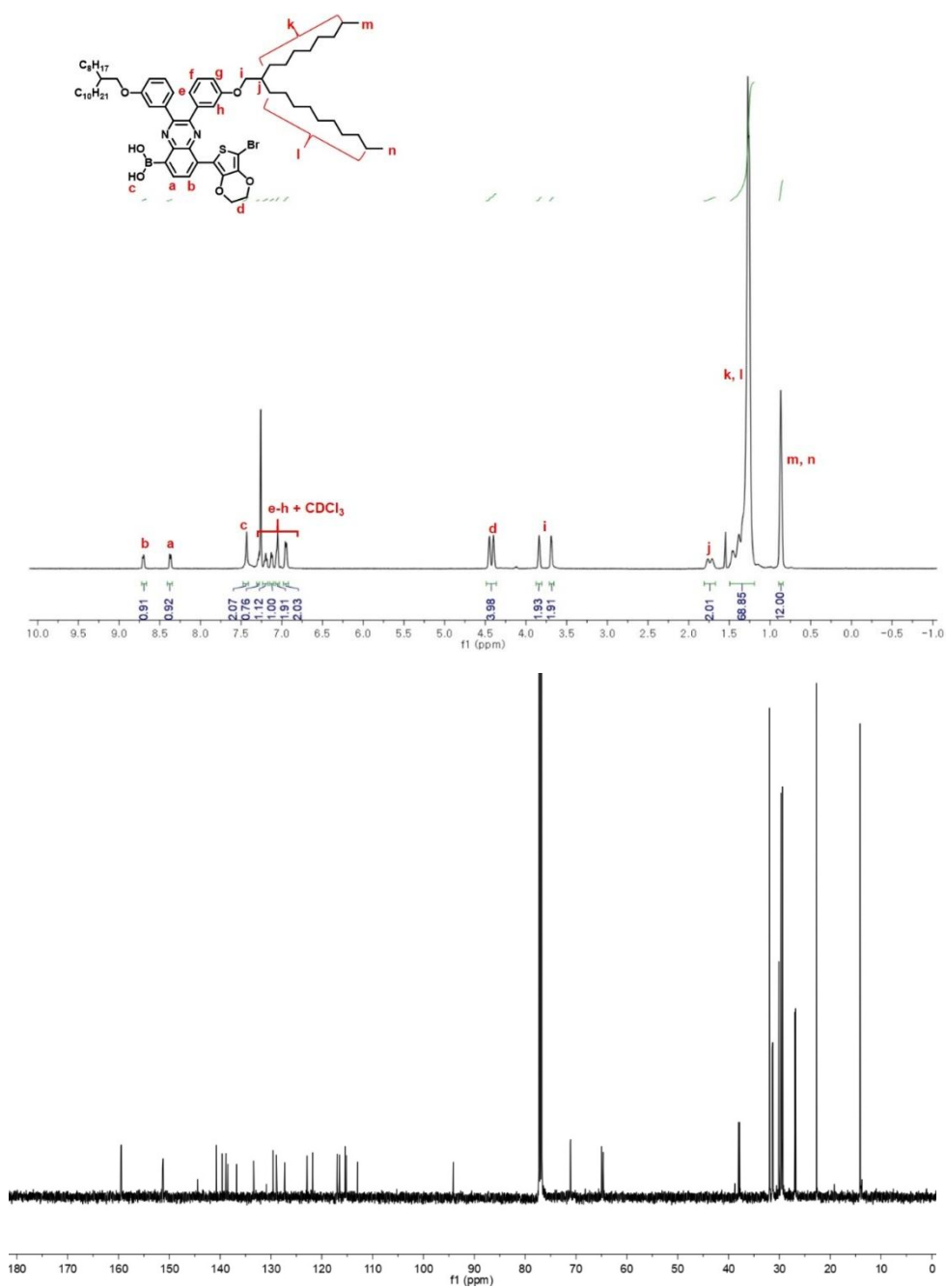


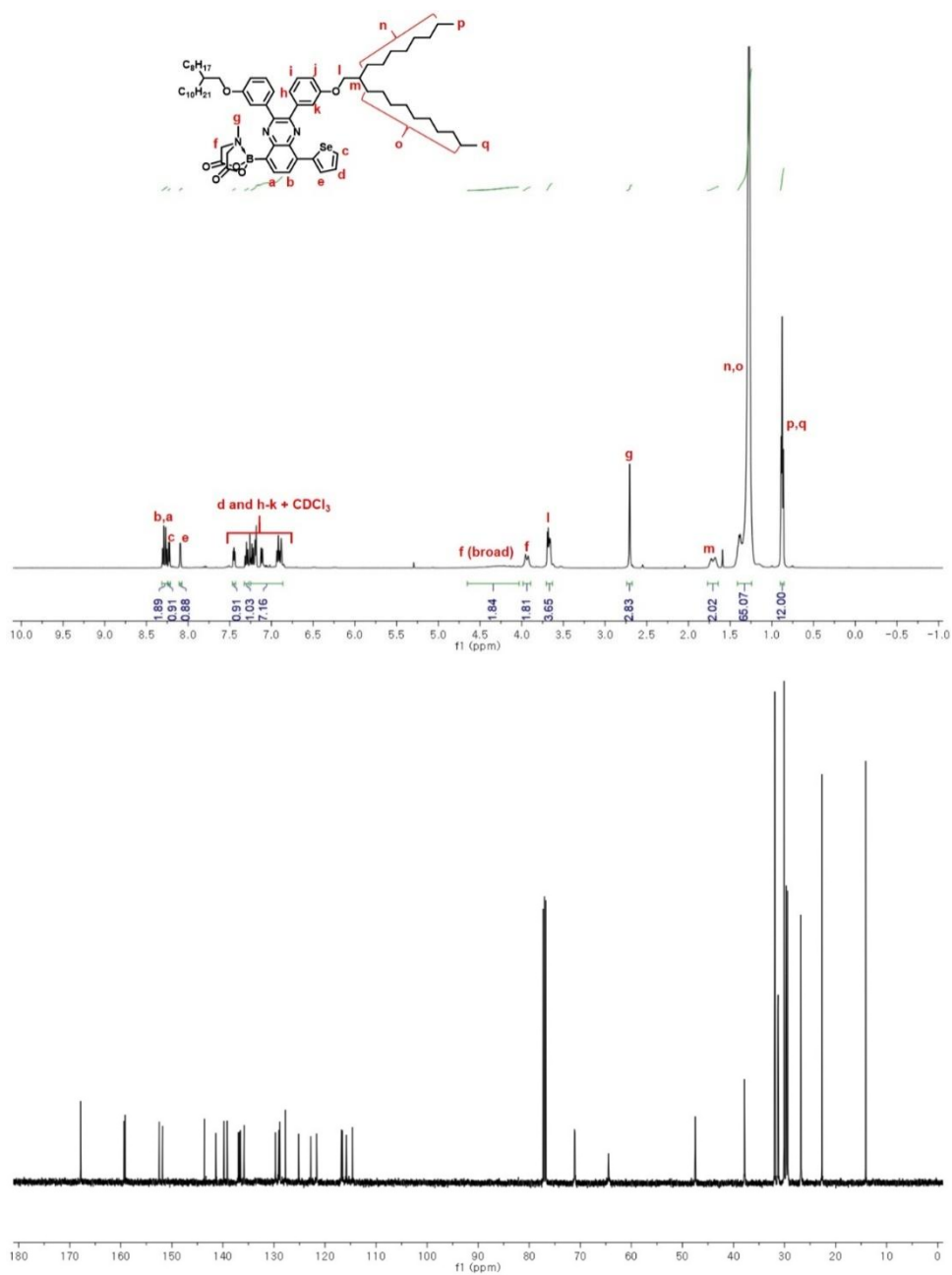


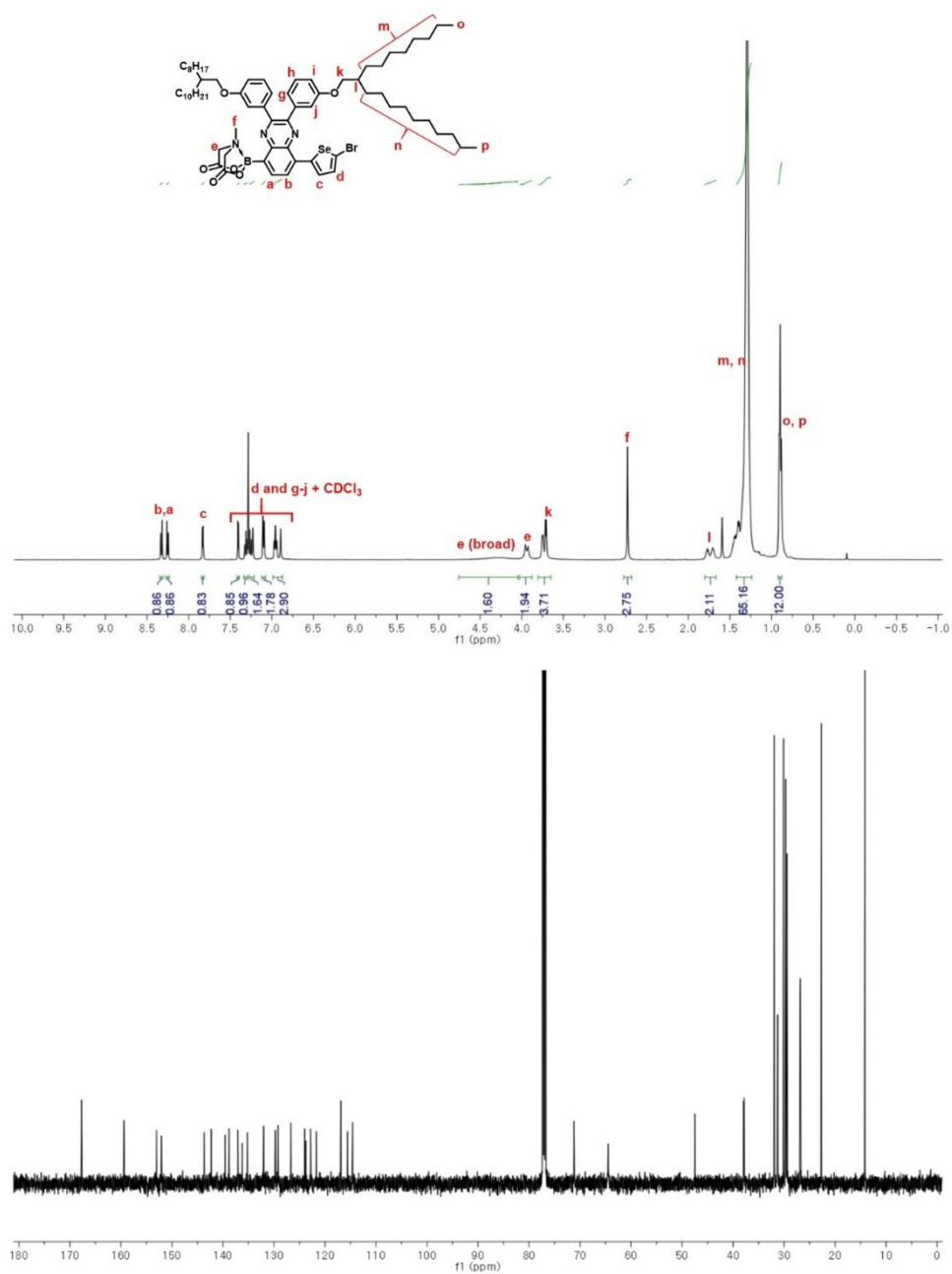


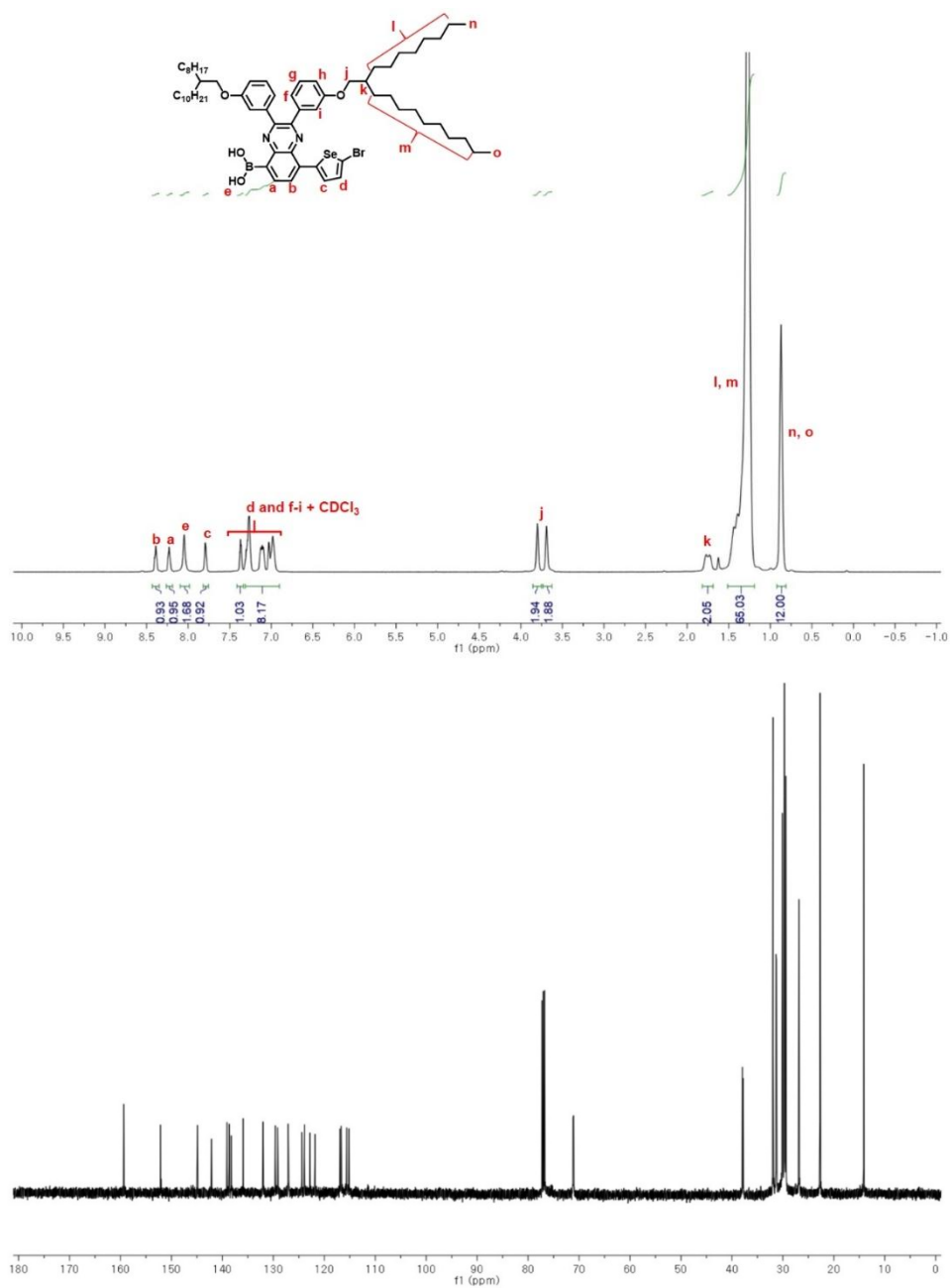


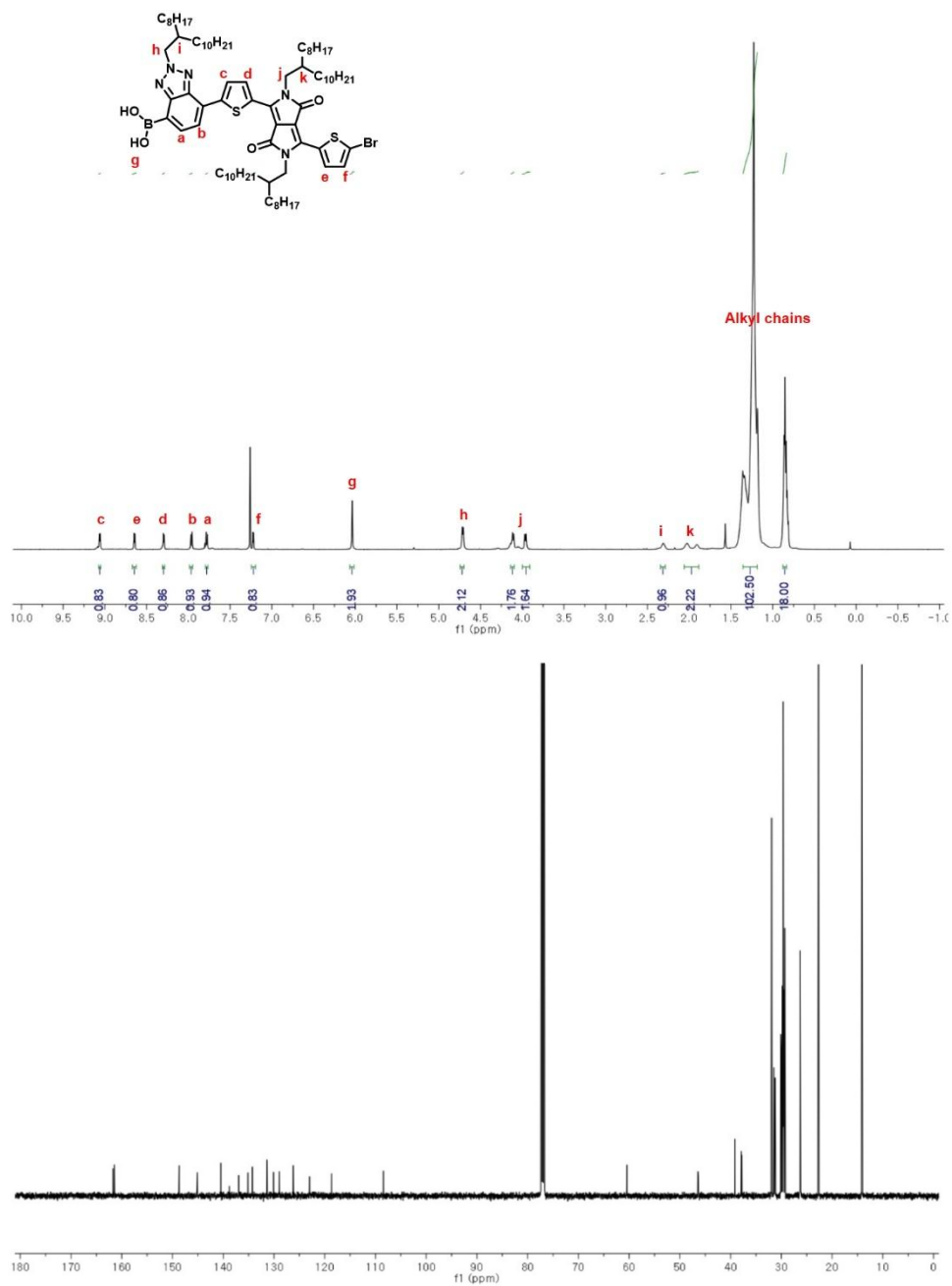


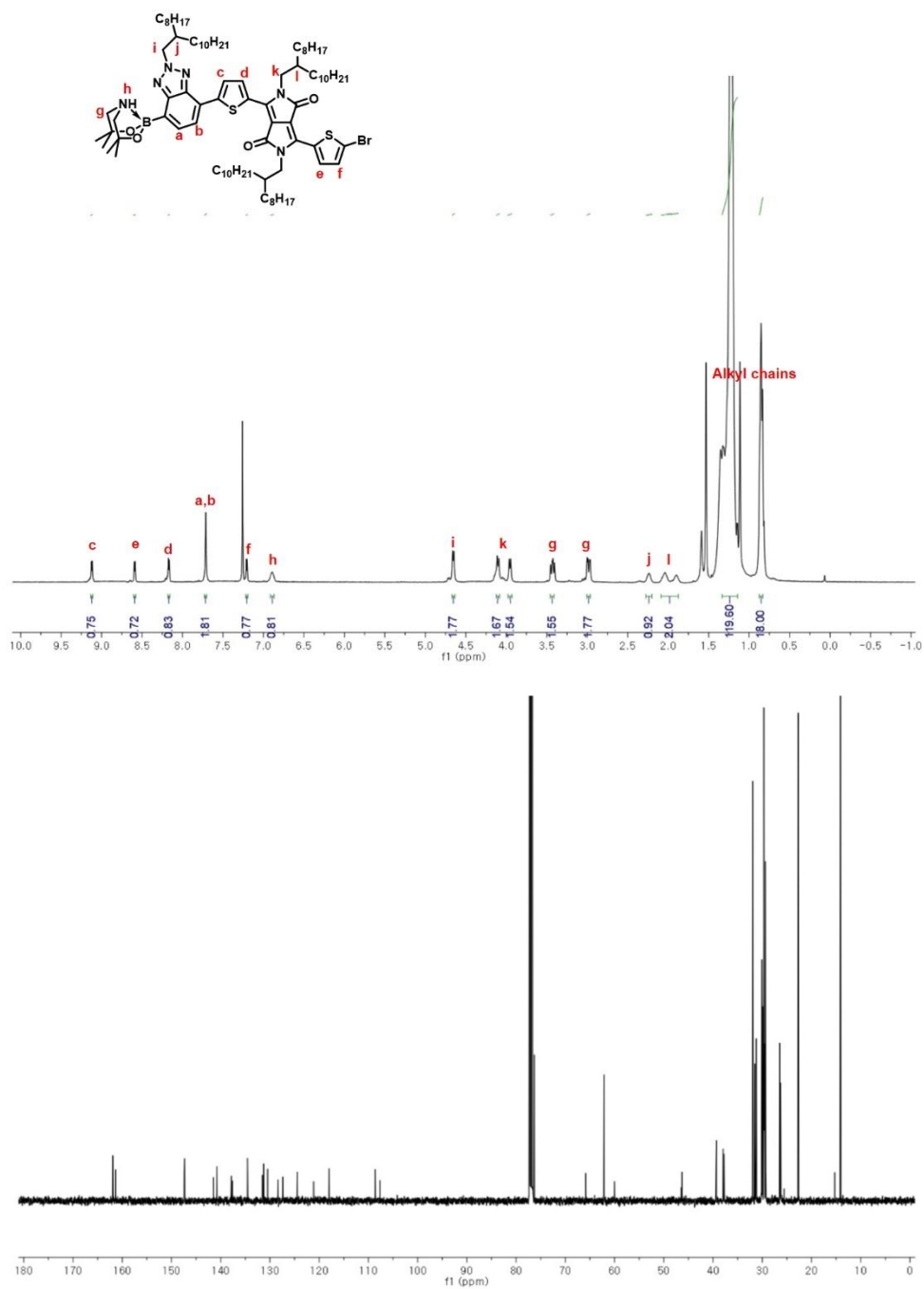












5. References

- (1) H. Huang, L. Yang, A. Facchetti, T. J. Marks, *Chem. Rev.* **2017**, *117*, 10291–10318.
- (2) A. C. Arias, J. D. MacKenzie, I. McCulloch, J. Rivnay, A. Salleo, *Chem. Rev.* **2010**, *110*, 3–24.
- (3) E. Wang, L. Wang, L. Lan, C. Luo, W. Zhuang, J. Peng, Y. Cao, *Appl. Phys. Lett.* **2008**, *92*, 033307.
- (4) M. Kim, S. U. Ryu, S. A. Park, K. Choi, T. Kim, D. Chung, T. Park, *Adv. Funct. Mater.* **2020**, *30*, 1904545.
- (5) T.-W. Chen, K.-L. Peng, Y.-W. Lin, Y.-J. Su, K.-J. Ma, L. Hong, C.-C. Chang, J. Hou, C.-S. Hsu, *J. Mater. Chem. A* **2020**, *8*, 1131–1137.
- (6) R. Ma, T. Liu, Z. Luo, Q. Guo, Y. Xiao, Y. Chen, X. Li, S. Luo, X. Lu, M. Zhang, Y. Li, H. Yan, *Sci. China Chem.* **2020**, *63*, 325–330.
- (7) J. Sakamoto, M. Rehahn, G. Wegner, A. D. Schlüter, *Macromol. Rapid Commun.* **2009**, *30*, 653–687.
- (8) B. Sharma, Y. Sarothia, R. Singh, Z. Kan, P. E. Keivanidis, J. Jacob, *Polym. Int.* **2016**, *65*, 57–65.
- (9) L. Wang, C. Pan, A. Liang, X. Zhou, W. Zhou, T. Wan, L. Wang, *Polym. Chem.* **2017**, *8*, 4644–4650.
- (10) F. Lombeck, H. Komber, A. Sepe, R. H. Friend, M. Sommer, *Macromolecules* **2015**, *48*, 7851–7860.
- (11) B. Carsten, F. He, H. J. Son, T. Xu, L. Yu, *Chem. Rev.* **2011**, *111*, 1493–1528.
- (12) Z. Yuan, C. Buckley, S. Thomas, G. Zhang, I. Bargigia, G. Wang, B. Fu, C. Silva, J.-L. Brédas, E. Reichmanis, *Macromolecules* **2018**, *51*, 7320–7328.
- (13) W. Shin, W. Ko, S.-H. Jin, T. Earmme, Y.-J. Hwang, *Chem. Eng. J.* **2021**, *412*, 128572.
- (14) M. Wakioka, N. Torii, M. Saito, I. Osaka, F. Ozawa, *ACS Appl. Polym. Mater.* **2021**, *3*, 830–836.
- (15) M. Wakioka, H. Morita, N. Ichihara, M. Saito, I. Osaka, F. Ozawa, *Macromolecules* **2020**, *53*, 158–164.

- (16) E. Iizuka, M. Wakioka, F. Ozawa, *Macromolecules* **2015**, *48*, 2989–2993.
- (17) H. Bohra, H. Chen, Y. Peng, A. Efrem, F. He, M. Wang, *J. Polym. Sci. Part A Polym. Chem.* **2018**, *56*, 2554–2564.
- (18) S. Chen, Y. An, G. K. Dutta, Y. Kim, Z. G. Zhang, Y. Li, C. Yang, *Adv. Funct. Mater.* **2017**, *27*, 1603564.
- (19) L. Lu, T. Zheng, T. Xu, D. Zhao, L. Yu, *Chem. Mater.* **2015**, *27*, 537–543.
- (20) A. Yokoyama, R. Miyakoshi, T. Yokozawa, *Macromolecules* **2004**, *37*, 1169–1171.
- (21) M. C. Iovu, E. E. Sheina, R. R. Gil, R. D. McCullough, *Macromolecules* **2005**, *38*, 8649–8656.
- (22) R. Tkachov, V. Senkovskyy, H. Komber, J.–U. Sommer, A. Kiriya, *J. Am. Chem. Soc.* **2010**, *132*, 7803–7810.
- (23) K. Mikami, M. Nojima, Y. Masumoto, Y. Mizukoshi, R. Takita, T. Yokozawa, M. Uchiyama, *Polym. Chem.* **2017**, *8*, 1708–1713.
- (24) N. Doubina, A. Ho, A. K. Y. Jen, C. K. Luscombe, *Macromolecules* **2009**, *42*, 7670–7677.
- (25) M. Yuan, K. Okamoto, H. A. Bronstein, C. K. Luscombe, *ACS Macro Lett.* **2012**, *1*, 392–395.
- (26) A. K. Leone, P. K. Goldberg, A. J. McNeil, *J. Am. Chem. Soc.* **2018**, *140*, 7846–7850.
- (27) A. K. Leone, K. D. Souther, A. K. Vitek, A. M. LaPointe, G. W. Coates, P. M. Zimmerman, A. J. McNeil, *Macromolecules* **2017**, *50*, 9121–9127.
- (28) L. M. Gao, Y. Y. Hu, Z. P. Yu, N. Liu, J. Yin, Y. Y. Zhu, Y. Ding, Z. Q. Wu, *Macromolecules* **2014**, *47*, 5010–5018.
- (29) M. Su, S. Y. Shi, Q. Wang, N. Liu, J. Yin, C. Liu, Y. Ding, Z. Q. Wu, *Polym. Chem.* **2015**, *6*, 6519–6528.
- (30) A. Yokoyama, H. Suzuki, Y. Kubota, K. Ohuchi, H. Higashimura, T. Yokozawa, *J. Am. Chem. Soc.* **2007**, *129*, 7236–7237.
- (31) K. Kosaka, T. Uchida, K. Mikami, Y. Ohta, T. Yokozawa, *Macromolecules* **2018**, *51*, 364–369.
- (32) M. A. Baker, S. F. Zahn, A. J. Varni, C. H. Tsai, K. J. T. Noonan, *Macromolecules* **2018**, *51*, 5911–5917.

- (33) S. Kobayashi, K. Fujiwara, D. H. Jiang, T. Yamamoto, K. Tajima, Y. Yamamoto, T. Isono, T. Satoh, *Polym. Chem.* **2020**, *11*, 6832–6839.
- (34) S. Kobayashi, M. Ashiya, T. Yamamoto, K. Tajima, Y. Yamamoto, T. Isono, T. Satoh, *Polymers* **2021**, *13*, 4168.
- (35) H. Zhang, C. Xing, Q. Hu, *J. Am. Chem. Soc.* **2012**, *134*, 13156–13159.
- (36) J. Dong, H. Guo, Q. S. Hu, *ACS Macro Lett.* **2017**, *6*, 1301–1304.
- (37) Y. Qiu, J. Mohin, C. H. Tsai, S. Tristram–Nagle, R. R. Gil, T. Kowalewski, K. J. T. Noonan, *Macromol. Rapid Commun.* **2015**, *36*, 840–844.
- (38) R. J. Ono, S. Kang, C. W. Bielawski, *Macromolecules* **2012**, *45*, 2321–2326.
- (39) Y. Qiu, A. Fortney, C. H. Tsai, M. A. Baker, R. R. Gil, T. Kowalewski, K. J. T. Noonan, *ACS Macro Lett.* **2016**, *5*, 332–336.
- (40) H. H. Liu, W. W. Liang, Y. Y. Lai, Y. C. Su, H. R. Yang, K. Y. Cheng, S. C. Huang, Y. J. Cheng, *Chem. Sci.* **2020**, *11*, 3836–3844.
- (41) M. P. Van Den Eede, J. De Winter, P. Gerbaux, G. Koeckelberghs, *Macromolecules* **2018**, *51*, 9043–9051.
- (42) A. D. Todd, C. W. Bielawski, *ACS Macro Lett.* **2015**, *4*, 1254–1258.
- (43) Elmalem, E.; Kiriya, A.; Huck, W. T. S. *Macromolecules* **2011**, *44*, 9057–9061.
- (44) S. Govaerts, P. Verstappen, H. Penxten, M. Defour, B. Van Mele, L. Lutsen, D. Vanderzande, W. Maes, *Macromolecules* **2016**, *49*, 6411–6419.
- (45) Y. Tokita, M. Katoh, Y. Ohta, T. Yokozawa, *Chem. – A Eur. J.* **2016**, *22*, 17436–17444.
- (46) V. Senkovskyy, R. Tkachov, H. Komber, M. Sommer, M. Heuken, B. Voit, W. T. S. Huck, V. Kataev, A. Petr, A. Kiriya, *J. Am. Chem. Soc.* **2011**, *133*, 19966–19970.
- (47) W. Liu, R. Tkachov, H. Komber, V. Senkovskyy, M. Schubert, Z. Wei, A. Facchetti, D. Neher, A. Kiriya, *Polym. Chem.* **2014**, *5*, 3404–3411.
- (48) R. Tkachov, H. Komber, S. Rauch, A. Lederer, U. Oertel, L. Haußler, B. Voit, A. Kiriya, *Macromolecules* **2014**, *47*, 4994–5001.
- (49) Y. Karpov, J. Maiti, R. Tkachov, T. Beryozkina, V. Bakulev, W. Liu,

- H. Komber, U. Lappan, M. Al-Hussein, M. Stamm, B. Voit, A. Kiriya, *Polym. Chem.* **2016**, *7*, 2691–2697.
- (50) P. Pahlavanlu, S. Y. An, J. R. Panchuk, A. A. Pollit, D. S. Seferos, *Macromolecules* **2021**, *54*, 3130–3138.
- (51) D. Bhardwaj, Shahjad, S. Gupta, P. Yadav, R. Bhargav, A. Patra, *ChemistrySelect* **2017**, *2*, 9557–9562.
- (52) P. Leysen, S. Quattrosoldi, E. Salatelli, G. Koeckelberghs, *Polym. Chem.* **2019**, *10*, 1010–1017.
- (53) P. Willot, G. Koeckelberghs, *Macromolecules* **2014**, *47*, 8548–8555.
- (54) T. Yokozawa, Y. Nanashima, Y. Ohta, *ACS Macro Lett.* **2012**, *1*, 862–866.
- (55) Z. J. Bryan, A. J. McNeil, *Macromolecules* **2013**, *46*, 8395–8405.
- (56) K. B. Seo, I. H. Lee, J. Lee, I. Choi, T. L. Choi, *J. Am. Chem. Soc.* **2018**, *140*, 4335–4343.
- (57) J. Lee, H. Park, S.-H. Hwang, I. H. Lee, T. L. Choi, *Macromolecules* **2020**, *53*, 3306–3314.
- (58) J. Lee, H. Kim, H. Park, T. Kim, S.-H. Hwang, D. Seo, T. D. Chung, T.-L. Choi, *J. Am. Chem. Soc.* **2021**, *143*, 11180–11190.
- (59) S.-H. Hwang, S.-Y. Kang, S. Yang, J. Lee, T.-L. Choi, *J. Am. Chem. Soc.* **2022**, *144*, 5921–5929.
- (60) P. A. Cox, A. G. Leach, A. D. Campbell, G. C. Lloyd-Jones, *J. Am. Chem. Soc.* **2016**, *138*, 9145–9157.
- (61) E. Wang, L. Hou, Z. Wang, S. Hellström, F. Zhang, O. Inganäs, M. R. Andersson, *Adv. Mater.* **2010**, *22*, 5240–5244.
- (62) Y. Kim, H. R. Yeom, J. Y. Kim, C. Yang, *Energy Environ. Sci.* **2013**, *6*, 1909–1916.
- (63) M. Al-Hashimi, M. A. Baklar, F. Colleaux, S. E. Watkins, T. D. Anthopoulos, N. Stingelin, M. Heeney, *Macromolecules* **2011**, *44*, 5194–5199.
- (64) B. Kim, H. R. Yeom, M. H. Yun, J. Y. Kim, C. Yang, *Macromolecules* **2012**, *45*, 8658–8664.
- (65) A. J. Kronemeijer, E. Gili, M. Shahid, J. Rivnay, A. Salleo, M. Heeney, H. Sirringhaus, *Adv. Mater.* **2012**, *24*, 1558–1565.
- (66) Bautista, M. V.; Varni, A. J.; Ayuso-Carrillo, J.; Tsai, C. H.; Noonan,

- K. J. T. *ACS Macro Lett.* **2020**, *9*, 1357–1362.
- (67) Tieke, B.; Rabindranath, A. R.; Zhang, K.; Zhu, Y. *Beilstein J. Org. Chem.* **2010**, *6*, 830–845.
- (68) H. Bronstein, Z. Chen, R. S. Ashraf, W. Zhang, J. Du, J. R. Durrant, P. Shakya Tuladhar, K. Song, S. E. Watkins, Y. Geerts, M. M. Wienk, R. A. J. Janssen, T. Anthopoulos, H. Sirringhaus, M. Heeney, I. McCulloch, *J. Am. Chem. Soc.* **2011**, *133*, 3272–3275.
- (69) T. Beryozkina, V. Senkovskyy, E. Kaul, A. Kiriy, *Macromolecules* **2008**, *41*, 7817–7823.
- (70) A. Kleine, U. S. Schubert, M. Jäger, *Macromolecules* **2022**, *55*, 3688–3698.
- (71) H.-N. Choi, I.-H. Lee, *Polym. J.* **2021**, *53*, 1205–1211.
- (72) J. P. Wolfe, S. Wagaw, S. L. Buchwald, *J. Am. Chem. Soc.* **1996**, *118*, 7215–7216.
- (73) M. S. Driver, J. F. Hartwig, *J. Am. Chem. Soc.* **1996**, *118*, 7217–7218.
- (74) V. D. Mitchell, D. J. Jones, *Polym. Chem.* **2018**, *9*, 795–814.
- (75) L. Verheyen, P. Leysen, M. Van Den Eede; W. Ceunen, T. Hardeman, G. Koeckelberghs, *Polymer (Guildf)* **2017**, *108*, 521–546.
- (76) T. Yokozawa, Y. Ohta, *Chem. Commun.* **2013**, *49*, 8281–8310.
- (77) K. B. Woody, B. J. Leever, M. F. Durstock, D. M. Collard, *Macromolecules* **2011**, *44*, 4690–4698.
- (78) Y. Janpatompong, R. Marcial-Hernandez, D. J. Tate, M. L. Turner, *Polym. Chem.* **2021**, *12*, 6731–6736.
- (79) H. N. Choi, H. S. Yang, J. H. Chae, T.-L. Choi, I. H. Lee, *Macromolecules* **2020**, *53*, 5497–5503.
- (80) B. R. Gautam, R. Younts, J. Carpenter, H. Ade, K. Gundogdu, *J. Phys. Chem. A* **2018**, *122*, 3764–3771.

리빙 스즈키-미야우라 촉매-이동 중합을 통한 낮은 밴드갭을 갖는 다양한 전자 주개-받개 교대 공중합체의 정교한 합성

김 황 석

화학부 유기화학 전공

서울대학교 대학원

본 연구에서 우리는 RuPhos Pd G3 전촉매를 이용하는 리빙 스즈키-미야우라 촉매-이동 중합 (Suzuki-Miyaura catalyst-transfer polymerization, SCTP) 을 통한 다양한 전자 주개-받개 교대 공중합체의 정교한 합성을 보고한다. 먼저, 이런 리빙 중합을 다양한 전자 주개 및 받개를 조합한 단량체들에 적용하고 조건을 최적화하여 여러 교대 공중합체들을 조절된 평균 분자량 (M_n), 낮은 분산도 (D , 1.05-1.29), 그리고 높은 수득률 (>87%) 로 얻었다. 또한, 이 방법론을 다이케토피롤로피롤 (DPP, 강한 받개) 을 포함해 네 개의 방향족 고리를 가진 단량체까지 확장했을 때에도 조절된 M_n (9.2-40.0 kg/mol) 의 고분자를 합성할 수 있음을 발견하였다. 추가적으로, 이 리빙 중합법은 복잡한 구조를 가진 다양한 다이블록 및 트라이블록 공중합체의 한 단계 합성 또한 가능케 하였다. 마지막으로, 합성된 교대 공중합체들은 조절 가능한 광학적 밴드갭 (E_g^{opt} , 1.29-1.77 eV) 및 최고 피점 분자궤도함수 에너지 (HOMO, -5.57에서 -4.75 eV까지) 와 같은 광전기화학적 성질을 보여주었고 블록 공중합체의 넓은 흡광 범위는 이 물질들의 잠재적인 높은 가시광선 활용 능력을 암시하였다.

핵심어: 공액 고분자, 축매-이동 중합, 유기 반도체 물질, 전자 주개-받개 공중합체, 스즈키-미야우라 교차 짝지음 반응

학번: 2020-26902